General Disclaimer

One or more of the Following Statements may affect this Document

- This document has been reproduced from the best copy furnished by the organizational source. It is being released in the interest of making available as much information as possible.

- This document may contain data, which exceeds the sheet parameters. It was furnished in this condition by the organizational source and is the best copy available.

- This document may contain tone-on-tone or color graphs, charts and/or pictures, which have been reproduced in black and white.

- This document is paginated as submitted by the original source.

- Portions of this document are not fully legible due to the historical nature of some of the material. However, it is the best reproduction available from the original submission.

SGT

E84-10026

CR-174549

1

5089-3 (917)
October 3, 1983

I. Introduction

TITLE: CCRS Proposal for Evaluating LANDSAT-D MSS and TM Data

Investigation Number: LANDSAT-4, F-2

Authors: Dr. W.M. Strome, (PI)
Dr. J. Cihlar, (Co-I)
Dr. D.G. Goodenough, (Co-I)
Mr. F.E. Guertin, (Co-I)
Dr. B. Guindon, (Collaborator)
Ms. J.M. Murphy, (Collaborator)
Dr. P. Teillet, (Collaborator)

Organization: Canada Centre for Remote Sensing (CCRS)

Type of Report: First Progress Report

Reporting Date: May 2, 1983 to September 2, 1983

II. Techniques

The following LANDSAT-4 imagery was used in the study: 13 MSS scenes and 5 TM scenes.

Sensor	Path/Row	Identification	Date	Data Type
MSS	17/30	Niagara, Ont.	28/11/82	raw
MSS	18/23	Sakami L., Que.	09/12/82	raw
MSS	17/30	Niagara, Ont.	28/08/82	raw
MSS	36/23	Melfort, Sask.	02/09/82	raw
MSS	16/24	Mesgouez L., Que.	22/09/82	raw
MSS	34/23	Red Deer L., Man.	22/10/82	raw
MSS	39/22	Meadow L., Sask.	23/10/82	raw
MSS	41/18	Uranium City,Sask.	24/11/82	raw
MSS	35/21	Pukatawagan, Man.	01/01/83	raw
MSS	40/21	Churchill L.,Sask.	20/01/83	raw
MSS	40/25	Medicine Hat, Alt.	20/01/83	raw
MSS	36/23	Melfort, Sask.	04/10/82	raw
MSS	16/28	Ottawa, Ont.	24/10/82	raw
TM	20/31	Windsor, Ont.	25/09/82	P-type
TM	48/26	Vancouver Is.,BC	11/11/82	raw
TM	42/36	Oxnard, California	15/11/82	raw
TM	39/25	Medicine Hat,Alt.	10/10/82	P-type
TM	1628	Ottawa, Ont.	12/12/82	raw

Most data, exept for the TM scenes of Windsor and Medicine Hat, were in the uncorrected and raw form in order to develop the radiometric and geometric correction algorithms independent from any previous processing.

Except for the Windsor scene all the imagery was acquired at the Prince Albert satellite station. The MSS studies are conducted on CCRS image processing and analysis facilities (MIPS-TSS, DICS, CIAS) that were developed for previous LANDSAT missions and were upgraded in 1982 for LANDSAT-4. The TM studies have access to two new systems: Thematic Mapper Transcription System (TMTS), and the LANDSAT-4 Digital Image Analysis System (LDIAS), (Reference 1).

CCRS is developing LDIAS, a dual VAX 11/780 system for analysis of LANDSAT-4 Thematic Mapper (TM) and Multispectral Scanner (MSS) data. The LDIAS includes two image displays, two map displays, and various array and special purpose processors.

Most of the hardware has been delivered for the system. We are awaiting delivery of upgraded image displays capable of easily handling 7-channel TM scenes. We will also receive in August, 1984 a fast, processing subsystem which will perform the following functions on a full TM scene (at disk access rates for functions 1,4):

(1) table look-up of 7 channels simultaneously for a full TM scene;
(2) parallelepiped classification of up to 21 channels;
(3) maximum likelihood classification with or without parallelepiped preclassification;
(4) ratioing and linear combinations of channels.

Initial software comes from the CCRS Image Analysis System (CIAS) developed earlier for the LANDSAT-1, 2, 3 MSS images. We have converted 330,000 lines of code to the VAX and have commenced preprocessing research and development reported below.

III. Accomplishments

The objectives of the Canadian proposal are:

(1) to quantify the LANDSAT-4 sensors and system performance for the purpose of updating the radiometric and geometric correction algorithms for MSS and for developing and evaluating new correction algorithms to be used for TM data processing;

(2) to compare and access the degree to which LANDSAT-4 MSS data can be integrated with MSS imagery acquired from earlier LANDSAT missions;

(3) to apply image analysis and information extraction techniques for specific user applications such as forestry or agriculture.

The accomplishments toward these objectives have been:

(1) adaptation of radiometric and geometric correction algorithms for LANDSAT-4 MSS, (Reference 2);

(2) comparison of LANDSAT-4 MSS products with earlier MSS missions, (Reference 2);

(3) investigation of various algorithms for TM radiometric calibration, (References 3, 4). Also, using a ground-based spectroscopic laboratory the magnitude of the view angle effects expected for crops has been measured;

(4) investigation of specific algorithms toward Tm geometric correction. Methods for automated control point acquisition has been investigated using simulated TM data. The best edge operator is the magnitude of the gradient. Single band GCP accuracy provides comparable accuracy to that achieved with multiple bands. The preferred bands are TM1 for road intersections and field boundaries and TM2 for land-water interfaces and field-forest boundaries. Normalized or average correlation gave the lowest mismatch rates. The performance of 32 by 32 chips was not worse than that of 64 by 64 chips. Below 32 by 32 chips mismatch rates increase with decreasing chip size. Neither peak correlation thresholding nor correlation surface curvature can be readily used to identify mismatch cases.

IV. Significant Results

(1) System-corrected and geocoded LANDSAT-4 MSS products are offered operationally to users.

(2) It has been determined that the radiometric calibration algorithms developed for MSS cannot be used for TM data if a ±1 quantum level accuracy is required.

V. Publications

The following papers were presented at the LANDSAT-4 Early Results Symposium, 22-24 February 1983: N83-29754

1. Canadian Plans for Thematic Mapper Data by W.M. Strome, F.E. Guertin, A.B. Collins and D.G. Goodenough;

2. Radiometric Calibration and Geocoded Precision Processing of LANDSAT-4 Multispectral Scanner Products by the Canada Centre for Remote Sensing by J. Murphy, D. Bennett and F. Guertin;

3. Preliminary Evaluation of the Radiometric Calibration of LANDSAT-4 Thematic Mapper Data by the Canada Centre for Temote Sensing by J. Murphy, W. Park and A. Fitzgerald;

4. A Preliminary Assessment of LANDSAT-4 Thematic Mapper Data by D.G. Goodenough, E.A. Fleming and K. Dickinson.

There were also related presentations made at the Canadian LANDSAT-4 Workshop in Ottawa, 28-29 June 1983.

VI. Problems

The main problem has been the limited availability of suitable TM imagery over Canada, in particular the lack of data and ground truth during the summer of 1983.

VII. Data Quality and Delivery

The two TM scenes to be processed at the Goddard Space Flight Center were: Mistassini and Starbuck. According to the list of images provided by the LANDSAT-4 Science Office on August 5, 1983, there is no good quality cloud free TM images for these two sites.

VIII. Recommendation

We recommend that NASA provide us with the raw high density tape and the ground truth for the Arkansas scene (Path 23, Row 35) acquired on August 22, 1982 and corresponding to the LACIE supersites in this area.

We also recommend that NASA provide the following two TM scenes as substitutes for Mistassini and Starbuck:

Sensor	Path/Row	Identification	Date	Date Type
TM	14/26	St. Jean, Que.	10/10/82	P-type
TM	14/28	Sorel, Que.	10/10/82	P-type

We would appreciate if we could receive the above data as soon as possible and not later than the end of the next reporting period.

IX. Conclusions

For MSS our studies have demonstrated that LANDSAT-4 can provide data continuity with the previous three LANDSAT missions.

For TM our simulation studies dramatically indicate that LANDSAT-4 will substantially enhance Canadian capability to execute resource management incorporating remote sensing. We expect large benefits in forestry, agriculture and geology.

CANADIAN PLANS FOR THEMATIC MAPPER DATA

Authors W.M. Strome, F.E. Guertin,
A.B. Collins and D.G. Goodenough

Canada Centre for Remote Sensing
2464 Sheffield Road
Ottawa, Ontario, Canada
K1A 0Y7

ABSTRACT

Canada was the first country outside the U.S.A. to receive, process and distribute data from the original LANDSAT series. The data from these satellites have been used to improve the state-of-the-art of resource management and environmental monitoring in Canada over the past decade. The utility of MSS data has been proven in a wide range of applications, from ice reconnaissance, through agriculture and forestry to geological exploration, to name a few. Despite the usefulness of MSS, its limitations prevented full use of satellite remote sensing technology for some purposes. Thus, it was decided to upgrade the Canadian facilities to receive and process the data from LANDSAT-4.

The modifications to the existing equipment for processing MSS data from the new satellite were relatively straightforward and are now complete. The Prince Albert Satellite Station has been modified to permit reception and recording of TM data for western North America. A small scale system has been built to transcribe TM data from the high density station tapes to computer compatible tape. The throughput of this system is very low - two to five scenes per week. However, it does enable us to develop and test the algorithms to be used in our Thematic Mapper Bulk Processing system and our Multi Observation Satellite Image Correction System (MOSAICS). These will be operational in 1984 and 1986 respectively. The latter system will provide geocoded image data, keyed to maps and independent of satellite orbit and sensor resolution. To analyze the TM imagery a new facility called the LANDSAT-D Image Analysis System (LDIAS) is being developed and will be phased gradually into operation starting in 1983.

INTRODUCTION

Remote sensing data from satellites are particularly suited for providing information required for resource management and environmental monitoring in a country such as Canada, which has a large geographical area and a relatively low population. Satellite data is especially useful for remote areas. Because of the importance of this new tool for gathering resource and environmental data, Canada was the first country outside the U.S. to build facilities to receive, record, process and distribute data from the original LANDSAT series. Over the past decade, MSS data have been used extensively to improve the state-of-the-art of resource management and environmental monitoring in Canada for a wide range of application from ice reconnaissance through agriculture and forestry to geological exploration, to name just a few. While the MSS data have been valuable, the limitations of this instrument prevented the achievement of the maximum benefits possible from remote sensing satellite technology in many instances. To improve the quality of data which can be obtained from remote sensing satellites, and thereby improve Canada's resource management capability, it was decided to upgrade our facilities to enable them to receive, record, process, distribute and analyze the Thematic Mapper and MSS data from LANDSAT-4.

LANDSAT-4 MSS

Because of the orbit chosen for LANDSAT-4 as well as changes in the sensor itself, the MSS processing facility required several changes. These were completed in December, 1982. In addition, Canada changed its CCT format to the new Standard Format Family, in order to be compatible with other ground stations, and now supplies all LANDSAT MSS data in that format. The earlier format is no longer supported. However, CCRS has offered to provide assistance to users having difficulty in converting their software to read the new tape format.

THEMATIC MAPPER RECEPTION

Data from the Thematic Mapper (TM) are transmitted at X-band (compared to S-band for MSS), and have a much higher data rate than that of the MSS. To receive the TM data, the antenna at Prince Albert was modified, an additional feed system installed and a new receiver added. The High Density Digital Tape Recorders (HDDTR) were replaced to permit recording of the higher data rates of TM. These changes were completed in October, 1982. Since that time, the Prince Albert Station has been recording all North American data within its coverage circle (see Figure 1). Under an arrangement with NASA, the Prince Albert Station is recording Western U.S. data which cannot be acquired at Greenbelt, MD. In return, NASA is recording Eastern Canadian data which cannot be recorded at Prince Albert. The tapes are exchanged so that each country can process its own data.

TM TRANSCRIPTION SYSTEM

CCRS has developed a transcription system which can convert the HDDT recorded at the receiving station to CCT format. This is required in order to develop the correction algorithms to be used in the TM pre-processing production system. A block diagram of this system is shown in Figure 2. The system, which was completed in December 1982, has limited correction and throughput capabilities. It can transcribe two scenes per week and only provides corrections for detector placements and sampling delays, and for major differences between scan directions. It can also extract the house-keeping data contained in the X-band data stream. At NASA, these data are obtained from a separate low data rate telemetry recorder, which is not used in the Canadian system.

TM BULK PROCESSING SYSTEM

A high throughput (30-40 scenes per day) TM Bulk Processing System is now under construction to provide system corrected data for distribution to users. This system, for which the block diagram is shown in Figure 3, will be completed by May 1984. The computer used in this system is a DEC VAX-11/780. The data are formatted by a special hardware front end and digital interface. Corrections are performed by an array processor. Curently, a STAR Technology ST-100 is being evaluated for this purpose. There is some concern that this new product may not be available in time to meet our schedule. If this is the case an alternative processor will be considered. A colour MDA FIRE recorder will be used to generate photographic products. The CCT peripherals are standard 1600/6250 bpi devices.

The design goals of the TMBPS are to provide simple operator interaction instruction; to take data from HDDT or CCT; to provide Worldwide Reference System framing; to provide radiometric and along-scan systematic geometric correction; to produce either "raw" or system corrected CCT products in the Standard LANDSAT Ground Station Operators Working Group (LGSOWG) format; to provide black and white or colour film products; and to provide full scene or quarter scene (quadrant) products.

Absolute detector calibration will be provided as well as striping removal and correction for sensor non-linearity. Output to the film recorder will be adjusted for film gamma distortion. Compensation for detector failures will be performed by substitution of data from an adjacent detector. Contrast stretch and corrections for sun angles will also be made.

Corrections will be applied to remove band to band misregistration, detector offsets within a band, forward and reverse scan non-linearity and misregistration and scan line length errors. In addition, geometric errors resulting from earth rotation, altitude changes, panoramic distortion, earth curvature and attitude changes will be corrected to the extent possible with a priori and telemetry data.

MOSAICS

When CCRS began providing users with MSS precision geometrically corrected products, it was decided to adopt a philosophy which differed significantly from that of all other ground station operators. The standard approach was to produce images which were corrected to match a Space Oblique Mercator projection, which most closely matched the geometry of the satellite orbit. After a careful survey of Canadian users, it was decided to provide corrected products matching quadrants at standard 1:250,000 scale map sheets, with 50x50 m pixels aligned along the northings and eastings of this projection (Guertin, 1981). This choice made it much easier to combine LANDSAT data with that in existing geocoded data bases. In addition, this choice makes it possible to provide data products which are geometrically independent of the data source. Thus, the geometrically corrected products from LANDSAT-4 MSS match precisely those produced from LANDSAT-1, 2 and 3. Figure 4 depicts the standard platform independent approach. The MOSAICS system will provide geometrically corrected MSS, TM and SPOT products which match the current MSS data, except for the pixel size, which will be 25x25 m for TM. In this case, four TM pixels cover a single MSS pixel as shown in Figure 5.

A block diagram of MOSAICS is shown in Figure 6. Its configuration is similar to that of the TMBPS with the addition of two work stations which are used for Ground Control Point (GCP) selection and digitizing as well as production control. Indeed, MOSAICS is physically the TMBPS with more hardware and extensive software additions. This system will be completed in 1986.

MOSAICS will provide precision geocoded products which can be corrected for terrain relief where suitable Digital Terrain Models (DTM) are available. Scenes may be corrected using GCPs within the scene or throughout a satellite pass. It will feature extensive quality assessment functions and secure data base archives. Output CCTs will be in the standard LGSOWG format. Throughput will be 25 geocoded products per day, 30-40 system corrected products or a mixture of these. In addition, the system will be capable of producing a mosaic using adjacent scenes both along an orbital track and from adjacent orbits. Geometric correction will be to sub-pixel accuracy. In Canada, products will be in the UTM projection and based upon standard map quadrangles. However, the system could be adapted to any standard map projection.

The MOSAICS concept should simplify the task of the user in combining data from different satellites, as well as those from geocoded data bases.

LANDSAT DIGITAL IMAGE ANALYSIS SYSTEM

In order to make effective use of the data from the TM, CCRS is developing a new LANDSAT Digital Image Analysis System (LDIAS). A block diagram of this system is shown in Figure 7. The major design goal of this system is to provide a capability to analyse a full TM scene in the time now required to process a LANDSAT MSS scene on the CCRS Image Analysis System (CIAS), (Goodenough, 1978). This will be achieved using a special pre-processor which will include special hardware functions for image analysis and a powerful array processor as well as image display subsystem with considerable internal processing capabilities. In addition, an Intergraph MAP I/O subsystem will facilitate conversions between raster and vector geocoded data formats to permit effective use of map data in the analysis process, and to provide geocoded data outputs which can be used directly for updating geocoded data bases.

While the hardware and basic software for this system will be completed by the end of 1984, there are several problems which must be solved in order to take full advantage of the higher spatial and spectral resolution as well as the additional bands provided by the TM. Several studies have demonstrated that the application of standard MSS analysis techniques to TM data will often result in poorer classifications than can be achieved with MSS. This is attributed to the reduction of homogeneity with increased spatial resolution. To overcome this difficulty, research and development efforts are required to develop better segmentation algorithms in order to define the areas which contain given materials of interest. Once segments are defined, new algorithms are needed for their classification. Better labelling techniques and methods for use of a priori information are also required. Much better use of textural features will be required to effectively analyze the higher resolution data from the TM. Also, it will be necessary to determine the level of supervision which is required for different applications.

Research is required to determine effective methods for the integration of multiple pixel data from different satellites and other data sources, and to analyse the resulting high dimensional data sets in an effective manner. More care will be required in correcting the data for geometric and radiometric effects. Appropriate techniques must be developed.

Some of the R&D activities to be undertaken in the LDIAS project will be aimed at improving the geometric and radiometric correction applied to user products from the TMBPS and MOSAICS.

The LDIAS project will not be completed until 1987. However, by early 1984, most of the hardware and standard analysis software will be installed. In addition, the MAP I/O facility will be fully integrated and tested. By early 1985, the high speed processor will be added to the system and plans for incorporating DTM data will be complete. It is expected that the R&D activity leading to the development of effective algorithms for the analysis of high resolution, multidimensional data, such as that obtained with the TM, will be completed by early 1986.

USE OF TM DATA

In preparation for Canada's participation in the LANDSAT-4 program, a cost-benefit study was conducted by A.K. McQuillan (1978) and a Workshop on Canadian Plans for Participation in LANDSAT Follow-On Programs was held (CCRS, 1979). The results of these two reports were summarized by A.K. McQuillan and W.M. Strome (1979).

Most of the advantages of TM data over that for MSS were envisaged to result in improved accuracy in existing applications. However, several applications which are marginal at best with MSS could become practical with TM data. These include, for example, regional land use planning, wetland and intertidal mapping, several geological applications and snow mapping.

At this stage in the evolution of satellite remote sensing technology, it is most important that the users be given high quality products, the analysis tools to take advantage of the increased information in order to offset the costs associated with handling much higher data volumes, and most important of all, the assurance that the data will continue to be available from some source. Without this assurance, operational resource management agencies cannot afford to abandon traditional information gathering methods in favour of the new technology, despite its possible advantages.

REFERENCES

CCRS, (1978) Report on CCRS Workshop on Canadian Plans for Participation in Landsat Follow-on Programs, CCRS, March 1978.

Goodenough, D.G., Strome, W.M., (1978) The Canada Centre for Remote Sensing Image Analysis System (CIAS) CIPS Review, Canada Information Processing Society.

Guertin, F.E., Shaw, E., (1981) Definition and Potential of Geocoded Satellite Imagery Products, 7th Canadian Symposium on Remote Sensing, Winnipeg, pp. 384-394.

McQuillan, A.K., (1978) Application and Potential Benefits of Landsat-D, CCRS Research Report.

McQuillan, A.K., Strome, W.M., (1979) An Evulation of Landsat-D for Canadian Applications, Proceedings of the 13th International Symposium on Remote Sensing of Environment, Ann Arbor, pp. 957-964.

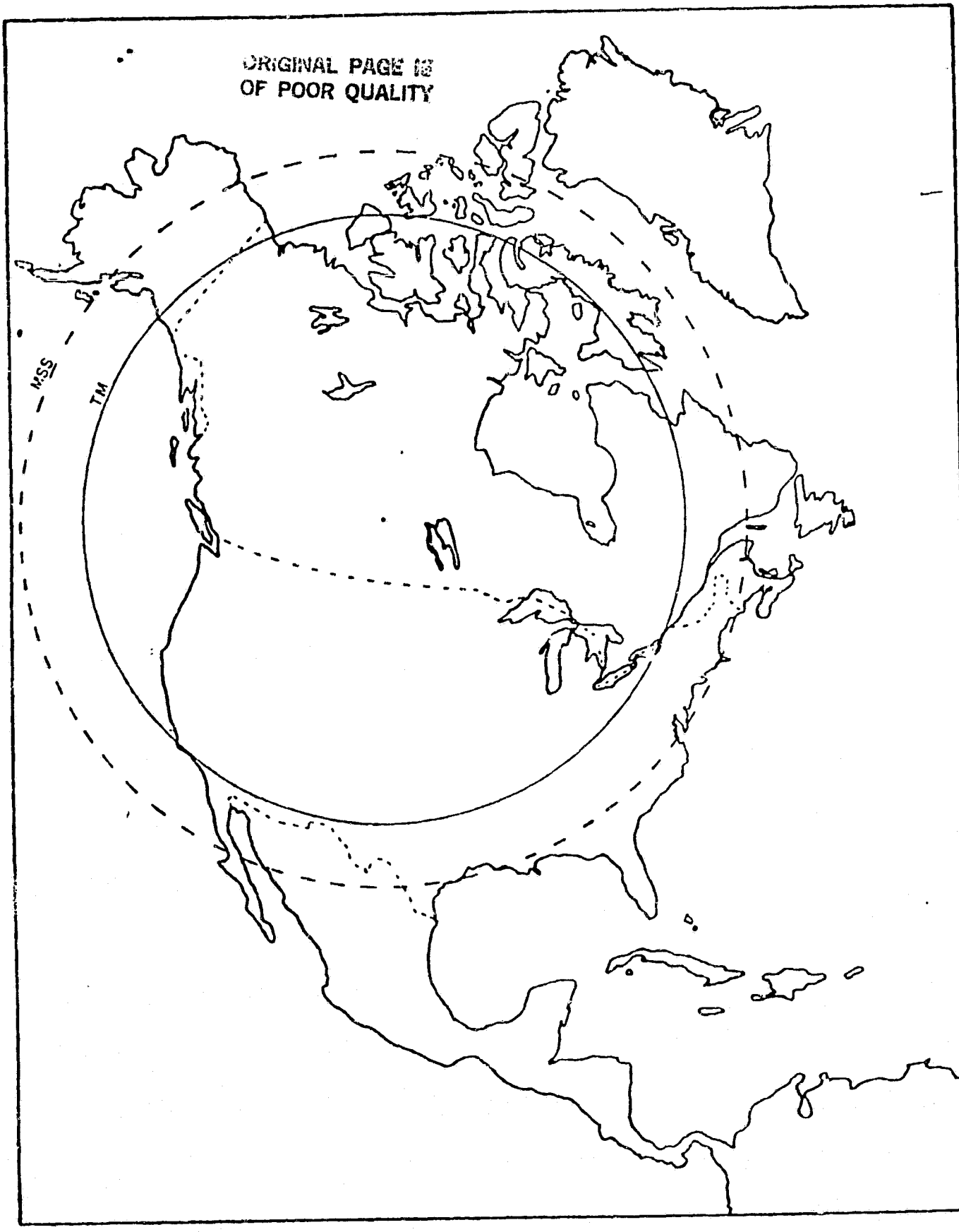

FIGURE 1: LANDSAT-4 COVERAGE CIRCLE FROM PASS

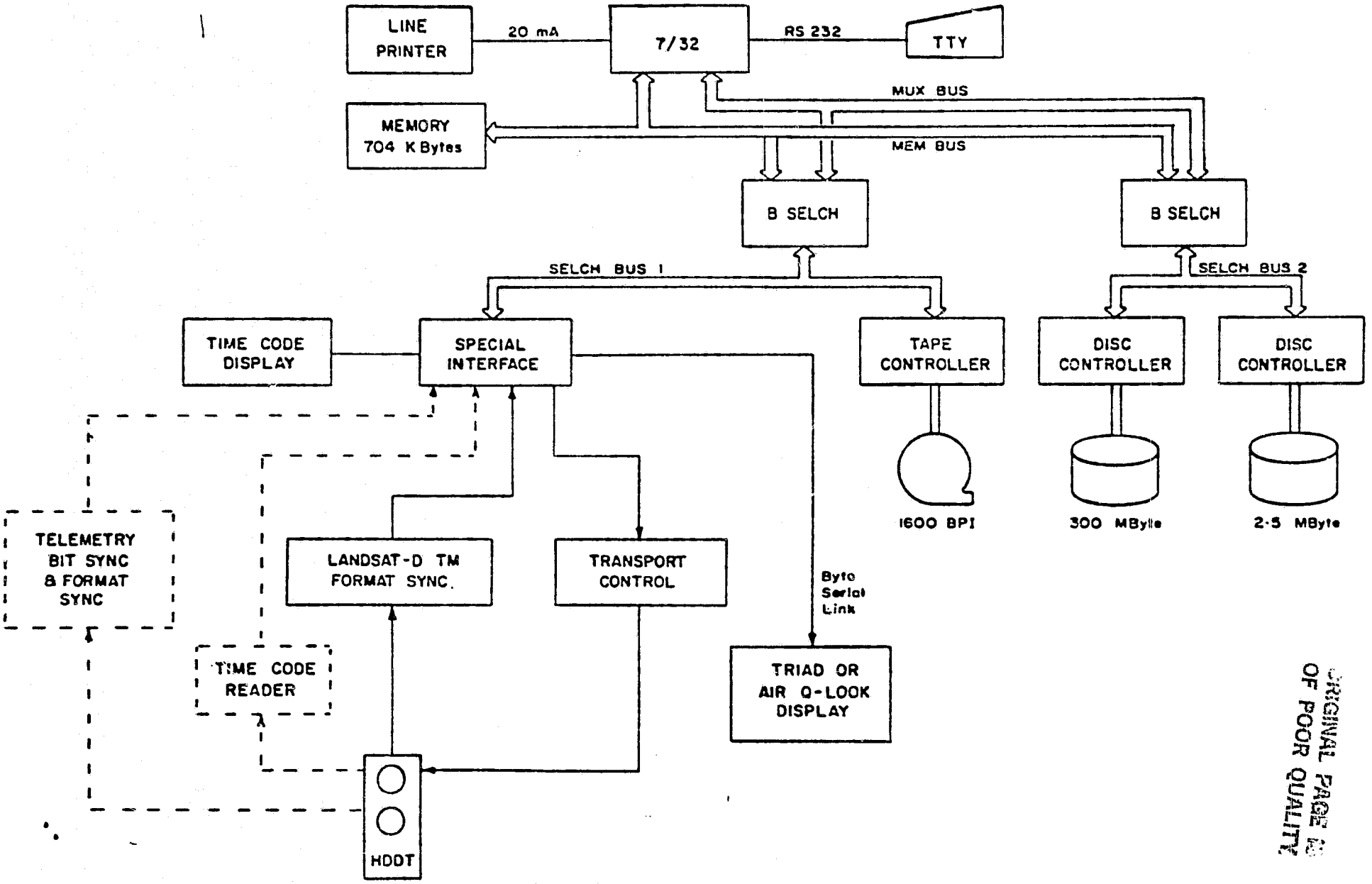

FIGURE 2: THEMATIC MAPPER TRANSCRIPTION SYSTEM

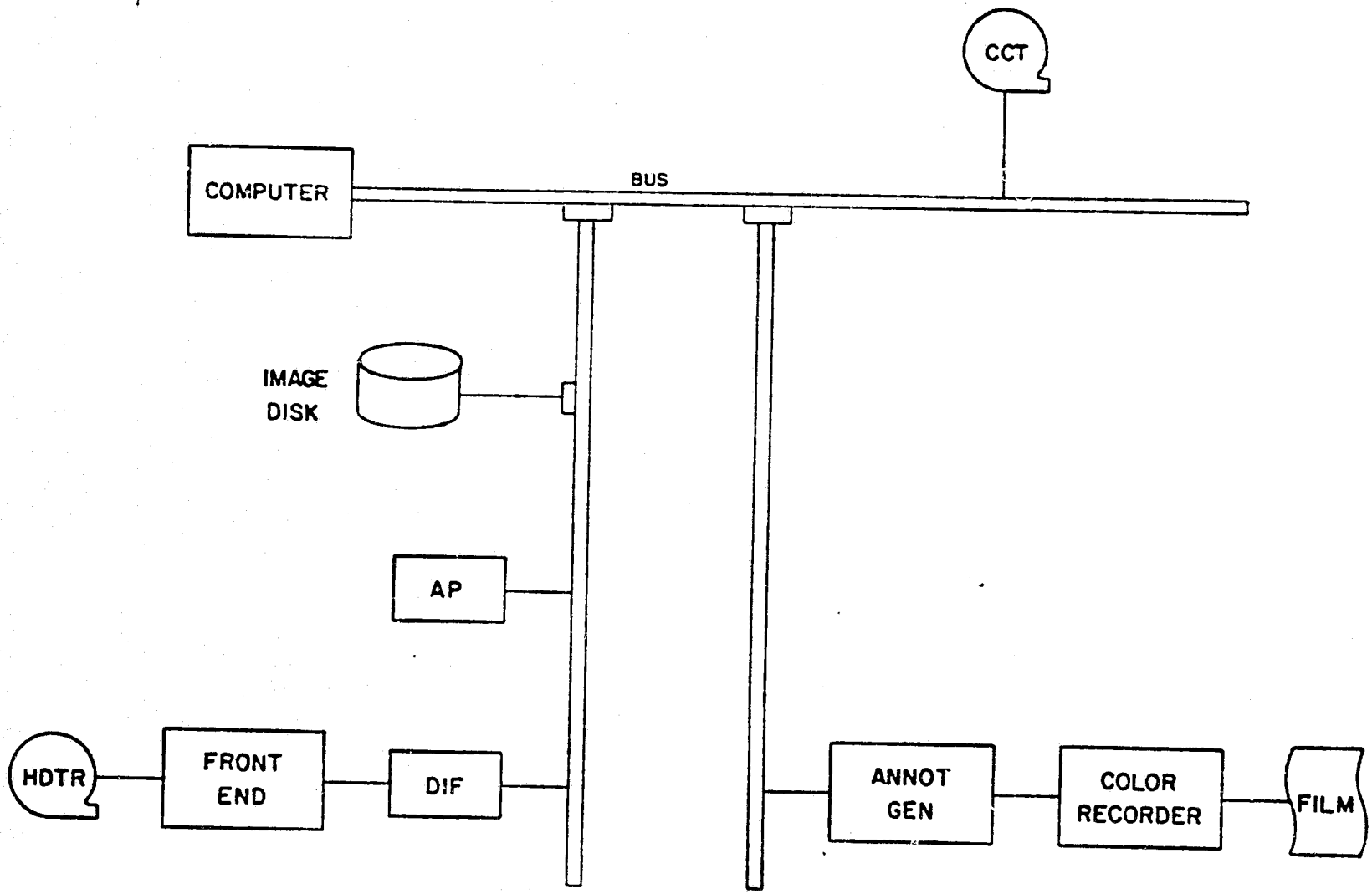

FIGURE 3: THEMATIC MAPPER BULK PROCESSING SYSTEM

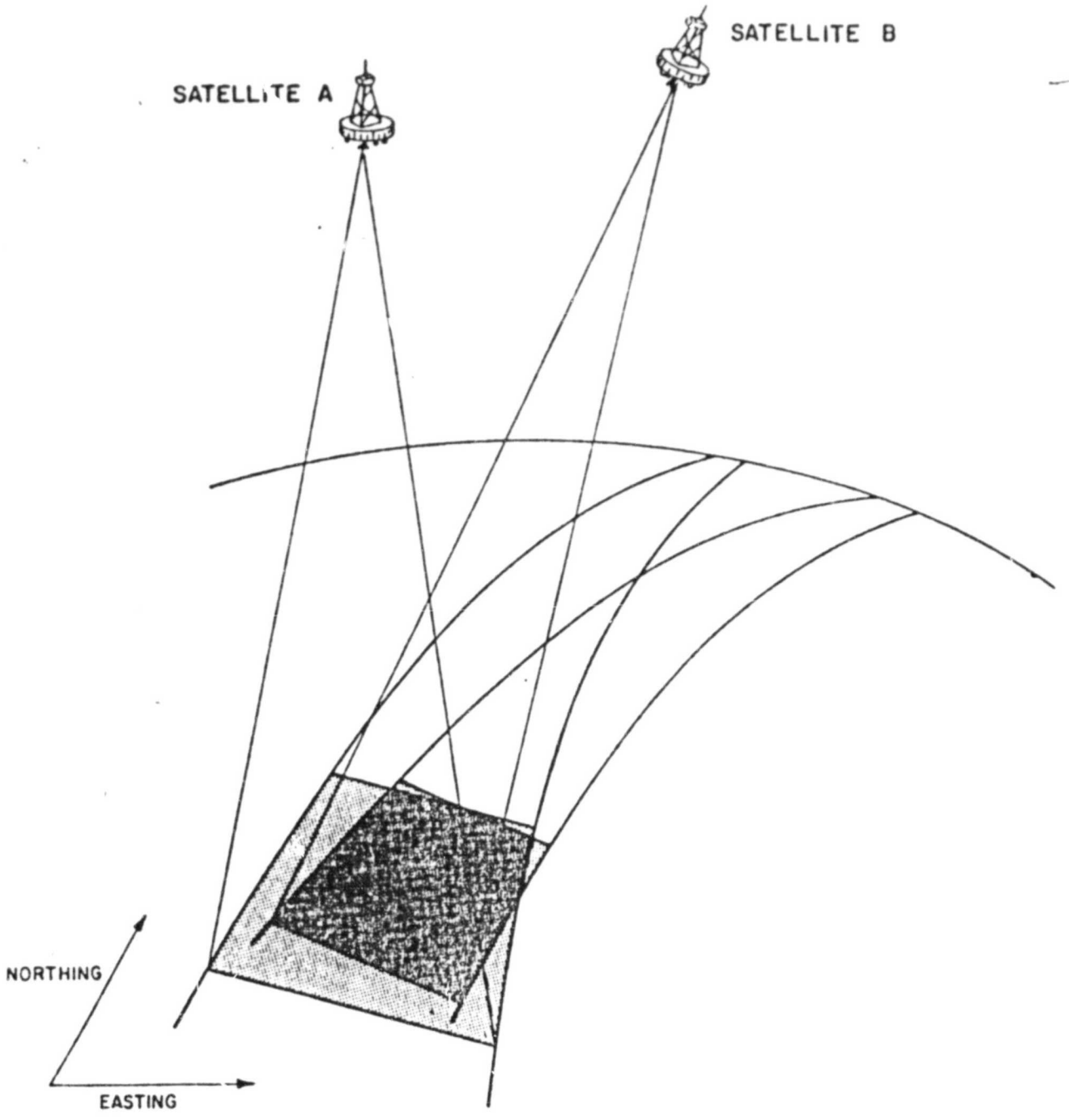

FIGURE 4: MISSION DEPENDENT IMAGERY

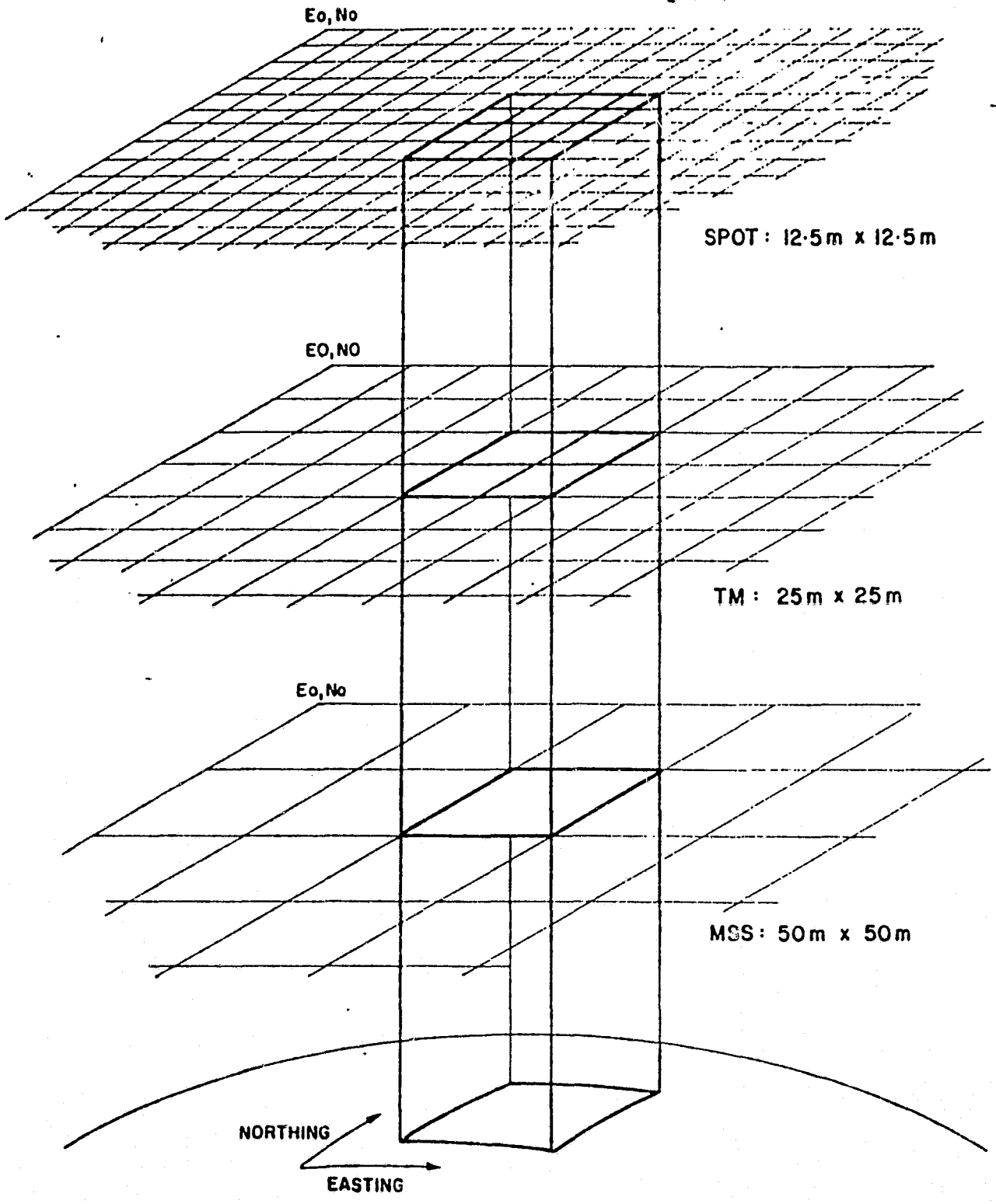

FIGURE 5: GEOCODED IMAGERY

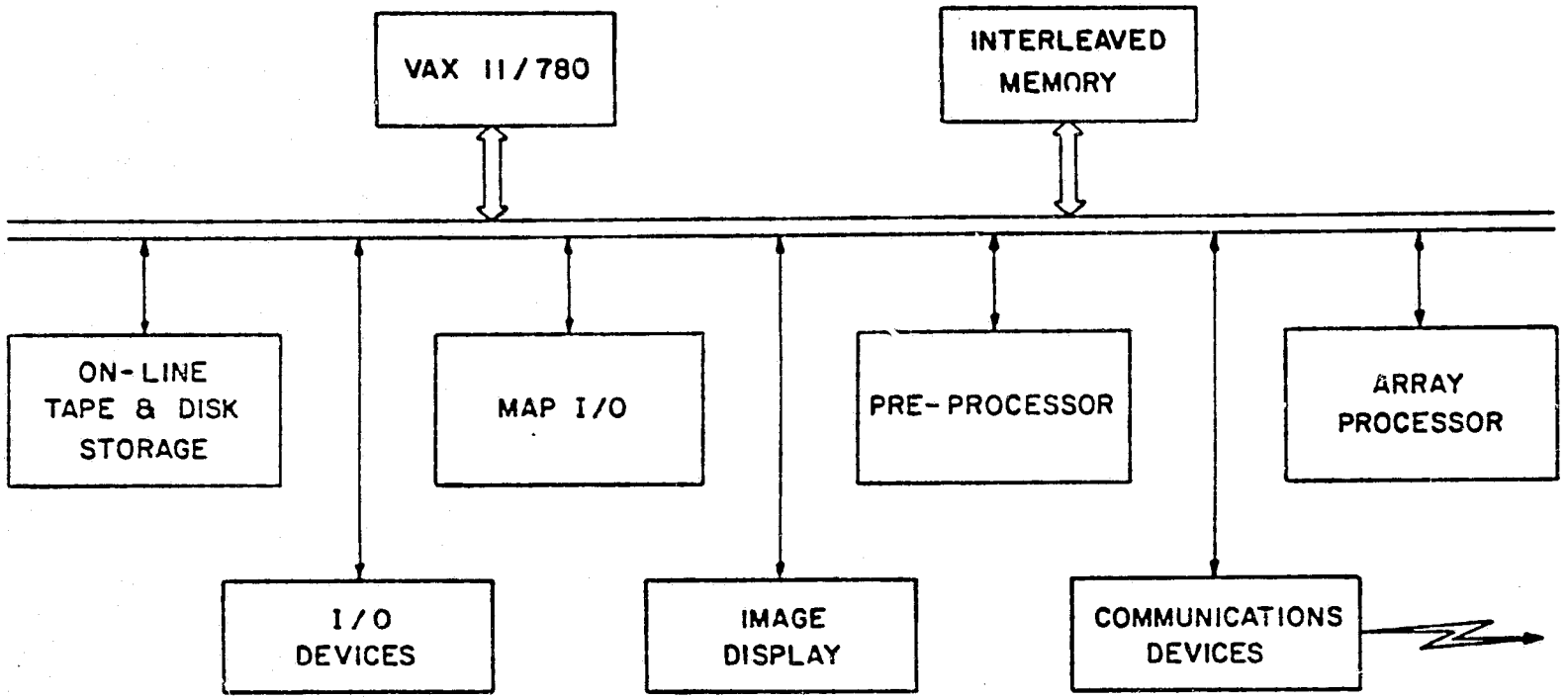

FIGURE 7: LANDSAT DIGITAL IMAGE ANALYSIS SYSTEM

ORIGINAL PAGE IS
OF POOR QUALITY

A PRELIMINARY ASSESSMENT

OF

LANDSAT-4 THEMATIC MAPPER DATA

D.G. Goodenough, E.A. Fleming, K. Dickinson

Department of Energy, Mines and Resources, Canada

ABSTRACT

The results of a preliminary assessment of both raw and NASA-processed Thematic Mapper (TM) data will be discussed.

Geometric correction of NASA-processed TM data has been carried out. Correction was possible to within 3 pixels in the along track direction and 2 pixels in the across track direction

A preliminary evaluation of TM imagery provided by the NASA LANDSAT Assessment System for geometric accuracy and map information content has been carried out on samples of imagery. The initial indications were that bands 3, 5 and 7 contain the most useful cartographic information. The resolution of rural and urban detail as well as the fit to plotted map detail was found to be improved over LANDSAT MSS, and such images may provide adequate revision information for 1:250,000 maps in areas where it is not currently profitable to use LANDSAT MSS.

As part of a study of the radiometric correction of TM data, the relative gains and offsets for each detector in each band of raw data were calculated. This was done for different subscenes as well as a full scene and the variation of the results with direction of scan and position of subscene were studied.

INTRODUCTION

The geometric errors for image to map rectification of one Thematic Mapper (TM) scene of an area near Windsor, Ontario were studied. The scene had been produced on computer compatible tape by NASA and contained radiometric and system corrections for geometric distortions.

The role of the LANDSAT MSS and RBV sensors has been well-established for topographic map revision in Canada. (Fleming, 1981; Moore, 1982) and it is fully anticipated that satellite-derived information for map revision and change detection will form an ever-increasing part of map revision programs of the future. At present resolution levels this information is suited to the revision of 1:250,000 maps and change detection in 1:50,000 maps over approximately 30% of the country. With the increased resolution promised by the Thematic Mapper and eventually SPOT, it is hoped to increase the area of information reliability using satellite sources to between 60% and 100% of the country.

Two images from the Thematic Mapper have been examined for cartographic content. Both images fall within geographic zones that are currently classified as not suitable for the application of satellite techniques for revision purposes, one in the urban-rural area south of Windsor, Canada, and one in the prairie region of Medicine Hat.

The extraction of information relating to ground cover from digital imagery requires that the data be radiometrically as well as accurately geometrically corrected. It is essential to be able to assess the quality of these corrections before the data are analyzed. As a first step, a preliminary study of Thematic Mapper detector response has been carried out. Raw TM scenes of Vancouver Island and the sea off California were used. These scenes were received by the Prince Albert Satellite Station and transcribed to computer compatible tapes at the Canada Centre for Remote Sensing.

OBSERVATIONS

A. GEOMETRIC CORRECTION OF NASA TM DATA

A computer compatible tape was received from NASA-GSFC containing Thematic Mapper data of Windsor-Detroit (WRS track 37, row 34) imaged by LANDSAT-4 on July 20, 1982. The scene had been previously geometrically and radiometrically corrected on the LANDSAT-D Assessment System (LAS) of NASA-GSFC.

Using the CCRS Image Analysis System (CIAS) (Goodenough, 1979), we selected 27 map ground control point (GCP)-image GCP pairs spanning à 1000 by 1000 pixel area of the scene near Windsor. The scale of the map sheets was 1:50,000. GCPs were usually road intersections. An affine transformation of the image to map was derived. The root-mean-square (rms) error in the across-track direction was 32.0 m and in the along-track direction, 40.6 m. We noted a systematic effect; namely, that errors along track were consistently greater than position errors across track.

This NASA product had only geometric corrections for system errors (without GCPs) applied. It was most impressive how good a relative geometric correction had been made with LAS. It is clear that such images of flat terrain can be rectified to have errors less than 41 m. However, multitdate classification requires that these errors be less than 0.5 IFOV or 15 m for Thematic Mapper data if classification accuracy is to be improved with the additional information.

B. CARTOGRAPHIC POTENTIAL OF NASA TM DATA

1. Geometric Accuracy

Band 5 of a scene of the Medicine Hat area, imaged on November 10, 1982 (E40117-17392) was used for this study.

During the revision tests using photographic TM imagery, we found that the fit of the imagery to the map base was much better than when system corrected MSS imagery is used. In an effort to quantify the overall geometry of the Medicine Hat image relative to a U.T.M. map grid, map-based control points were identified on the photograph and their positions measured using a Wild STK-1 stereocomparator.

Thirty control points were selected, and although coordinate position determinations to within 20 m could be made from 1:50,000 maps, larger uncertainties in position result from the fact that the water levels are variable in this region and 21 of the selected points were on water-related features. Although some road intersections were better defined on band 7, band 5 provided the best overall source for control points and all identifications and measurements were made on this band.

The result of the transformation of image coordinates to map coordinates is given in Table 1.

A slight improvement in fit is noted when the affine transformation is used. However, since most people using imagery are scaling to a map using simple enlargement procedures, the residual displacements for the points after a similarity transformation to 5 points (#2 in table) is shown graphically in Figure 1. The area of large displacements in the north-west portion of the image was characteristic of all the transformations.

2. Map Information Content

Two scenes were examined for cartographic content: Band 3 of the Windsor-Detroit scene imaged on July 20, 1982 (track 37, row 34) and bands 1-7 of the Medicine Hat scene described in the previous subsection.

The image quality and cartographic information content of the Windsor area image approached that of a Skylab 190B photograph of the same area. All the road patterns mapped at a scale of 1:250,000 were clearly visible in both the semi-urban and rural areas, railways were not discernible and the land-water interface was not well-defined. Although individual rural buildings were not resolved, the difference between roads having houses or built-up areas and these on which no development had taken place, was quite obvious. Wooded areas were poorly defined.

The total topographic map content of the image with respect to cultural details fell somewhere between that contained on 1:250,000 maps and that contained on 1:50,000 maps. Such images would provide road revision information for both scales and excellent change detection capability for 1:50,000 revision planning.

About 5% of the country has similar cultural patterns to that of the Windsor area, and is a category in which LANDSAT MSS is not currently considered useful for revision purposes. Thus the availability of Thematic Mapper data would increase the boundaries of where satellite data is useful into these urban-rural areas.

The Medicine Hat images supplied in transparency form by NASA were too dense for use on the projection equipment used in revision work and it was necessary to make secondary negatives and positives, increasing by two the number of generations removed from the original image. Interpretations were confirmed by reference to the original images.

It was established that band 3 (0.63-0.69 μm), band 5 (1.55-1.75 μm) and band 7 (2.03-2.35 μm) contained cartographic information. Band 4 (0.76-0.90 μm) which should have provided a good land-water interface was lacking in contrast and did not provide any useful information.

The area covered by this photograph is prairie and rangeland dotted with numerous intermittent lakes and water storage areas. This is a geographic zone in which LANDSAT MSS is not a useful source of revision information. Detailed study of the three potentially best bands of the Thematic Mapper would lead to a similar conclusion for this sensor.

Roads and railroads were best delineated on band 5, but they were fragmentary and did not include all road classes mapped at 1:250,000. Some roads through range-land were clearer in band 7. The airport at Medicine Hat showed most clearly on band 3 but other cultural features showed up poorly. Water details were best rendered on band 5.

The determination of changes to road pattern is probably the primary consideration in evaluating revision sources for 1:250,000 mapping. If this basic requirement is not met from a satellite sensor then it is more advantageous to get all revision information from other sources. In this area of the prairies the cultivation pattern of the fields dominates, over-riding any road pattern. LANDSAT MSS fails as a revision tool for this reason and it would appear that the Thematic Mapper would likewise fail.

C. RADIOMETRIC CORRECTION OF RAW TM DATA

The scene used for this analysis was of the Vancouver Island area, imaged on November 9, 1982 (track 48, frame 26). The solar azimuth and elevation with respect to the frame centre were 158.1° and 22° respectively.

Relative gains and offsets were calculated using the method described by Strome and Vishnubhatla (1973). The calculations were based on the following equations:

$$G_K = \sqrt{\left(\frac{Q_L - P_L^2}{Q_K - P_K^2}\right)} \quad , \quad O_K = P_L - P_K G_K$$

where G_K = Relative gain of detector K

O_K = Offset of detector K

$$P_K = \frac{1}{N_K} \sum_{I=1}^{N_K} I_K(I)$$

$$Q_K = \frac{1}{N_K} \sum_{I=1}^{N_K} [I_K(I)]^2$$

and $G_L = 1$ = Gain of reference detector

$O_L = \emptyset$ = Offset of reference detector

$I_K(I)$ = Intensity of Ith pixel for detector K

N_K = Number of pixels in sample for detector K

Throughout this paper, the G_K's are referred to as relative gains. In actual fact, G_K is the relative gain of detector L relative to detector K (or relative attenuation of detector K relative to detector L). O_K is the offset that must be added to detector K so that its zero level will correspond to detector L. Note that we use the expression in the form calibrated output is a function of uncalibrated input. This is the reverse of NASA representation, so the gains in this paper are the inverse of those in NASA papers.

The relative gains and offsets were calculated for the forward and reverse scan directions separately and detector 16 (forward scan) was used as the reference detector.

First of all, the calculations were performed on the full scene for bands 1,2,3,4,5 and 7. The results for the reverse scan direction were seen to be correlated with those of the forward direction for each band. The forward direction gains were greater than the reverse for the lower numbered detectors but smaller for the higher numbered detectors. The actual cross-over point depended on the band as follows:

- Detectors 1-6, Bands 1-4: Forward Gain > Reverse Gain
  Detectors 7-16, Bands 1-4: Forward Gain < Reverse Gain

- Detectors 1-7, Band 5: Forward Gain > Reverse Gain
  (Detector 3 of Band 5 was dead in this scene and therefore was not included in the analysis)
  Detectors 8-16, Band 5 Forward Gain < Reverse Gain

- Detectors 1-10, Band 7: Forward Gain > Reverse Gain
  Detectors 11-16, Band 7: Forward Gain < Reverse Gain

Figure 2 shows the results for band 4.

The same calculations were performed on subscenes of the image formed by dividing the scene into 11 non-overlapping horizontal swaths, each 500 lines deep. The number of pixels contributing to the calculation of each gain and offset was at least 82,500. An area of bad data was found to extend from line 4913 to 4927. The swath containing these lines was excluded from the analysis. The results were analyzed for bands 1 and 4.

The amount of variation of gain with swath was found to be a factor of typically 2 and 3 times greater than for LANDSAT-1 MSS, as reported by Shlien and Goodenough (1974), allowing for the difference in dynamic range between the TM and MSS sensors. The same algorithm for calculating gains and offsets was used in each case.

The amount of variation in the gain of a given detector over the scene was found to depend on the distance of the detector from its nearest reference detector in the image. As the distance from a reference detector increased, so did the amount of variation in the gain. This is shown in Figure 3 which is a plot of relative gain versus swath start line number for a subset of detectors from band 1.

A convenient way to observe this effect is to plot the range of gain for each detector versus the relative detector position, as shown in Figure 4 for band 1. The range of gain is defined to be the difference between the largest and the

smallest gains obtained from the calculations for the different swaths. The relative detector position is the position of a detector relative to its nearest reference detector in the image. Thus, the relative detector positions of detectors 16 to 1 in the forward scan direction are 0 to 15 when detector 16 is the reference detector. The relative detector positions of detectors 16 to 1 in the reverse scan direction are 16 to 1 because they are closer to the next line imaged by the reference detector rather than the previous one.

The swath size was then halved; i.e. the image was divided into 22 swaths each 250 lines deep. A plot of range of gain versus relative to detector position for band 1 was generated from these results for the forward scan direction. Its shape was similar to the 500 line swath case but the spread of values of the range increased by approximately 40%, indicating considerable sensitivity in the correction algorithm for the scene content in this image.

The scene was also divided into 11 non-overlapping vertical strips, each 500 pixels wide. The number of pixels contributing to the calculation of each gain and offset was at least 85,500. The results of the gain and offset calculations were examined for bands 1 and 4. A tendency of the range of gain to increase with relative detector position was again observed. The mean intensity was also calculated for each detector and each vertical strip. The variation of mean intensity across the image was similar for each detector: a typical example is shown in Figure 5.

A comparison was made between this method for calculating gains and offsets and that used by J. Murphy (1983). The gains calculated for the same TM data were closely correlated, although those calculated by the present method tended to be shifted to higher values. It should be noted that it was necessary to invert one set of gains before the comparison could be made.

Some of the above analysis was repeated on another scene of TM data. The second scene was of California (track 42, frame 36), and had much less intensity variation than the Vancouver Island scene. The gains were calculated over the full scene for bands 1-5 and 7. The forward and reverse scan direction results showed strong correlation for each band. The forward direction gains were smaller than the reverse for all detectors; i.e.

- Detectors 1-16, Bands 1-5,7: Forward Gain < Reverse Gain

Figure 6 shows the results for band 4. Detector 10 can be seen to have significantly lower gain than the other detectors in both scenes. The dependence of the amount of variation in the gain on the distance to the nearest reference detector was not observed in this second scene. This implies that the observed variation is a scene-dependent effect.

CONCLUDING REMARKS

The geometric properties of TM photographic imagery permitted very good fitting to map detail using simple scaling techniques to localized areas and, using simple scaling, the overall geometry remained within 500 metres or 0.4 mm at the image scale of 1:1,141,600. An affine transformation, permitting differential scaling, slightly improves the fit to about 400 metres or 0.35 mm at image scale.

The imagery shows promise of having the needed additional resolution and spectral discrimination to provide map revision information in urban-rural areas where the MSS sensor is now considered inadequate. The late-season prairie image, however, did not hold such promise, and judgement must be reserved until images are acquired at other seasons in this particular geographic area.

The relative gains and offsets of TM detectors calculated over two full scenes of raw data showed correlations between the forward and reverse scan directions. It was noted that for the bands studied in one scene (bands 1-5 and 7), the forward gain was always greater than the corresponding reverse gain for detectors 1 to 6 but always less than the corresponding reverse gain for detectors 11 to 16. In a second scene studied, the forward and reverse scan direction gains again showed correlation. In this case, the forward gain was less than the corresponding reverse gain for all detectors.

The amount of variation of gain over the Vancouver Island scene was found to be larger than that for LANDSAT-1 MSS by a factor of 2 to 3, allowing for the difference in dynamic range.

The amount of variation in the gain of a given detector over the scene was found to depend on its distance from the nearest reference detector in the image. However, this effect was not observed in a second scene; one which contained considerably less intensity variation. The relative radiometric correction algorithm may be inadequate for TM scenes with large intensity variations across them.

Future work in this area includes the study of the variation in detector response with time over many scenes. The approach described in this paper must be tested by using the relative gains and offsets to radiometrically correct the data and then re-analyzing the corrected scenes. In addition, the absolute calibration of TM detectors will be studied.

REFERENCES

Fleming, E.A., "Monitoring revision requirements for Canadian maps". Proceedings of the 7th Canadian Symposium on Remote Sensing, Winnipeg, 1981.

Goodenough, D.G., "The Image Analysis System (CIAS) at the Canada Centre for Remote Sensing," Canadian Journal of Remote Sensing, 5, 3-17, 1979.

Moore, H.D., "LANDSAT increases efficiency of topographic map revision". CIS Proceedings, Centennial Convention Vol. 2, Ottawa, Canada, April 1982.

Murphy, J., W. Park and G. Fitzgerald, "Preliminary evaluation of radiometric calibration of LANDSAT-4 Thematic Mapper data by the Canada Centre for Remote Sensing". Proceedings of the LIDQA Symposium, February 22-24, 1983.

Shlien, S. and D.G. Goodenough, "Quantitative methods of processing the information content of ERTS imagery for terrain classification". Proceedings of the 2nd Canadian Symposium on Remote Sensing, Guelph, 1974.

Strome, M. and S. Vishnubhatla, "A system for improving the radiometric corrections for ERTS-1 MSS data". Proceedings, XXIV International Astronautical Congress, Baku, USSR, 1973.

TABLES

FIGURES

TABLE 1

RESIDUAL DISPLACEMENTS FROM UTM CONTROL IN TM IMAGE E40117-17392(5)

(1:1,141,600)

TRANSFORMATION	No. of Points USED	No. of Points CHECK	RMS (X) M	RMS (Y) M	RMS (XY) M
1. Similarity	27		422	324	532
2. Similarity	5		394	308	501
		22	430	327	540
3. Affine	27		318	206	379
4. Affine	5		212	36	216
		22	352	256	436

RESIDUAL DISPLACEMENTS AT CHECK POINTS AFTER A SIMILARITY TRANSFORMATION TO UTM CONTROL

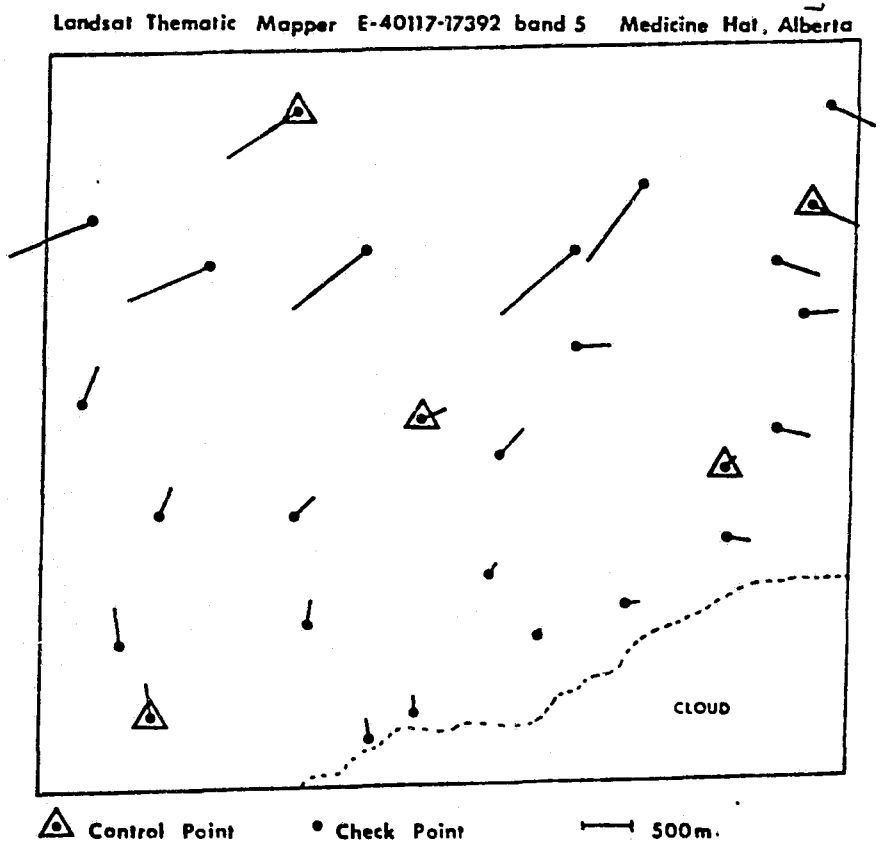

Figure 1

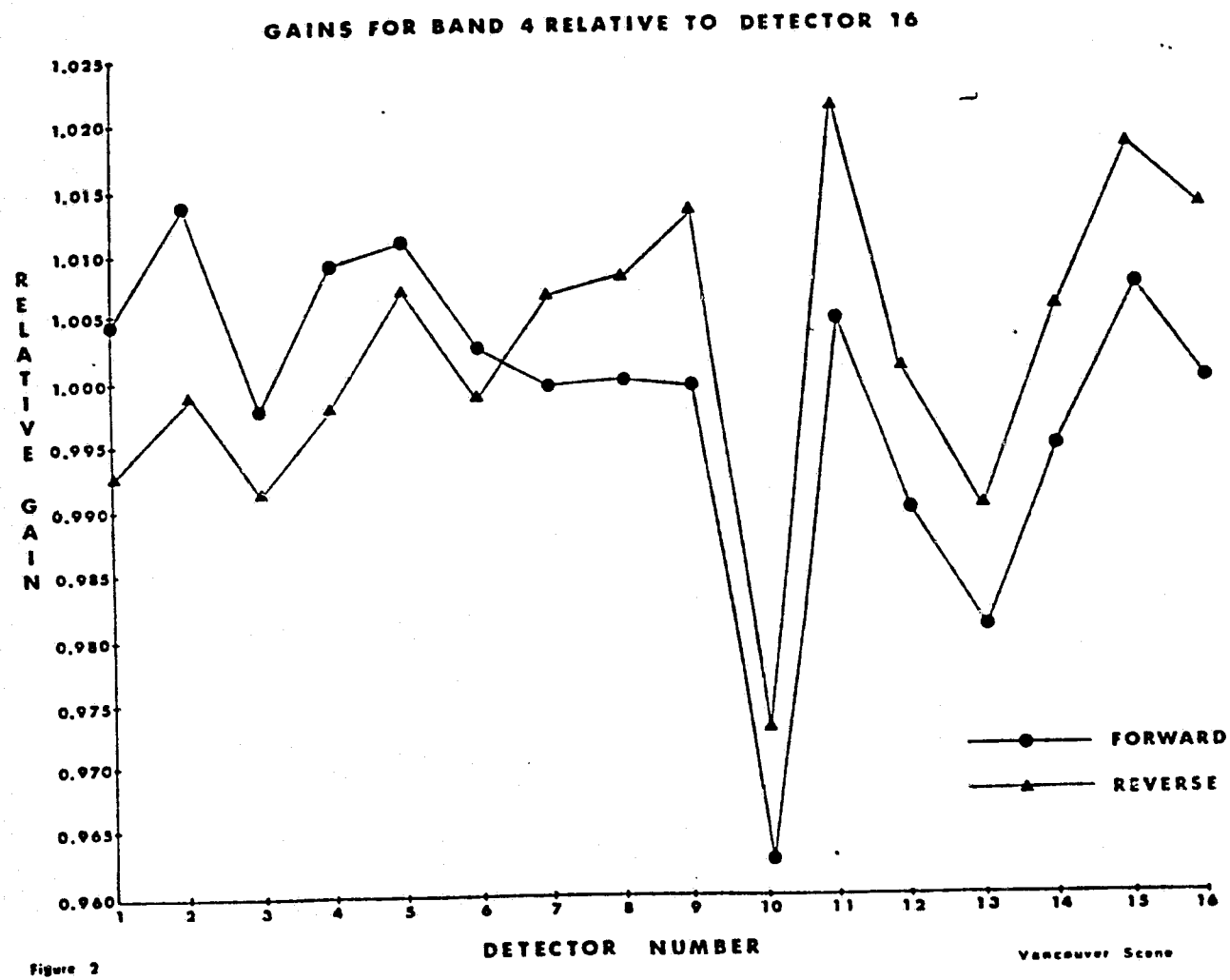

Figure 2

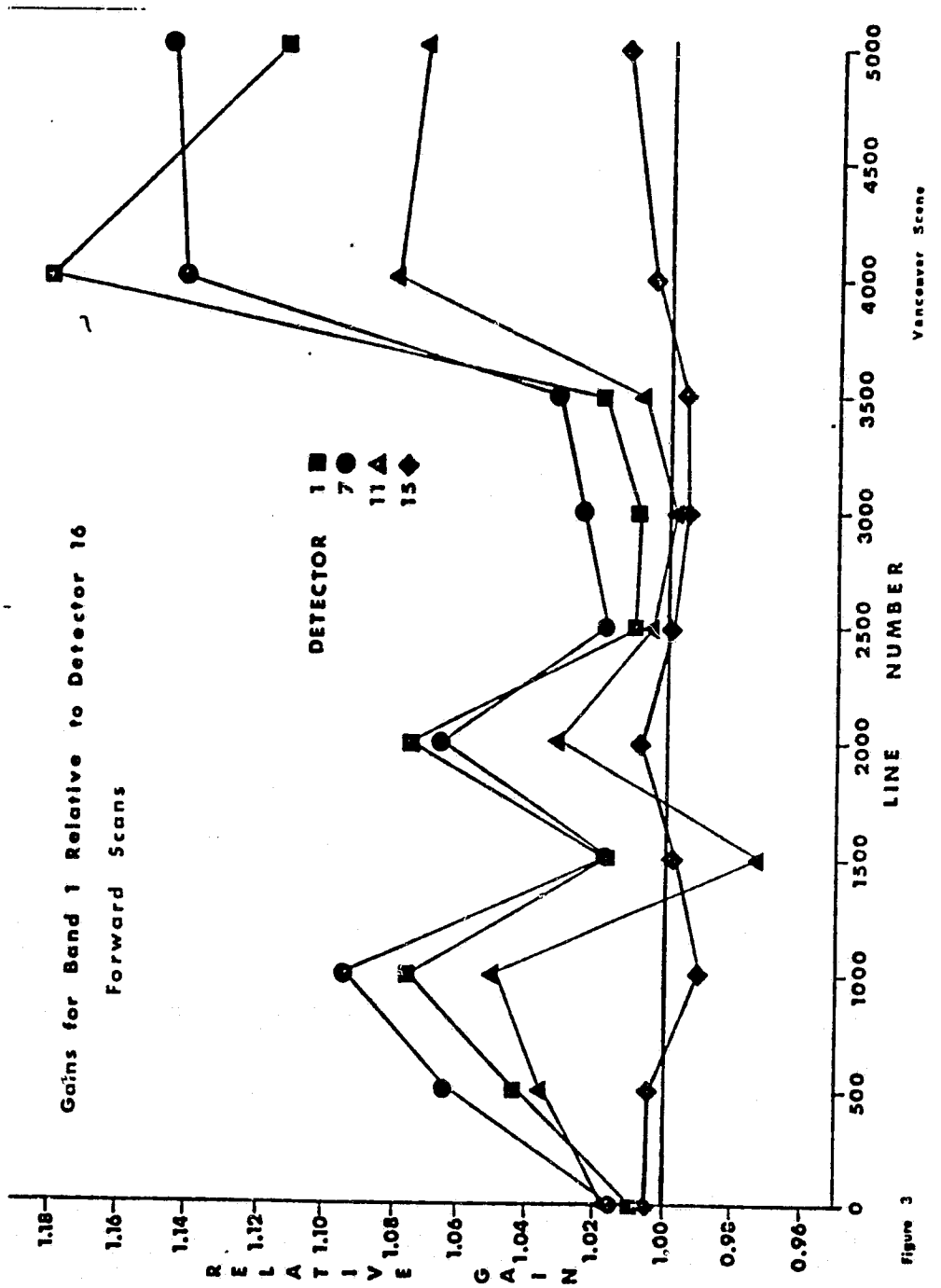

Figure 3

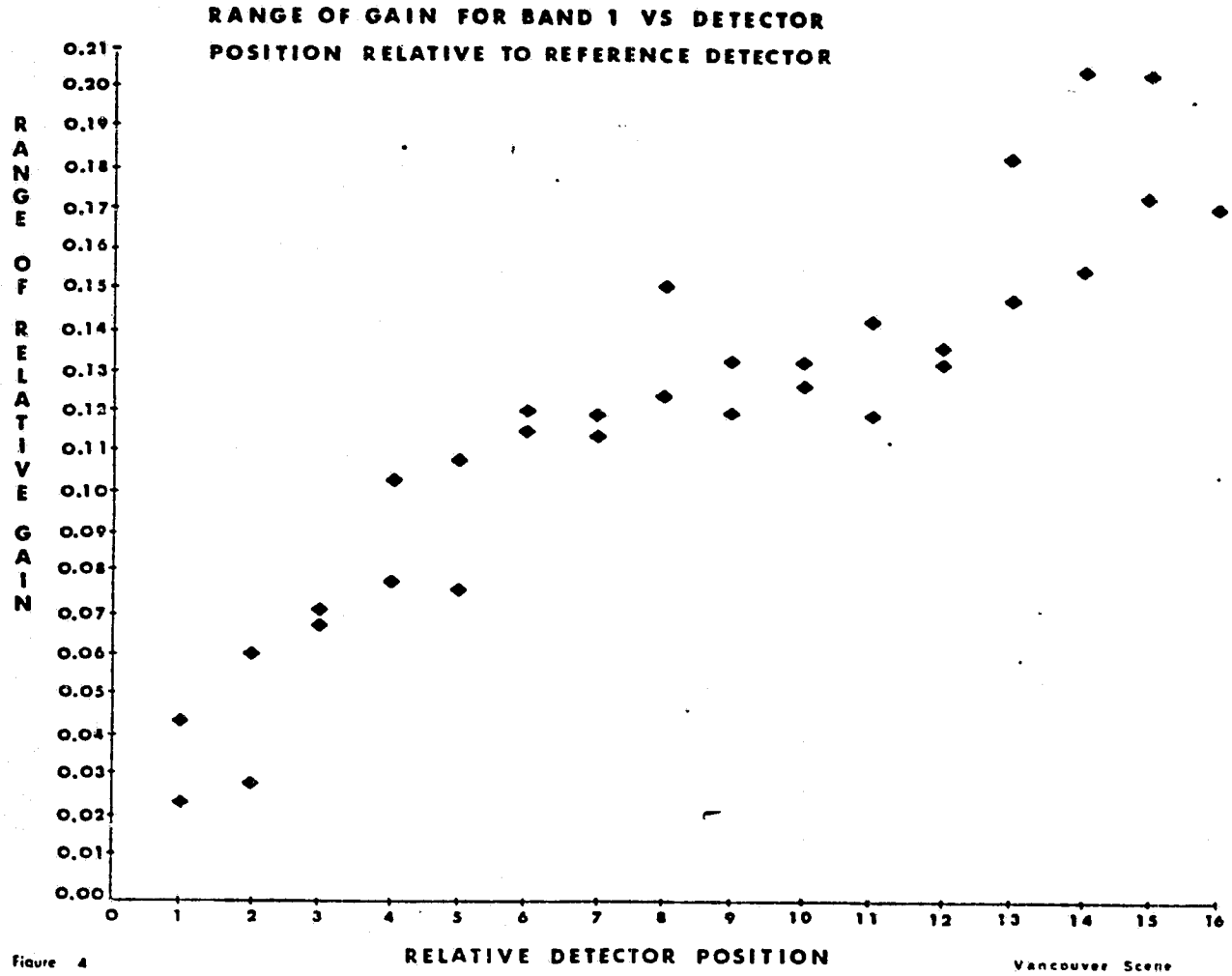

Figure 4

Vancouver Scene

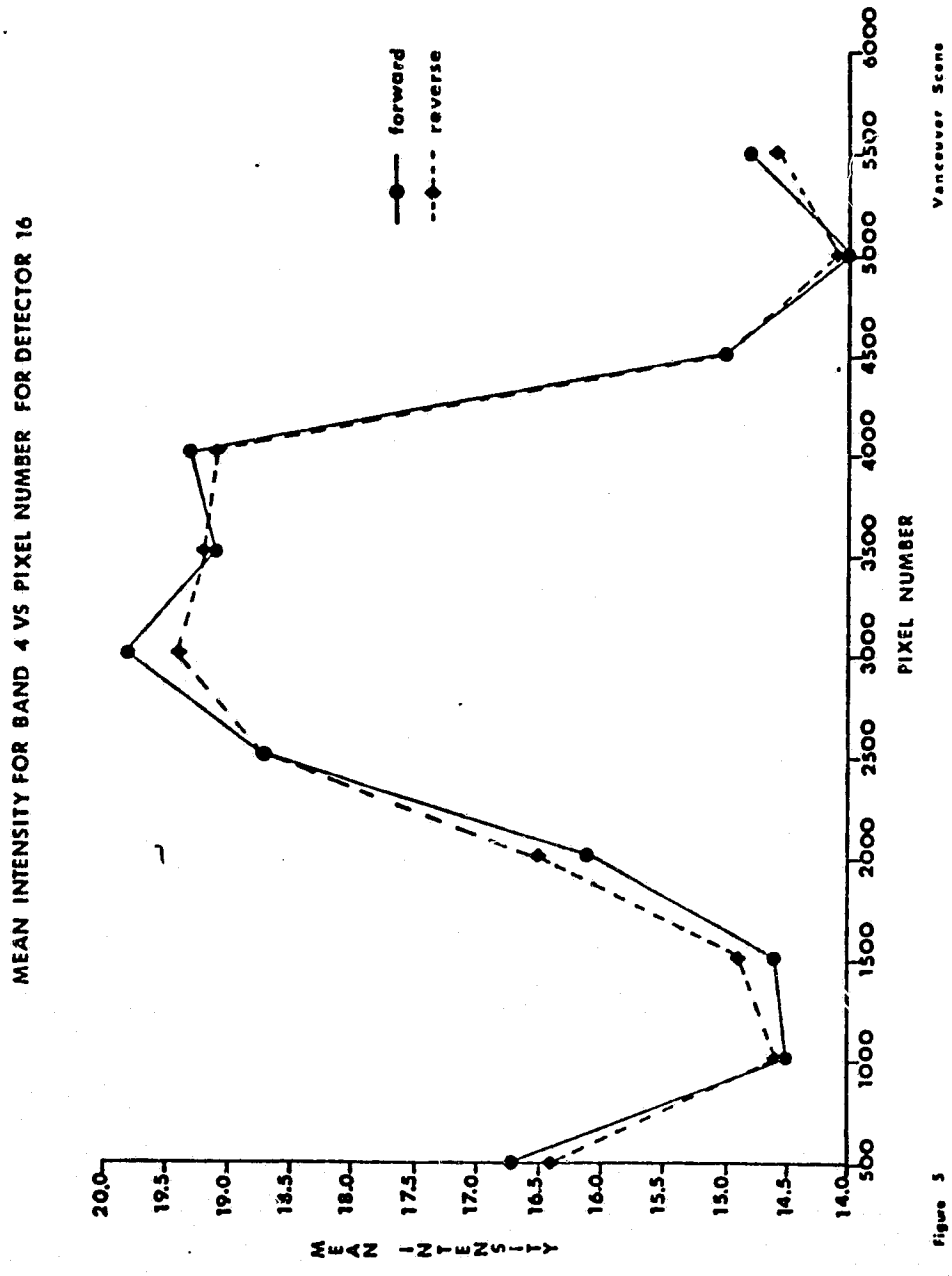

Figure 5

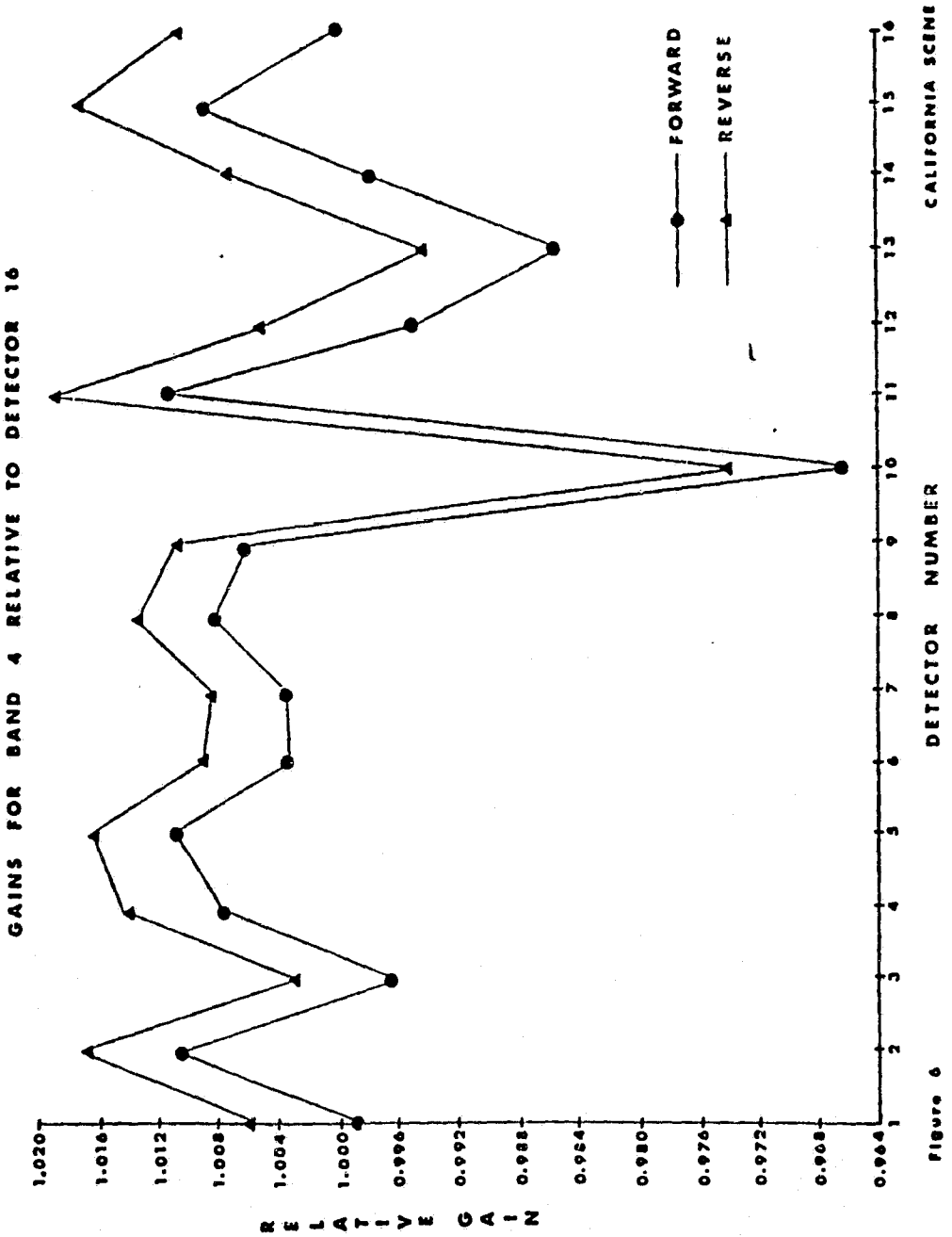

Figure 6

RADIOMETRIC CALIBRATION AND GEOCODED PRECISION PROCESSING OF LANDSAT 4 MULTISPECTRAL SCANNER PRODUCTS BY THE CANADA CENTRE FOR REMOTE SENSING

AUTHORS: J. Murphy, D. Bennett, F. Guertin

PRESENTED BY: Jennifer Murphy

Canada Centre for Remote Sensing
2464 Sheffield Road
Ottawa, Ontario
Canada

ABSTRACT

The method used by the Canada Centre for Remote Sensing (CCRS) for the radiometric calibration of LANDSAT-4 Multispectral Scanner (MSS) data is reviewed, with reference to the methodology used by the Centre for LANDSAT-1, 2 and 3 MSS data. Inherent in this technique is the possibility for the user to convert the corrected digital values to the absolute scene radiance of the target under observation. The generation of the constants needed for this final conversion requires both the pre-launch and post-launch radiometric calibration constants as supplied by NASA. Results of some preliminary comparative studies of the radiometric properties of the LANDSAT-4 MSS versus earlier satellites in the LANDSAT series are presented. In addition, early observations on the stability of the calibration data, firstly, within one scene, secondly, within one orbit, and thirdly, over a period of several months, are presented. Estimates of residual striping in the corrected products are also presented.

The method used by CCRS, to perform precision processing of LANDSAT MSS data for generating geocoded or map compatible LANDSAT MSS products in the Universal Transverse Mercator projection, is reviewed. LANDSAT-4 MSS precision processed products are evaluated for geodetic accuracy, and are compared to similar products from the previous LANDSAT satellites to assess the orbit independent registration accuracy.

1.0 CCRS RADIOMETRIC CORRECTION METHOD

The radiometric correction process used by CCRS, as described by Ahern and Murphy (1978), may be divided into three stages.

a) a reference detector is chosen for each spectral band, and the corrections required to place the data from this detector on an absolute scale are calculated using the calibration wedge data, pre-launch calibration data and the maximum and minimum radiance values associated with the response of the band.

b) the relative differences between all other detectors in each band and the reference detector are calculated, using the means and standard deviations of the decompressed raw data values as calculated from the sums and the sums of the squares of the scene data values. (Excluded from the scene statistics are those pixels which cause any one detector to saturate, such that only that portion of the curve for which the response of all detectors within the band is essentially linear is used.)

c) finally, the absolute calibration of the reference detector is combined with the relative calibration of the other five detectors within the band, to provide an absolute calibration of all six detectors in each of the four bands.

Inherent in the technique is the assumption that the response of each detector is linear, that is, the voltage output varies in a linear fashion with the radiance input. Hence the calibration process may be represented by the equation:

$$V' = (V - a) / b \qquad (1)$$

where V' is the calibrated digital value, (0-255)
V is the uncalibrated decompressed digital value, (0-255)
b is the gain,
and a is the offset.

1.1 USE OF THE CALIBRATION WEDGE

Each calibration wedge for the selected reference detector is sampled at the six predefined locations, and the histogram for each of the six samples is accumulated over the entire scene. Since one full scene contains 186 complete calibration wedges for each detector, the histogram is first used to isolate any outliers. This is

accomplished by generating a smoothed histogram, where each of the histogram bins contains a count of all sample values falling within a window which is five digital values wide. The mean value is then calculated using only those samples which contribute to the smoothed histogram bin with the largest count.

The stability of the calibration wedge, and the choice of a reference detector for each band, are discussed further in Section 3.

The values of a and b in equation (1) are calculated using the formulae:

$$a = \sum_{i=1}^{6} C_i'' * V_i \qquad (2)$$

$$b = \sum_{i=1}^{6} D_i'' * V_i \qquad (3)$$

where the V_i's are the mean decompressed samples of the calibration wedge at the six locations.

NASA (Reference 1) supplied, before the launch of LANDSAT-4, tables for C_i' and D_i' in a band normalized form, and exemplified their generation and use (NASA, Reference 2). The pre-launch maximum and minimum radiance values to which the pre-launch C_i' and D_i' apply are shown, for each band, in Table 1.1 as RMAX and RMIN respectively.

However, the maximum radiance values for bands 1 and 3 were modified by NASA (Reference 3) using post-launch observations, and these are shown as RMAX' in Table 1.1. In order to obviate the necessity of changing the C_i' and D_i', multiplicative (M) and additive (A) modifiers to be used in the modified detector response equation (4) were supplied.

$$V' = (V - a)/M*b - A \qquad (4)$$

However, these modifiers include the effects of relative detector differences within the band, a process which is treated by CCRS completely independently from the absolute calibration. The C_i' and D_i' were therefore used in combination with the maximum and minimum radiance to give band normalized C_i'' and D_i'' appropriate to the revised RMAX'.

$$C_i' = C_i + RMIN * D_i \quad (5)$$

$$D_i' = (RMAX - RMIN) * D_i \quad (6)$$

From (6), $D_i = D_i'/(RMAX - RMIN)$ (7)

From (5) and (7), $C_i = C_i' - RMIN*(D_i'/(RMAX - RMIN))$ (8)

For RMAX' and RMIN'

$$C_i" = C_i + RMIN' * D_i \quad (9)$$

$$C_i" = C_i + RMIN' * D_i'/(RMAX - RMIN) \quad (9')$$

$$D_i" = (RMAX' - RMIN') * D_i \quad (10)$$

From (7), $D_i" = (RMAX' - RMIN') * D_i'/(RMAX - RMIN)$ (11)
From (8) and (9'),

$$Ci" = C_i - (RMIN - RMIN') * D_i'/(RMAX - RMIN) \quad (12)$$

The $C_i"$ and $D_i"$ used by CCRS are shown in Table 1.4. For changes in maximum and minimum radiance values shown in Table 1.1, the Ci" and Di" are related to Ci' and Di' in the following way:

Bands 2 and 4 - No Change
Bands 1 and 3 - Ci" = Ci'
Band 1 - Di" = 0.919355*Di'
Band 3 - Di" = 0.863014*Di'

In addition to supplying products calibrated using the values of RMAX' and RMIN' as discussed above, which CCRS terms the "CAL2" option, an alternative calibration, termed the "CAL3" option, can be supplied by CCRS, where the maximum and minimum radiance values are shown as RMAX" and RMIN" in Table 1.1.

The "CAL3" absolute gains and offsets are calculated from the "CAL2" absolute gains and offsets using the expressions:

a' = a - 255 * (RMIN'-RMIN")/(RMAX'-RMIN') (13)
b' = b * (RMAX"-RMIN")/(RMAX'-RMIN') (14)

where a' and b' are the "CAL3" absolute offset and gain corresponding to the equivalent "CAL2" absolute offset and gain, a and b.

1.2 RELATIVE CALIBRATION

The relative correction of the individual detectors within each band is performed using information from the scene being viewed by the MSS, and this method has the advantage of using a calibration source with the spectrum of the scene rather than the very much redder spectrum of the calibration lamp. It has been shown (Strome et al., 1975) that the gain of one detector relative to the gain of the reference detector is equal to the ratio of the standard deviations of the data acquired with these detectors. Similarly, the difference in zero offset is equal to the difference between the mean of the data values acquired with one detector and the mean of the data values acquired with the reference detector. The mean and standard deviation can be calculated from the sum and the sum of the squares of the scene data values, which in turn, are calculated from the decompressed histogram of the raw data values. In order to ensure that the histograms correspond only to pixels with radiance values for which the response of each detector is linear, all those pixels which saturate any one detector within a band are removed from the histograms of EACH detector within that band. This process is performed for each band independently. This technique was shown by Murphy (1981) to reduce residual striping in scenes with very bright snow and clouds.

1.3 CREATION OF LOOK-UP TABLES

After combining the relative gains and offsets with the absolute gains and offsets of the reference detectors, a radiometric look-up table is created for each detector i by means of the equation:

$$L_i(N) = (1/b_i) * (V_i(N) - a_i) \qquad (15)$$

where L_i is the look-up table entry for each of the 64 possible data values N recorded by detector i; $V_i(N)$ is the decompressed data value corresponding to the compressed data value N; a_i and b_i are the absolute offset and gain of detector i. The decompression tables, obtained from those supplied by NASA (Reference 1) by expanding to a range of 0 to 255, are shown in Table 1.3.

1.4 CONVERSION OF DIGITAL VALUES TO SCENE RADIANCE

The scene radiance, R', (in watts/m^2sr) in each band can be calculated from the corrected linear digital value V', by means of the expression:

$$R' = A0 + V' * A1 \qquad (16)$$

where A0 and A1 for the CAL2 and CAL3 options are shown in Table 1.2.

1.5 TEST SCENES

A variety of test scenes was chosen, spanning the time period from late August 1982 to late January 1983, and each scene is identified in Table 1.5. The scenes were used for monitoring the calibration wedge, for studying the residual striping and for comparisons of LANDSAT-3 and LANDSAT-4 MSS data, as discussed in Sections 3, 4 and 5 respectively.

2.0 ABSOLUTE CALIBRATION OF TEST SCENE

The method outlined in Section 1 was used to calibrate a test scene recorded on December 9, 1982. First, however, the calwedge data was used for all six detectors in each band, and an absolute calibration for each was calculated as shown graphically in Figures 2.1 to 2.4 for bands 1 to 4 respectively. (Information obtained from these graphs was used in the choice of reference detectors, as described in Section 3.) The CAL3 gains and offsets are tabulated in Table 2.2.

Histograms for all six detectors in each band were accumulated, and are shown in Figures 2.5 to 2.8 for bands 1 to 4 respectively. From these were calculated the relative gains and offsets, shown in Table 2.1.

4.0 RESIDUAL RADIOMETRIC STRIPING

A simple method to assess the radiometric striping in MSS images consists of selecting arbitrary subscenes, and for each band plotting as a function of the line number the radiometric intensity values averaged over a fixed number of pixels. In such profiles the residual striping appears as a repetitive pattern with a period of six lines which is added to the scene content. Because the scene data is averaged over a number of pixels, for example 100 pixels, variations from line to line due to scene content tend to be small and gradual, particularly over uniform areas such as large water bodies. A detailed discussion and evaluation of this striping assessment method is given by Murphy (1981).

Figures 4.1 and 4.2 show the striping profiles for two subscenes extracted from a LANDSAT-4 MSS scene acquired on August 28, 1983, (path 17, row 30). All the data is presented on a 256 digital counts scale. Figure 4.1 illustrates the striping before and after radiometric calibration for all four bands over a 60-line by 100-pixel subscene in Lake Ontario. For example in band 1, the striping in the uncorrected data is more than four digital levels (peak to peak) while after radiometric calibration it has been reduced to less than one level. The other profiles for calibrated data show residual striping less than two levels. It should be noted that in this subscene, the uncalibrated data presented very little striping in bands 3 and 4. Figure 4.2 contains the corresponding profiles for a subscene acquired over land. Except for the scene information content, the profiles exhibit similar striping characteristics.

5.0 COMPARISON OF LANDSAT-3 AND LANDSAT-4 DATA

Because LANDSAT-3 and LANDSAT-4 have 18-day and 16-day coverage cycles respectively, it is possible to acquire MSS data from two overlapping passes recorded within a few minutes of each other. For example, LANDSAT-3 path 19 and LANDSAT-4 path 18 show considerable overlap over Canada and MSS data were acquired from these two paths by the Prince Albert Station on December 9, 1982. Similarly, data was recorded from LANDSAT-3 path 43 and LANDSAT-4 path 40 on January 20, 1983. With such passes, it is possible to compare LANDSAT-4 MSS to LANDSAT-3 MSS data under identical atmospheric and scene content conditions.

So far the evaluation has been limited to LANDSAT-3 path 19 row 23 and LANDSAT-4 path 18 row 23. It consisted of comparing the raw data histograms for the full scenes. In each of the four bands the histograms have the same general shapes and show less than 1.5 digital level differences in their mean values.

Taking into account the offset between the orbits and the fact that the width of the LANDSAT-3 image is limited to 135 kilometres the overlap between these two images is reduced to 75 kilometres. A more detailed analysis will consist of comparing the histograms for only the portion of the scene which is present in both images.

6.0 MSS GEOMETRIC CORRECTION

For LANDSAT-1, 2, 3 and 4 MSS data CCRS is offering two types of geometric corrections: a priori system corrected products and precision processed geocoded products. The geocoded products are generated on the Digital Image Correction System (DICS) which first went into production in 1979 for LANDSAT-1, 2 and 3 MSS data and was upgraded in 1982 in order to process LANDSAT-4 MSS data. This section discusses the characteristics of the geocoded products and presents the geometric correction model used in DICS.

Section 7 contains results on the geodetic accuracy of geocoded products using LANDSAT-4 MSS data.

6.1 GEOCODED PRODUCTS DEFINITION

Geocoded products consist of remote sensing imagery which has been transformed to a cartographic projection, such as the Universal Transverse Mercator (UTM) projection, and is largely independent of the sensor characteristics and the orbital parameters of the platform. The imagery is corrected to a subpixel accuracy both in multitemporal registration and in absolute geodetic control (as represented by topographic maps). The products are offered in a subscene format derived from the quadrangle division system used for maps. Irrespective of the sensor scan line orientation the processed image lines are aligned to the projection grid, and the pixel spacing meshes conveniently with the grid itself.

Each MSS geocoded product offered by CCRS corresponds to four maps (2x2 sheets) at 1:50,000 scale, that is a 0.5^{o} Latitude by 1.0^{o} Longitude quadrangle in the National Topographic System (NTS) or roughly an area of 60 x 80 kilometres for southern Canada. The actual dimensions of each geocoded product are functions of the quadrangle latitude and quadrangle position within the UTM zone and are defined in terms of the smallest rectangle falling on a one-kilometre grid unit and encompassing an entire NTS 0.5^{o} x 1.0^{o} quadrangle. Except at the centre of a UTM zone, adjacent products present a one or two-kilometre common strip due to the fact that NTS quadrangles are non rectangular. Each product contains a 4-band MSS subscene in the UTM projection where each line of image data is parallel to the Easting direction of the UTM metric grid. The imagery data is resampled to a 50x50-metre grid registered on the one-kilometre UTM grid.

Because the pixel grid is congruent to the UTM grid and the geocoded product dimensions are defined by the NTS quadrangles, geocoded MSS products from LANDSAT-1, 2, 3 and 4 are always in registration and can be superimposed directly; for example, pixel (i,j) in a LANDSAT-4 product covers the same 50x50-metre area as pixel (i,j) from one of the earlier satellites.

This is particularly important given the fact that compared to the earlier missions, LANDSAT-4 follows a different swathing pattern due to a lower orbit.

Figure 6.1 shows as a shaded area a common geocoded product which is extracted from LANDSAT-3 path 17, row 28 and from LANDSAT-4 path 16, row 28. If a particular LANDSAT orbit does not cover completely a given geocoded product in the across track direction, the uncovered portion will contain zero-intensity pixels. There is no attempt to mosaic the data from adjacent orbits on DICS. More information on the definition of geocoded products can be found in Guertin (1981).

6.2 MSS GEOMETRIC CORRECTION MODEL

The geometric correction model implemented on DICS uses Ground Control Points (GCP) measured on maps or extracted from reference image chips and requires only a minimum of ancillary information from the satellite, namely, the time code and the swath length code. It does not model the position and attitude of the platform and represents the geometric correction to be applied as a sequence of three transformations, Figure 6.2.

A product transformation translates the Northing and Easting of any GCP location (N,E) measured on the map into (U,V), the corresponding pixel location in the geocoded product. The product transformation is an affine completely defined by the origin of the product coordinates and the product pixel size. Two bivariate correction functions map (U,V) the corrected pixel location into (X,Y) the systematically corrected pixel location. This second transformation is based on a two-dimensional least-squares estimation process using the GCP information. The GCPs can be measured manually by an operator or by digital correlation. Manual GCPs are digitized on maps at 1:50,000 scale or at 1:250,000 for the northern regions of Canada where larger scale map coverage is not complete. GCPs are located in the MSS imagery by magnifying the image up to 16 times using either a simple pixel repeat or a damped sinc function interpolator and by contrast stretching the radiometric values of the data in order to enhance the features of interest.

The third transformation is an a priori along scan correction which maps (X,Y) into (P,L) the uncorrected pixel and line numbers. It corrects for earth rotation, sensor delay (inter and fractional intra band offsets), swath length variation, mirror velocity variation, panoramic error and earth curvature. These corrections are based on the following information. The earth rotation correction is derived from the nominal orbital parameters of the satellite. The band and detector offsets are known from the pre-launch data. The swath length variations are obtained from the telemetry. The mirror velocity, panoramic error and earth curvature are treated as a single error which is derived experimentally for each satellite by measuring from a LANDSAT scene some 100 to 200 GCPs evenly distributed along the scan lines, following the technique developed by Shlien (1979). For all LANDSAT satellites the mirror profiles have been extracted using prairie scenes containing a regular road network and very little elevation changes.

Having removed most of the along scan systematic errors through the third transformation the least-squares fit is correcting primarily for position and attitude errors, for mapping, aligning and rescaling the imagery to the UTM grid and for any residual errors in the a priori model. Experiments conducted using the MSS imagery from earlier satellites have demonstrated that an absolute geodetic accuracy of 50 metres RMS or better can be achieved consistently over an entire LANDSAT frame using least-squares fit second-order polynomials based on 25 to 35

GCPs. The large number of GCPs contributes to the reduction of the errors associated with the maps, which is estimated at 15 to 30 metres RMS for 1:50,000 scale maps. It has been shown by Fleming (1980) that the overall absolute residual geodetic error can be reduced to 30 metres RMS by replacing in the model the map GCPs with higher accuracy geodetic control from aerial photographs.

7.0 GEOMETRIC ACCURACY OF LANDSAT-4 MSS PRODUCTS

During the past four years, MSS data from the first three LANDSAT missions have been corrected to a 50-metre accuracy. In order to assess the absolute geodetic accuracy of LANDSAT-4 MSS imagery corrected on DICS two studies were conducted: residual errors on GCPs used in the transformation were compared, and independent test GCPs were measured in LANDSAT-4 products.

While the same geometric correction model is applicable to all four satellites, mission specific parameters are required for the along scan correction transformation. In particular, compared to the earlier MSS data, the LANDSAT-4 MSS swath length corrections are more important. Not taking into account the anomaly that had developed on LANDSAT-3, earlier MSS data had swath length differences of only one pixel. They were due primarily to the fact that the MSS mirror active scan and the sensor sampling sequences are not synchronized. For LANDSAT-4 swath length variations as large as eight pixels have been observed on adjacent swaths. For example, Table 7.1 shows a case where the swath length varies on a swath to swath basis in the range of zero to seven pixels. Examples have also been found where the range was only two pixels. This suggests variations in the mirror active scan period for consecutive scans. On DICS, the swath length variations are corrected linearly across the entire scan such that all swaths have the same number of pixels.

After having measured the GCPs and having derived the least-squares fit transformation the accuracy of the transformation can be assessed by the residual errors between the measured GCP locations and the computed locations. Knowing the characteristics of the geometric distortions and the validity of the second-order polynomial fit this can serve as an indication of the image accuracy. Figure 7.1 shows as vectors the residual errors for 34 GCPs measured over an entire LANDSAT-4 scene (Ottawa, path 16, row 28, cycle 5). The largest along scan and across scan errors are 1.00 pixel and 0.57 line respectively. The residual error for the 34 GCPs is 39.7 metres RMS (The RMS error is assuming 28 degrees of freedom for the case of 34 observations).

Table 7.2 compares the GCP residual errors for LANDSAT-4 and for the earlier three satellites. For five LANDSAT-4 MSS scenes it shows the RMS errors for similar scenes obtained from the earlier LANDSAT satellites. The earlier scenes have been selected to cover approximately the same regions as LANDSAT-4 in order to minimize effects due to map accuracy, relief distortions and image content. The acquisition dates have not been taken into account. For the earlier LANDSATs, the RMS error averaged over 15 scenes is 35.1 metres with a standard deviation of 5.7 metres compared to 38.3 metres with a standard deviation of 3.0 metres for LANDSAT-4. While the earlier LANDSAT images extracted from the archive had been corrected over a period of three years, differences in the operational procedures could have contributed to the larger standard deviation. For each of the LANDSAT-4 images "LL" indicates the swath length variations observed in the image. Taking into account the small number of scenes it can be stated that using the same correction model LANDSAT-4 MSS can be corrected to about the same accuracy as the earlier satellites and that swath length variations do not contribute significantly to the product errors.

In the second evaluation of product accuracy, a LANDSAT-4 image was corrected based on 34 well-distributed GCPs, and 14 new GCPs from a different set were measured in a single geocoded product extracted from that image. The selected geocoded product covers NTS maps 31G3, 31G4, 31G5 and 31G6 which include Ottawa in the top left quadrant. The product is located in the bottom right corner of path 16 row 28 and the top right corner of path 16 row 29. In such cases the geometric correction model is estimated for a full LANDSAT scene consisting of the bottom half of the first frame (row 28) and the top half of the second frame (row 29). Table 7.3 shows the Northing and Easting errors for the test GCPs, and their means and standard deviations. Based on the 14 GCPs the absolute geodetic error for the entire geocoded product is estimated at 48.1 metres RMS. The RMS error on the 34 original GCPs is 39.7 metres. Since geometric correction models based on bivariate second order polynomials show larger distortions at the edges, it would be necessary to measure the residual errors over each geocoded product from the same input image in order to assess further the absolute geodetic accuracy.

8.0 CONCLUSION

This early report has described the methodology used by CCRS to perform radiometric calibration and precision geometric correction of standard LANDSAT-4 MSS products. It has shown how the same algorithms are used to radiometrically correct and to place on a calibrated radiance scale the data from all four LANDSAT satellites. To assess the reliability of absolute calibration, the report has discussed the minor variations observed in the LANDSAT-4 calibration data and has proposed the comparison of overlapping LANDSAT-3 and LANDSAT-4 scenes acquired at the same time.

After reviewing the concept of geocoded products, this document has shown that the geometric correction model developed to precision process the MSS data from the earlier LANDSAT satellites can generate LANDSAT-4 MSS geocoded products with comparable geodetic accuracy.

The results presented here are seen as preliminary and are expected to be refined and augmented as more LANDSAT-4 data are acquired and processed by CCRS production facilities over a longer period.

9.0 REFERENCES

Ahern F., Murphy, J. (1978) Radiometric Calibration and Correction of LANDSAT 1, 2 and 3 MSS Data, CCRS Research Report 78-4, November 1978.

Fleming, E.A., Guertin, F.E. (1980) Determination of the Geographical Position of Isolated Islands using the Digital Image Correction System for LANDSAT MSS Imagery, 14th Congress of the International Society for Photogrammetry, Hamburg.

Guertin, F.E., Shaw, E. (1981) Definition and Potential of Geocoded Satellite Imagery Products, 7th Canadian Symposium on Remote Sensing, Winnipeg, pp. 384-394.

Murphy, J. (1981) A Refined Destriping Procedure for LANDSAT MSS Data Products, 7th Canadian Symposium on Remote Sensing, Winnipeg, pp. 454-470.

NASA Ref. 1 (1982) LANDSAT-D to Ground Station Interface Description, Revision 5, October, GSFC 435-D-400.

NASA Ref. 2 (1982) LANDSAT-D Investigations Workshop (LIDQA), May 13-14.

NASA Ref. 3 (1982) Third LANDSAT Technical Working Group Meeting (LTWG), October.

Shlien, S. (1979) Geometric Correction Registration and Resampling of LANDSAT Imagery, Canadian Journal of Remote Sensing, May, pp. 74-89.

Strome, W.M. et al. (1975) Format Specifications for Canadian LANDSAT MSS System Corrected Computer Compatible Tape, CCRS Research Report 75-3.

CHANNEL	RMIN	RMAX	RMIN´	RMAX´	RMIN´´	RMAX´´
1	0.02	2.5	0.02	2.3	0.0	2.5
2	0.04	1.8.	0.04	1.8	0.0	2.0
3	0.04	1.5	0.04	1.3	0.0	1.5
4	0.10	4.0	0 10	4.0	0.0	4.0

WHERE RMIN - NASA (CAL2) PRELAUNCH MINIMUM RADIANCE
RMAX - NASA (CAL2) PRELAUNCH MAXIMUM RADIANCE
RMIN´ - NASA (CAL2) POSTLAUNCH MINIMUM RADIANCE
RMAX´ - NASA (CAL2) POSTLAUNCH MAXIMUM RADIANCE
RMIN´´ - CAL3 MIMINUM RADIANCE
RMAX´´ - CAL3 MAXIMUM RADIANCE

TABLE 1.1 - MAXIMUM AND MINIMUM RADIANCE VALUES (MW/CM2SR)

CAL2 A0	CAL2 A1	CAL3 A0	CAL3 A1
2*10**-1	8941*10**-5	0	9804*10**-5
4*10**-1	6902*10**-5	0	7843*10**-5
4*10**-1	4941*10**-5	0	5882*10**-5
10*10**-1	15294*10**-5	0	15686*10**-5

WHERE
Absolute radiance value, R´ = A0 + A1 * V´
and V´ is the calibrated digital value.

TABLE 1.2 - A0 AND A1 COEFFICIENTS (W/M2SR)

DECOMPRESSION TABLES - BANDS 1 AND 3

0.0	1.8	3.6	5.4	7.2	9.0	11.0	13.0
14 8	16.6	18.6	20.6	22.6	24 6	26.8	29.0
31.2	33 6	36.2	38.8	42.0	45.0	48.0	51.0
54.6	58.0	61.6	65.0	68.8	72.8	77.0	81.0
85.0	88.8	92.6	96.2	99.8	103.6	108.0	113.2
118.8	124.0	129 0	134.4	139.8	146.0	151.8	157.8
163.6	169 6	175.4	181.0	186.6	192.2	198.0	204.0
210.0	216.2	222.4	228.6	234.8	241.0	247.2	254.0

DECOMPRESSION TABLES - BAND 2

0.0	1.6	3.2	5.0	6.8	8.8	10.6	12.4
14.4	16.4	18.4	20.6	22.6	24.6	26.8	29.0
31.2	33.6	36.2	38.8	42.0	45 0	48 0	51.0
54 6	58.0	61 6	65.0	68.8	72.8	77.0	81.0
85.0	88.6	92.2	95 8	99 4	103.0	107.4	112.8
118.4	123.6	128.6	134.0	139.6	145.6	151.4	157.4
163 2	169.2	175.0	180.6	186.2	192.2	198.0	204.0
210.0	216.2	222.4	228.6	234.8	241.0	247.2	254.0

TABLE 1.3 - DECOMPRESSION TABLES

OFFSETS (Ci"s) :

```
      DATA ((CIN4(I,J),I=1,6),J=1,6)/
     +          -0.05044050, -0.02074160,  0.00846760,
     +           0.03403190,  0.51373140,  0.51495150,
     +          -0.04896130, -0.01938700,  0.00774700,
     +           0.03452540,  0.51237920,  0.51369880,
     +          -0.04889510, -0.01909270,  0.00701670,
     +           0.03240320,  0.51355590,  0.51501270,
     +          -0.04896040, -0.01941010,  0.00730540,
     +           0.03306180,  0.51314260,  0.51486010,
     +          -0.04955080, -0.02222870,  0.00953270,
     +           0.03481040,  0.51269500,  0.51474140,
     +          -0.04973960, -0.01888300,  0.00796110,
     +           0.03248670,  0.51322930,  0.51494550
     + /
      DATA ((CIN5(I,J),I=1,6),J=1,6)/
     +          -0.05544900, -0.01940160,  0.01182860,
     +           0.04251390,  0.50862710,  0.51188080,
     +          -0.05443910, -0.01916970,  0.01063320,
     +           0.03967680,  0.50986750,  0.51343050,
     +          -0.05335200, -0.01817020,  0.01165940,
     +           0.03866120,  0.50908450,  0.51211670,
     +          -0.05441640, -0.01823660,  0.01291340,
     +           0.04082070,  0.50803260,  0.51088560,
     +          -0.05380060, -0.01977140,  0.01027140,
     +           0.04085980,  0.50946330,  0.51297680,
     +          -0.05412580, -0.01990290,  0.00992610,
     +           0.04152150,  0.50942310,  0.51315740
     + /
      DATA ((CIN6(I,J),I=1,6),J=1,6)/
     +          -0.05704220, -0.02197540,  0.00842300,
     +           0.03960200,  0.51324970,  0.51774330,
     +          -0.05796830, -0.02231510,  0.00827520,
     +           0.03914950,  0.51417110,  0.51868670,
     +          -0.05926110, -0.02706710,  0.00411550,
     +           0.03753270,  0.52006830,  0.52461070,
     +          -0.06023280, -0.02476510,  0.00752620,
     +           0.03826340,  0.51731030,  0.52189270,
     +          -0.05873130, -0.02233320,  0.00803440,
     +           0.03840670,  0.51492430,  0.51969520,
     +          -0.05866450, -0.02347670,  0.00884060,
     +           0.03874310,  0.51493910,  0.51961750
     + /
      DATA ((CIN7(I,J),I=1,6),J=1,6)/
     +          -0.08950200, -0.04144460, -0.00395170,
     +           0.03990730,  0.54677160,  0.54822120,
     +          -0.08913090, -0.04259440, -0.00207010,
     +           0.03881090,  0.54638960,  0.54859710,
     +          -0.08683630, -0.03995820, -0.00112650,
     +           0.03891670,  0.54373020,  0.54527510,
     +          -0.08828550, -0.04554920, -0.00276330,
     +           0.04064930,  0.54713930,  0.54881220,
     +          -0.08513990, -0.04298810, -0.00074280,
     +           0.03921280,  0.54410990,  0.54554780,
     +          -0.08418970, -0.04236670, -0.00032460,
     +           0.03645530,  0.54427150,  0.54615470
     + /
```

GAINS (Di"s) :

```
      DATA ((DIN4(I,J),I=1,6),J=1,6)/
     +           0.37384636,  0.32270623,  0.27240944,
     +           0.22838916, -0.59762505, -0.59972606,
     +           0.38377613,  0.33113939,  0.28285027,
     +           0.23518577, -0.61530140, -0.61764640,
     +           0.37538711,  0.32348751,  0.27801971,
     +           0.23381069, -0.60408416, -0.60662195,
     +           0.38663017,  0.33364509,  0.28574274,
     +           0.23956043, -0.62124962, -0.62432872,
     +           0.38408816,  0.33555321,  0.27913222,
     +           0.23422909, -0.61468358, -0.61831871,
     +           0.38633607,  0.33124962,  0.28332677,
     +           0.23954269, -0.61869547, -0.62175573
     + /
      DATA ((DIN5(I,J),I=1,6),J=1,6)/
     +           0.37615660,  0.31510970,  0.26222080,
     +           0.21025470, -0.57911560, -0.58462580,
     +           0.37683800,  0.31672710,  0.26593290,
     +           0.21643300, -0.58492920, -0.59100160,
     +           0.37715130,  0.31684350,  0.26571010,
     +           0.21942420, -0.58696560, -0.59216330,
     +           0.38476210,  0.32179640,  0.26758440,
     +           0.21901600, -0.59409660, -0.59906200,
     +           0.36968810,  0.31262660,  0.26224960,
     +           0.21095770, -0.57481520, -0.58070670,
     +           0.38075110,  0.32173450,  0.27029510,
     +           0.21580960, -0.59107530, -0.59751480
     + /
      DATA ((DIN6(I,J),I=1,6),J=1,6)/
     +           0.34998023,  0.29512022,  0.24756368,
     +           0.19878563, -0.54220993, -0.54923987,
     +           0.35163692,  0.29582634,  0.24794116,
     +           0.19961144, -0.54397333, -0.55104193,
     +           0.35757652,  0.30062272,  0.25227008,
     +           0.20438063, -0.55933005, -0.56651939,
     +           0.36876274,  0.31112576,  0.25864400,
     +           0.20868819, -0.56988652, -0.57733416,
     +           0.37168222,  0.31166160,  0.26158515,
     +           0.21149782, -0.57427970, -0.58214667,
     +           0.36463442,  0.30769303,  0.25539648,
     +           0.20700799, -0.56358048, -0.57115126
     + /
      DATA ((DIN7(I,J),I=1,6),J=1,6)/
     +           0.41613790,  0.33807030,  0.27716460
     +           0.20591720, -0.61746820, -0.61982300
     +           0.43228070,  0.35363710,  0.28515370
     +           0.21606760, -0.64170430, -0.64543500
     +           0.41927050,  0.34173870,  0.27751450
     +           0.21128650, -0.62362830, -0.62618350
     +           0.44784980,  0.37277860,  0.29762140
     +           0.22136270, -0.66833770, -0.67127640
     +           0.47547810,  0.39588420,  0.31611370
     +           0.24066650, -0.71271490, -0.71543020
     +           0.45994920,  0.38326690,  0.30618120
     +           0.23874470, -0.69234530, -0.69579840
     + /
```

Table 1.4 LANDSAT-4 Modified Ci"s & Di"s

The CAL3 gains and offsets for all detectors in all bands were then derived, as shown in Table 2.3, by using the absolute gains and offsets for one reference detector in each band combined with the relative gains and offsets of all the other detectors. Comparison of the absolute gains and offsets in Tables 2.2 and 2.3 shows small differences, as discussed in Section 1.2.

3.0 STABILITY OF THE CALWEDGE

The stability of the calwedge is being monitored by CCRS for two major purposes. Firstly, it is advisable to select as reference detectors for absolute calibration purposes the detector within each band which is most reliable in terms of both long term stability and constancy within one scene. Secondly, any long term drift in the absolute calibration of the MSS sensor should be monitored for quality assessment purposes.

3.1 STABILITY WITHIN ONE SCENE

The calwedges from seven scenes in the time period from the end of September 1982 to the end of January 1983 were investigated. For all twenty-four detectors, the mean and standard deviation of each of the six calwedge samples were calculated using data from all 186 calwedges per detector in the full scene. The accumulation of the histograms for each calwedge sample showed the distribution of points to fall either equally in two adjacent bins, or predominantly in one bin with a few points in the closest bin on either side. The only exceptions were samples 5 and 6 for all six detectors in bands 1, 2 and 3, where points fell in up to six bins.

The calwedge sample statistics are shown in Figures 3.1 to 3.24 for each of detectors 1 to 24 respectively. The horizontal scale on the charts shows the sample numbers 1 to 6. For each sample number, the mean and standard deviation for the seven test samples are shown, where each test sample is shown slightly displaced to the right in order of time sequence. The vertical scale, showing the raw digital value in the range 0 to 63, is shown separately for samples 1 to 4 and samples 5 to 6. the relative locations for all six samples within the full calwedge are shown schematically in Figure 3.0.

3.2 STABILITY WITHIN ONE ORBIT

The latest test scenes used by CCRS were from the same orbit on January 20, 1983. Inspection of the plots of the last two sets of calwedge samples shows that the mean value, calculated over each of the test scenes, did not drift by more than one half of one digital level. This study will be continued by CCRS towards the end of the first year of LANDSAT-4 data reception.

3.3 STABILITY OVER A PERIOD OF TIME

Of the twenty-four detectors, sixteen are seen to record calwedge samples with random fluctuations with a spread of approximately one digital level over a period of five months. Detector 16 shows a spread of two digital values. Those detectors for which the calwedge samples are drifting, either up or down, are of some concern since this may represent a change in the gain of that detector. From early September 1982 to late January 1983, the calwedge samples for detectors 5, 10, 19, 21 and 23 have drifted down one level; for detectors 3 and 9 they have drifted up two levels; and for detector 7 they have drifted down two levels.

3.4 CHOICE OF REFERENCE DETECTORS

Reference detectors have been chosen by CCRS using information from three sources. Firstly, those detectors shown to have drifted by one or more levels were rejected as candidates. Secondly, the absolute calibration graphs shown in Figures 2.1 to 2.4 for bands 1 to 4 respectively were used to reject those detectors for which the absolute gain and offset were significantly different from those for the other detectors in the same band. Finally, information supplied by NASA (Reference 2) concerning calwedge data was incorporated into the following choice of reference detectors. (The detector number in the sequence 1 to 24 is shown in parentheses.)

Band 1, detector 2 (2)
Band 2, detector 5 (11)
Band 3, detector 4 (16)
Band 4, detector 4 (22)

NASA SCENE IDENTIFICATION	PATH-ROW	ACQUISITION DATE
40043-152419	17-30	August 28, 1982
40048-171913	36-23	September 2, 1982
40068-151610	16-24	September 22, 1982
40098-170739	34-23	October 22, 1982
31695-17594	46-22	October 25, 1982
40101-173809	39-22	October 25, 1982
40131-17493	41-18	November 24, 1982
31726-17295	41-19	November 25, 1982
40146-15293	18-23	December 9, 1982
31740-15251	19-23	December 9, 1982
40169-171350	35-21	January 1, 1983
40188-17451	40-21	January 20, 1983
31782-17414	43-21	January 20, 1983
40188-17465	40-25	January 20, 1983
31782-17432	43-25	January 20, 1983
31782-17473	43-35	January 20, 1983

Table 1.5 Identification of Test Scenes

DETECTOR	BAND 1		BAND 2		BAND 3		BAND 4	
	GAIN	OFFSET	GAIN	OFFSET	GAIN	OFFSET	GAIN	OFFSET
1	0.9813	0.0856	0.9236	-0.7109	0.9474	0.0335	0.9611	0.3339
2	1.0000	0.0000 *	1.0458	-1.1507	0.9861	-0.1783	0.9795	0.0306
3	1.0379	1.2877	0.9313	-0.3736	1.0568	-0.8806	0.9696	-0.2955
4	1.0621	0.0233	0.9221	-0.0108	1.0000	0.0000 *	1.0000	0.0000 *
5	0.8356	0.9289	1.0000	0.0000 *	1.0246	-0.9832	0.9465	-0.1390
6	0.9601	0.3113	1.0225	-0.0948	0.9872	-0.2197	0.9676	-0.4966

RELATIVE GAINS AND OFFSETS, USING HISTOGRAMS

TABLE 2.1

DETECTOR	BAND 1		BAND 2		BAND 3		BAND 4	
	GAIN	OFFSET	GAIN	OFFSET	GAIN	OFFSET	GAIN	OFFSET
1	0.8416	-0.7195	0.8241	-2.2747	0.8584	-1.9502	0.8974	-5.7692
2	0.8583	-0.6319 *	0.9379	-2.1670	0.8969	-2.8125	0.9060	-6.3150
3	0.8931	0.5993	0.8295	-2.2191	0.9693	-5.0502	0.9203	-5.5261
4	0.9148	-0.5279	0.8281	-1.3401	0.9154	-3.2833 *	0.9253	-6.4430*
5	0.7177	-1.0117	0.8745	-1.3472 *	0.9414	-3.3754	0.8884	-5.9598
6	0.8381	-0.9245	0.9126	-1.3563	0.8999	-3.1385	0.8873	-5.8561

ABSOLUTE (CAL 3) GAINS AND OFFSETS, USING CALWEDGES

TABLE 2.2

DETECTOR	BAND 1		BAND 2		BAND 3		BAND 4	
	GAIN	OFFSET	GAIN	OFFSET	GAIN	OFFSET	GAIN	OFFSET
1	0.8422	-0.5343	0.8077	-1.9552	0.8672	-3.0770	0.8893	-5.8582
2	0.8583	-0.6319 *	0.9145	-2.5596	0.9072	-3.4160	0.9063	-6.2805
3	0.8909	0.6318	0.8144	-1.6282	0.9673	-4.3503	0.8971	-6.5426
4	0.9116	-0.6478	0.8064	-1.2530	0.9154	-3.2833*	0.9253	-6.4430*
5	0.7122	0.4008	0.8745	-1.3472 *	0.9379	-4.3474	0.8758	-6.2372
6	0.8240	-0.2954	0.8941	-1.4523	0.9036	-3.4608	0.8953	-6.7308

ABSOLUTE (CAL 3) GAINS AND OFFSETS

- COMBINING ABSOLUTE AND RELATIVE GAINS AND OFFSETS

TABLE 2.3

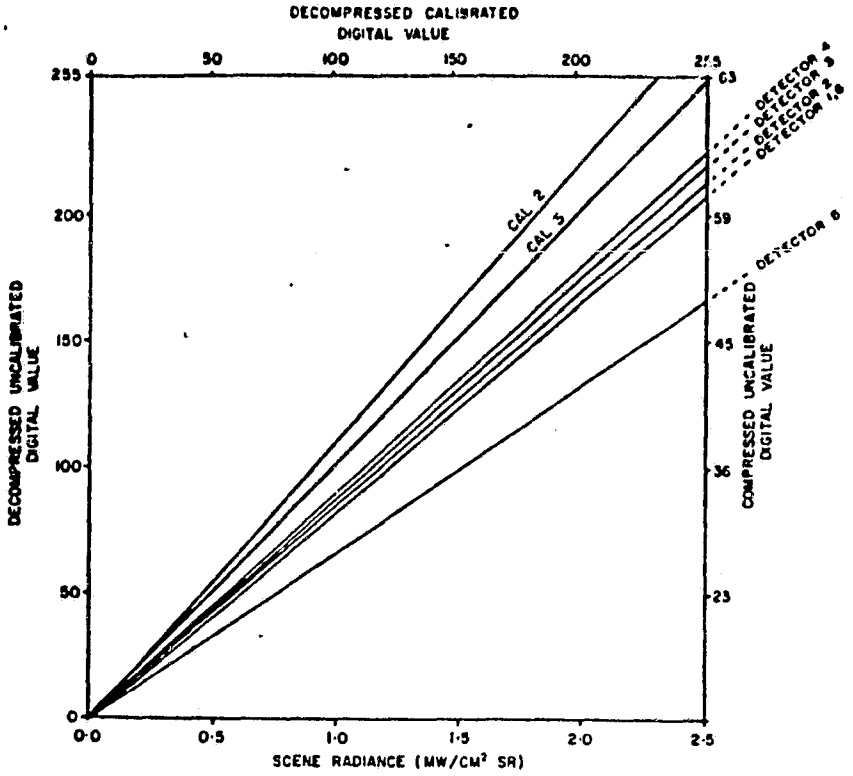

Relationship between Scene Radiance and Compressed, Decompressed and Calibrated Digital Values

Figure 2.1 ABSOLUTE CALIBRATION FOR BAND 1

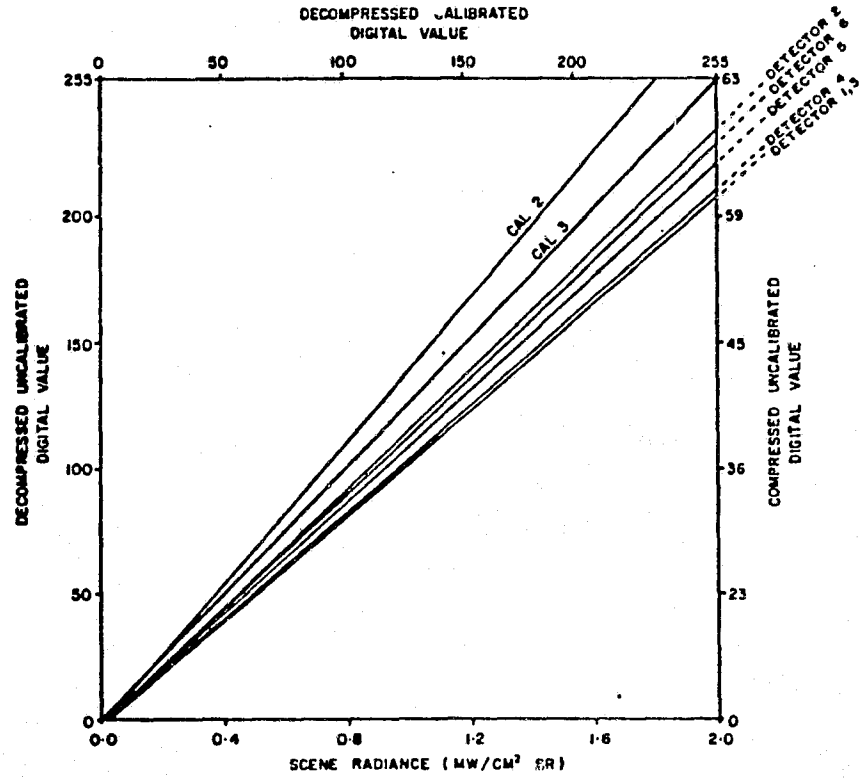

Relationship between Scene Radiance and Compressed Decompressed and Calibrated Digital Values

Figure 2.2 ABSOLUTE CALIBRATION FOR BAND 2

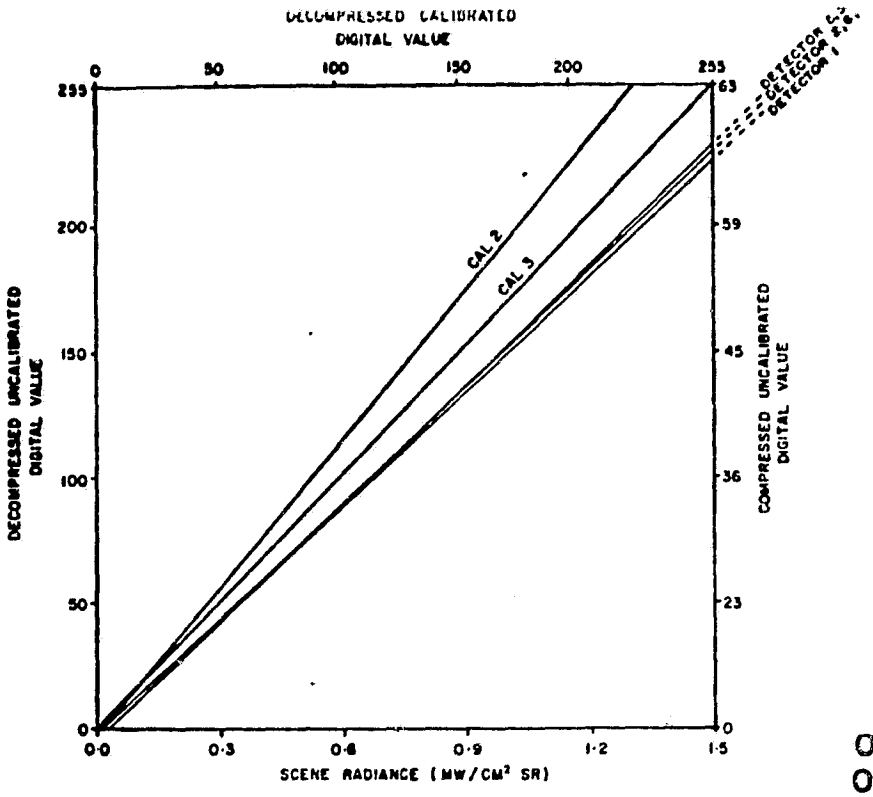

Relationship between Scene Radiance and Compressed Decompressed and Calibrated Digital Values

Figure 2.3 ABSOLUTE CALIBRATION FOR BAND 3

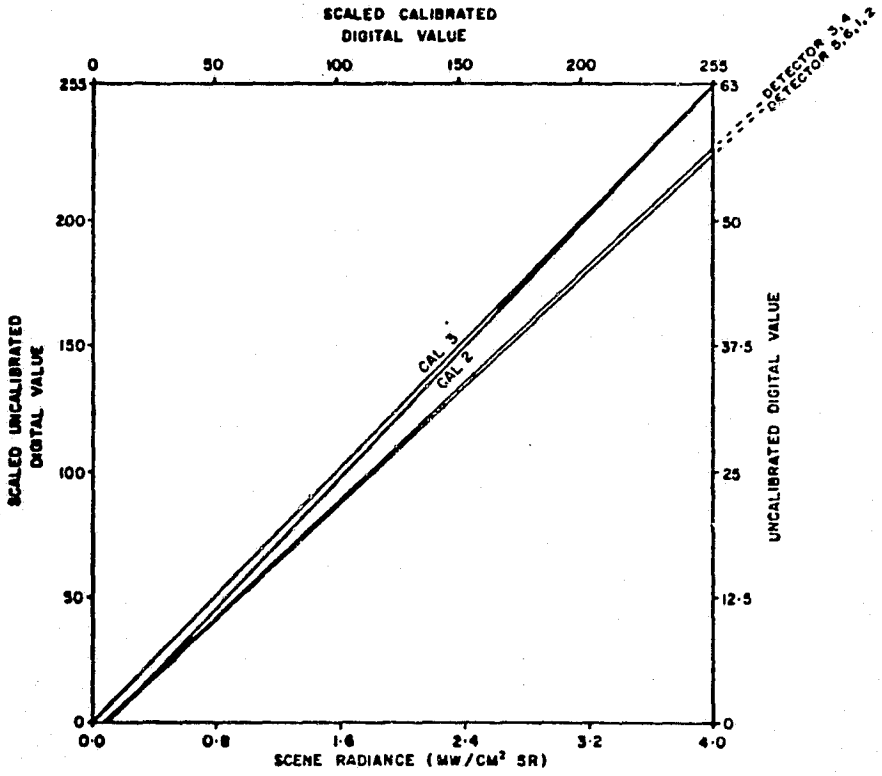

Relationship between Scene Radiance and Uncalibrated, Scaled Uncalibrated and Calibrated Digital Values

Figure 2.4 ABSOLUTE CALIBRATION FOR BAND 4

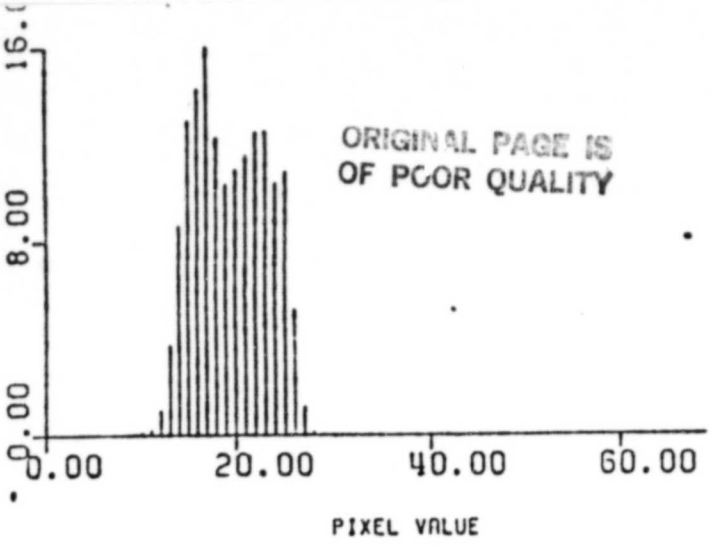

DETECTOR 1

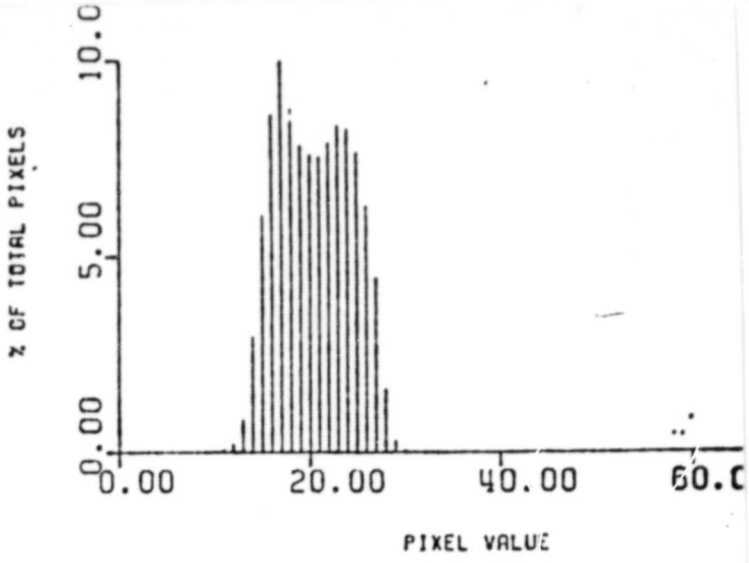

DETECTOR 4

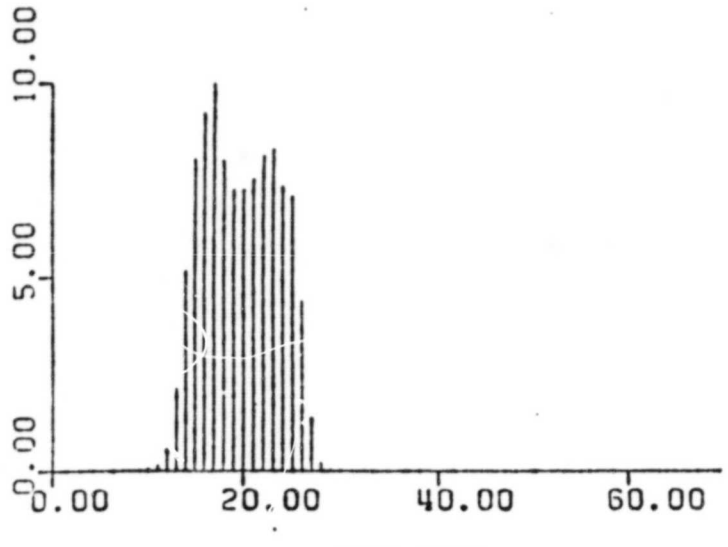

DETECTOR 2

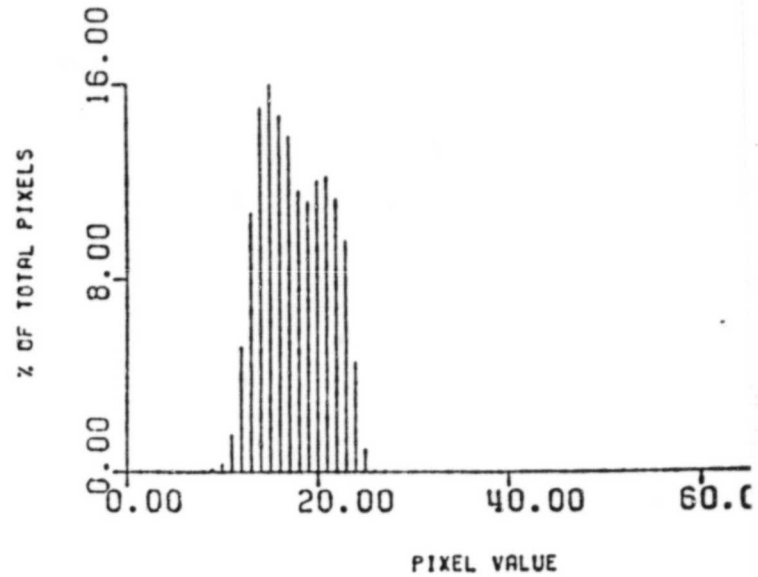

DETECTOR 5

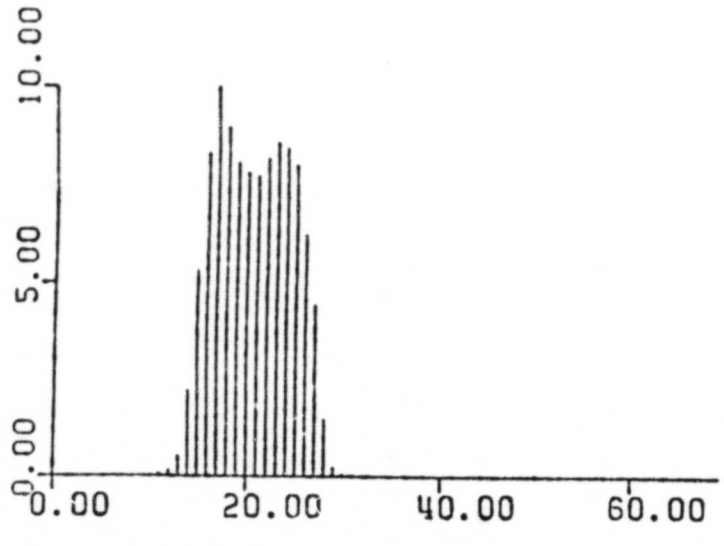

DETECTOR 3

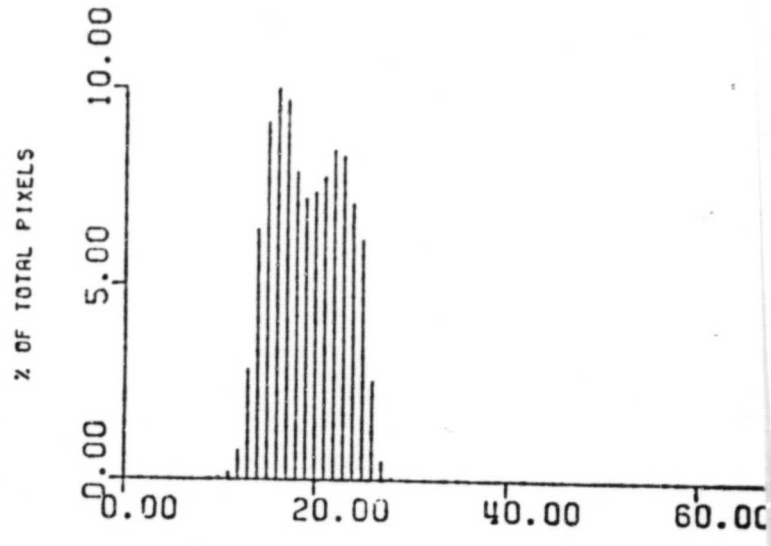

DETECTOR 6

FIGURE 2.5 BAND 1 RAW DATA HISTOGRAMS

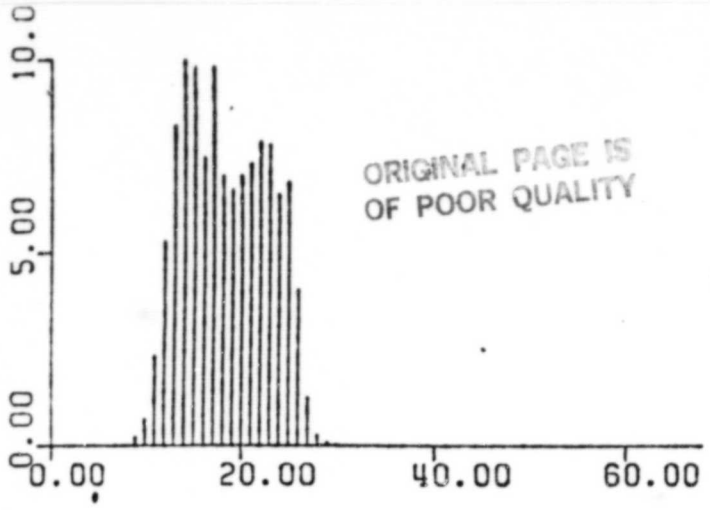

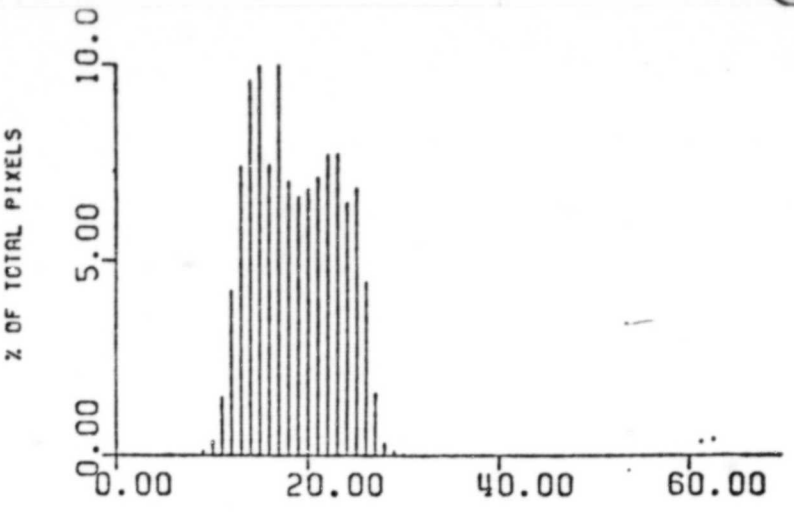

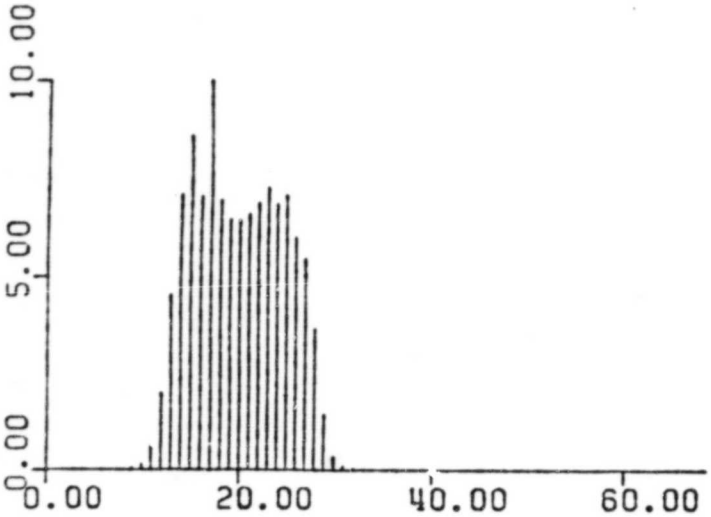

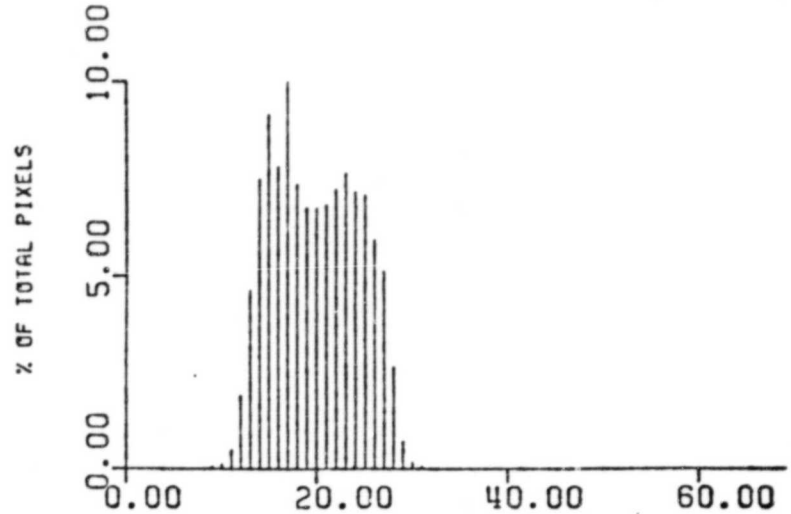

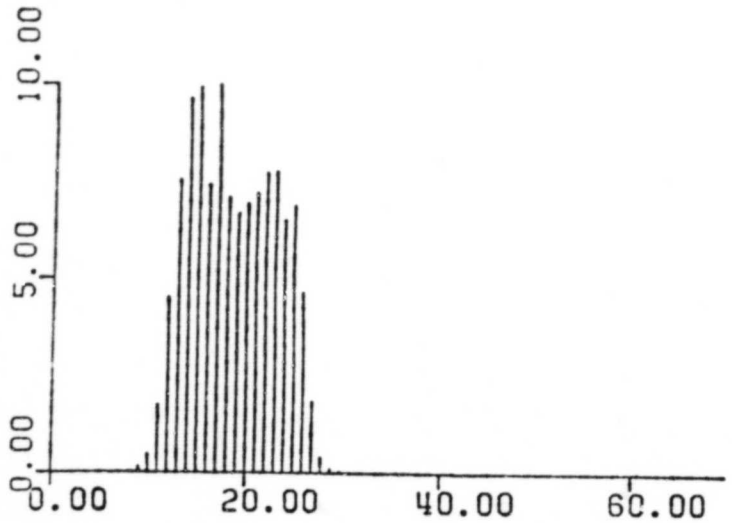

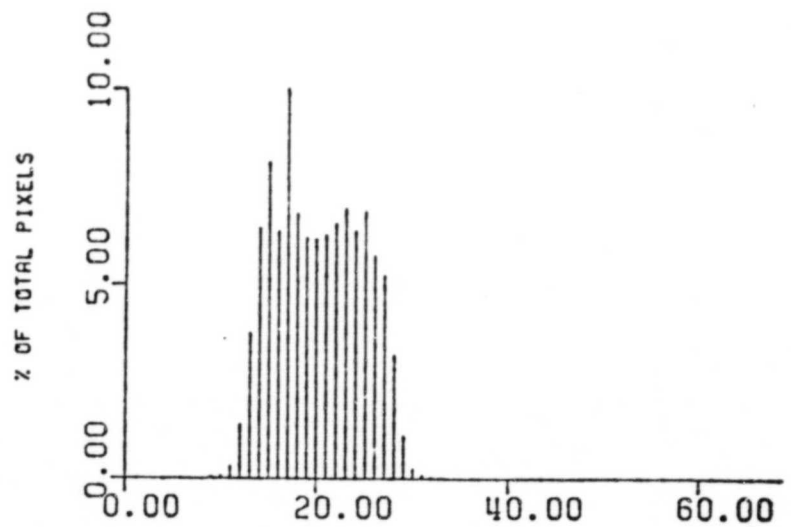

FIGURE 2.6 BAND 2 RAW DATA HISTOGRAMS

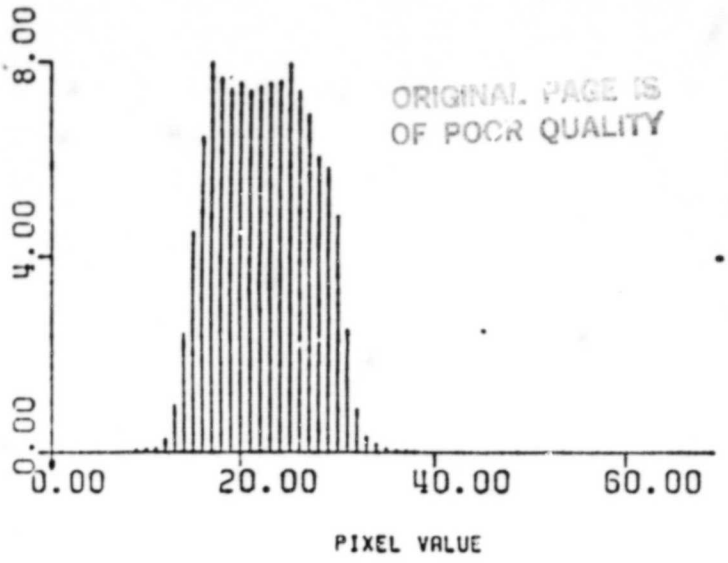

DETECTOR 1

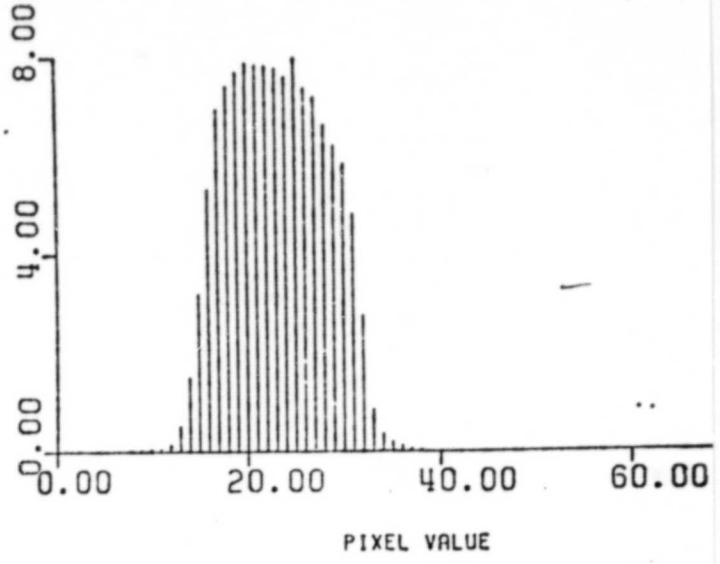

DETECTOR 4

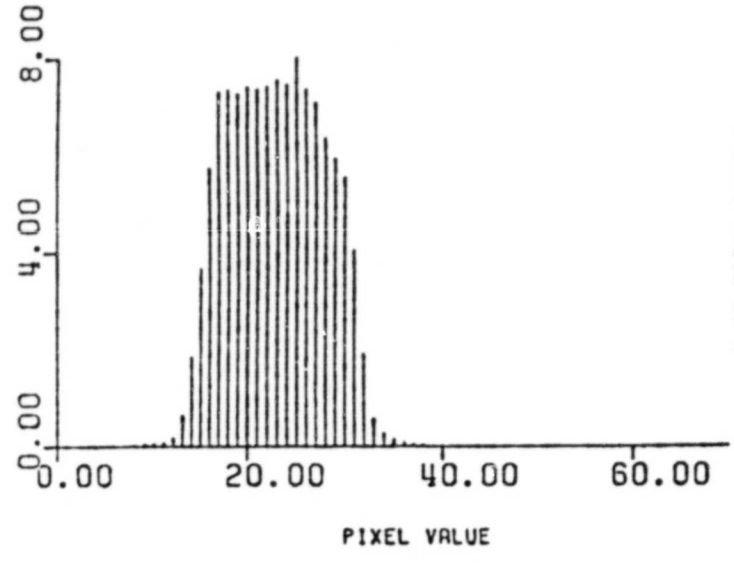

DETECTOR 2

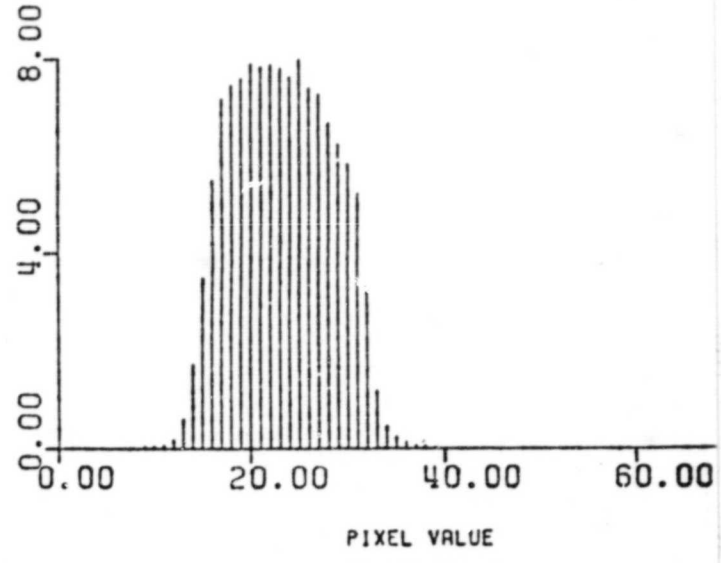

DETECTOR 5

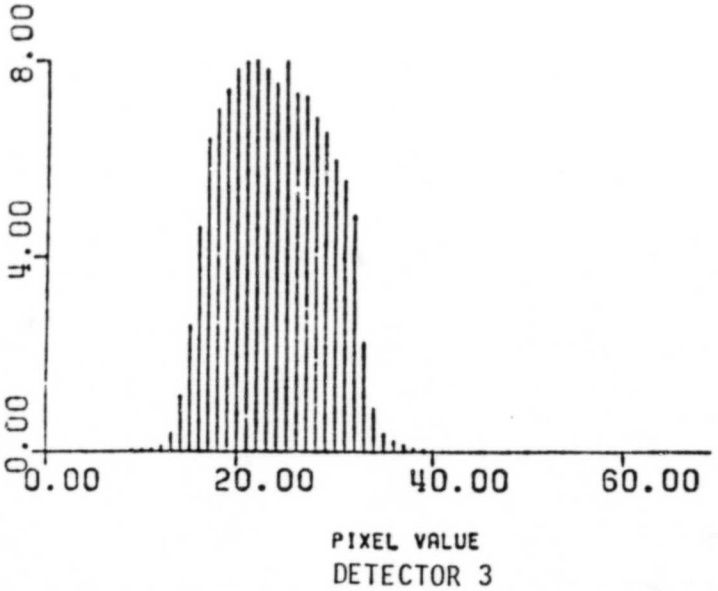

DETECTOR 3

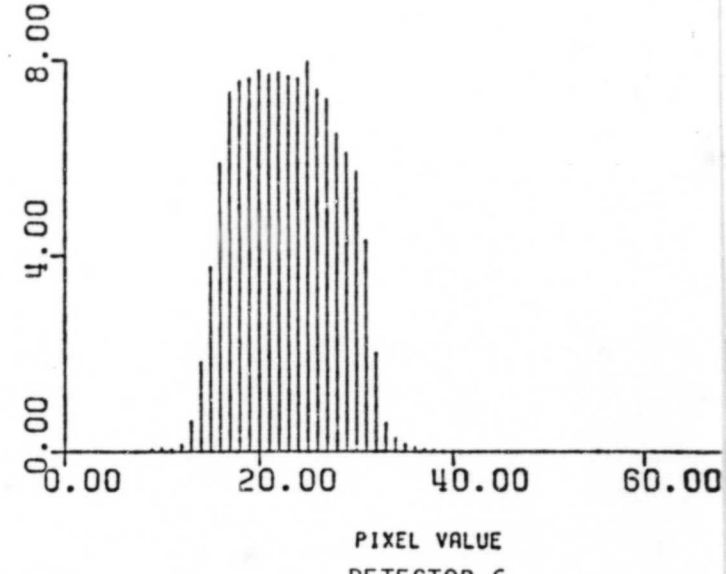

DETECTOR 6

FIGURE 2.7 BAND 3 RAW DATA HISTOGRAMS

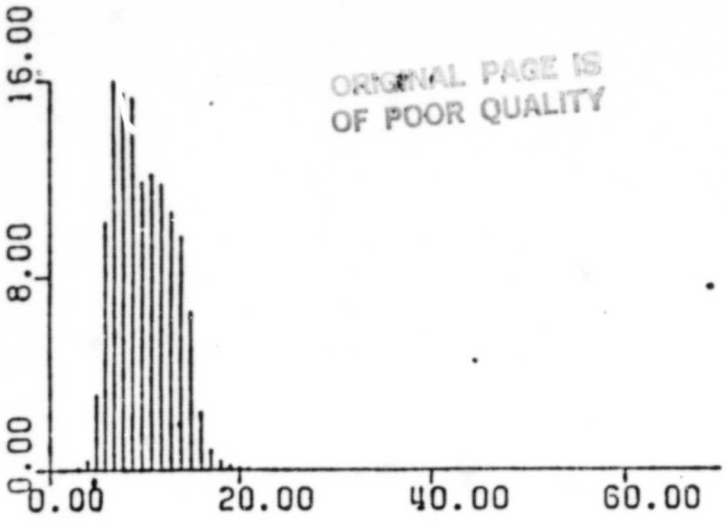

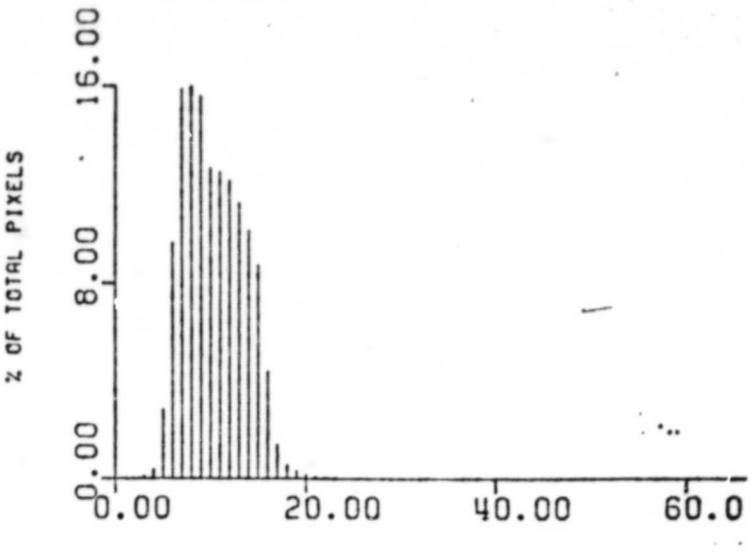

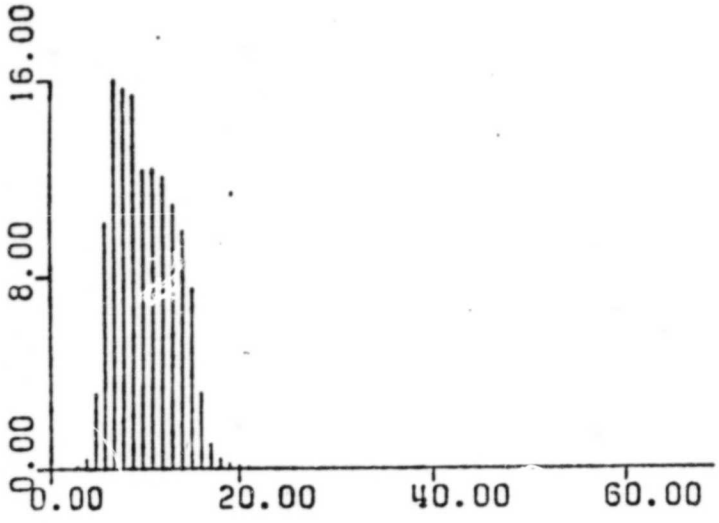

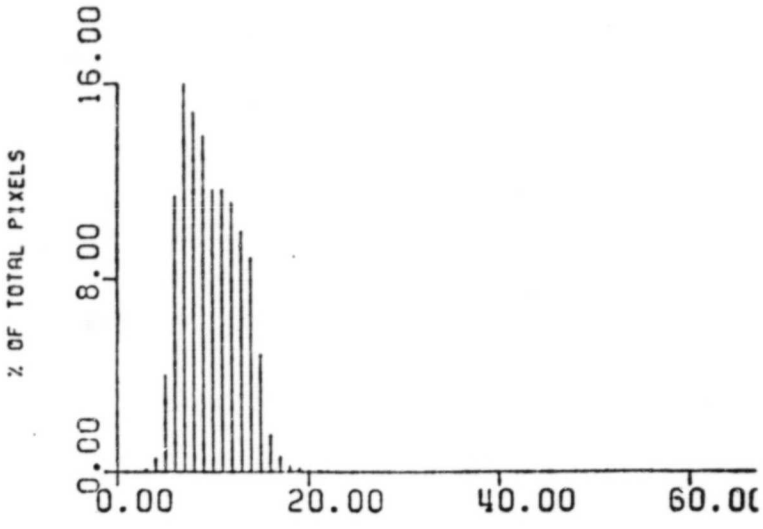

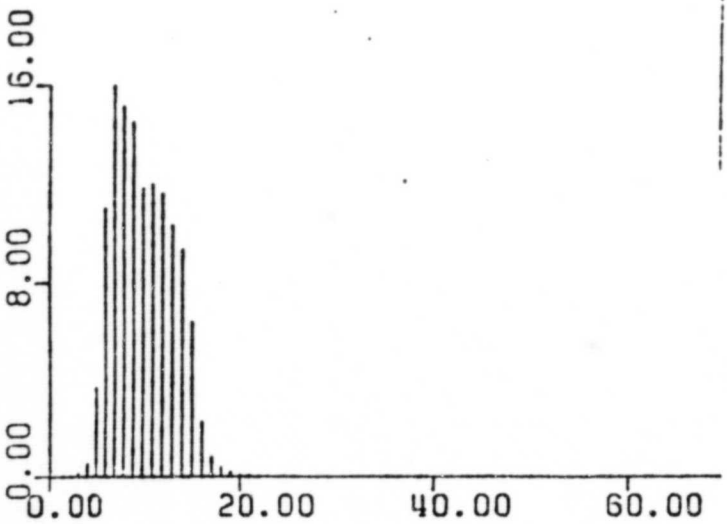

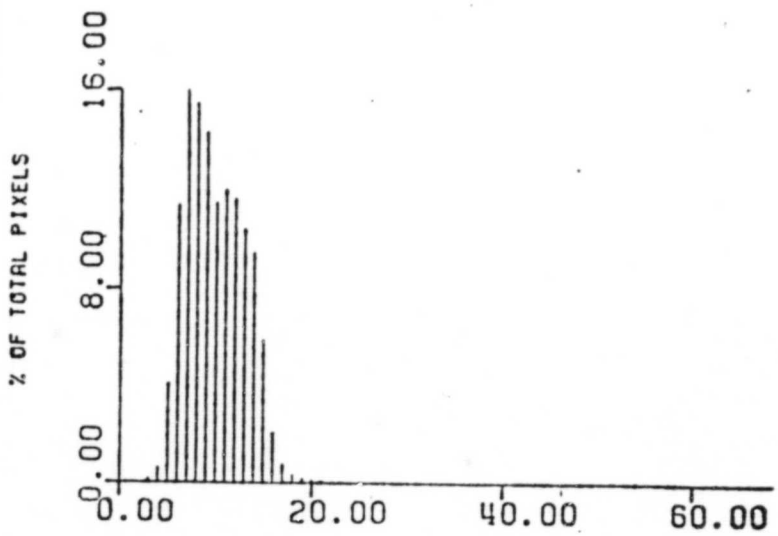

FIGURE 2.8 BAND 4 RAW DATA HISTOGRAMS

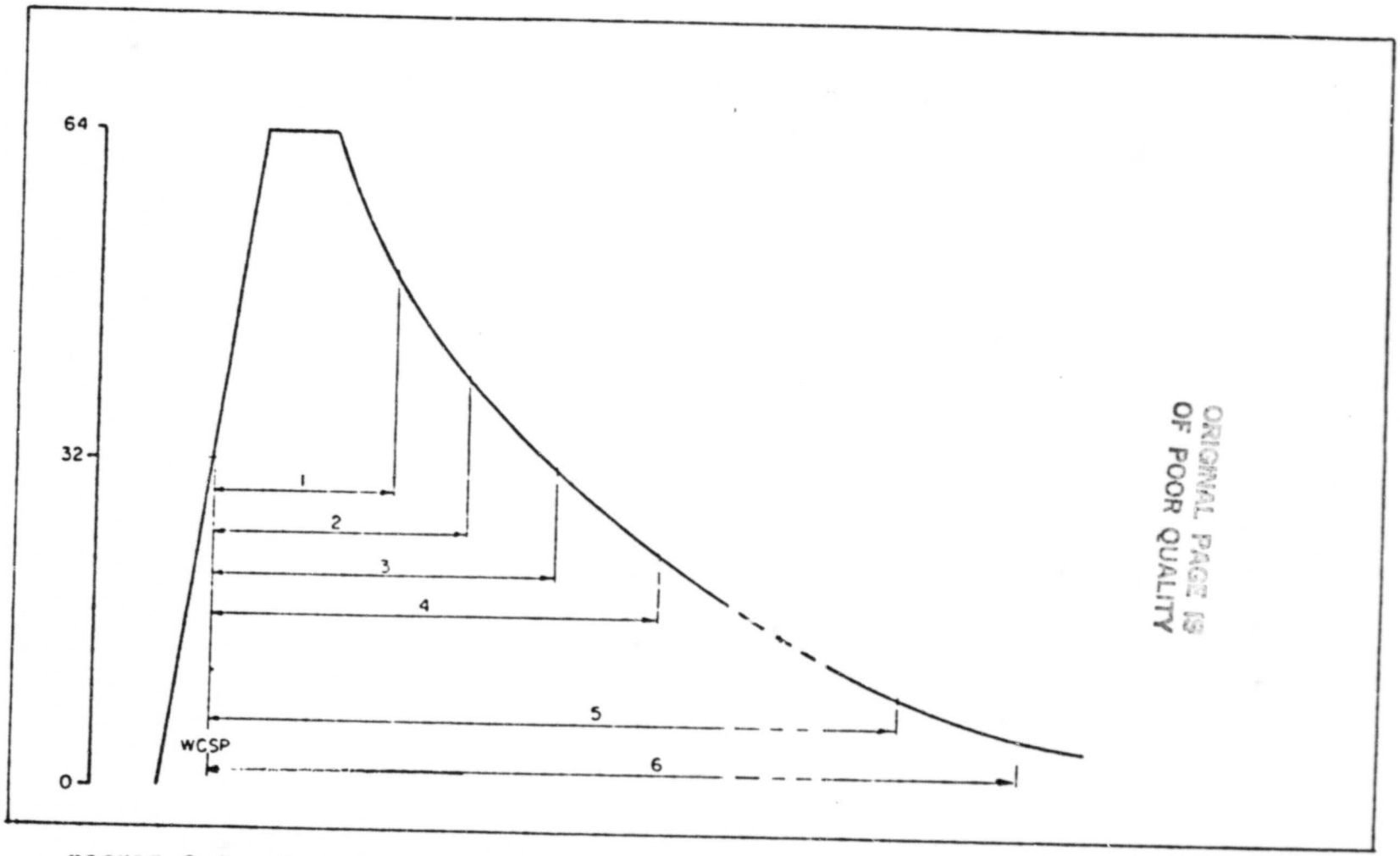

FIGURE 3.0 The calibration wedge. This is a schematic representation of a typical LANDSAT MSS calibration wedge showing the six sample locations relative to the word count start position (WCSP).

DETECTOR 1

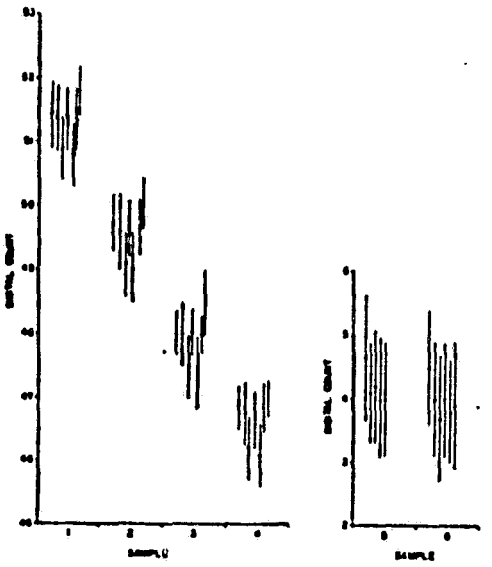

FIGURE 3.1

DETECTOR 2

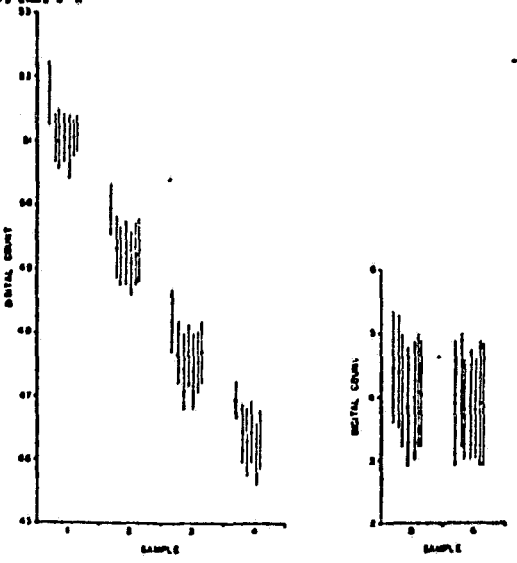

FIGURE 3.2

DETECTOR 3

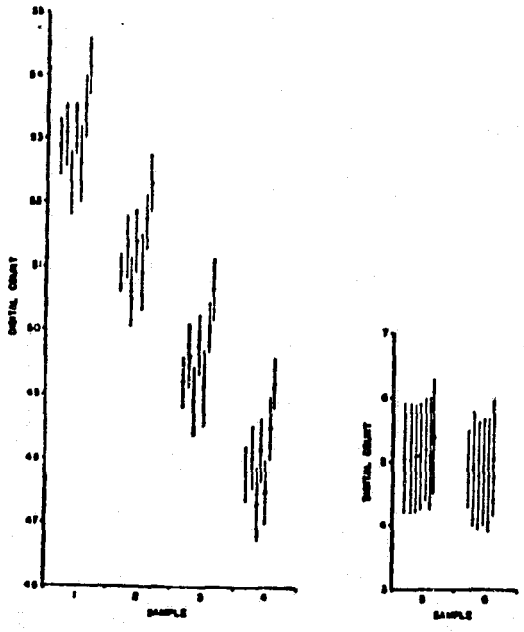

FIGURE 3.3

DETECTOR 4

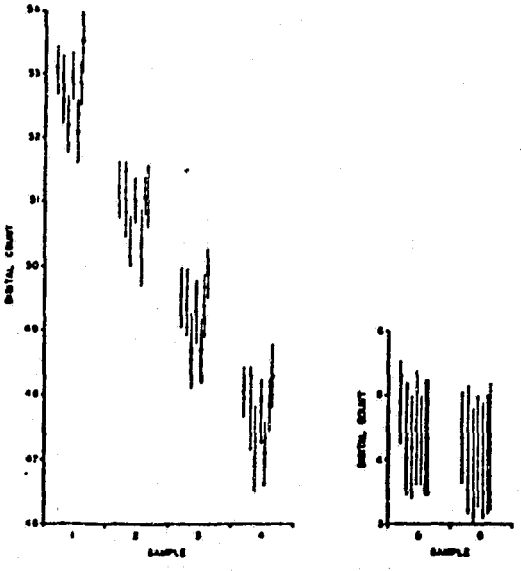

FIGURE 3.4

DETECTOR 9

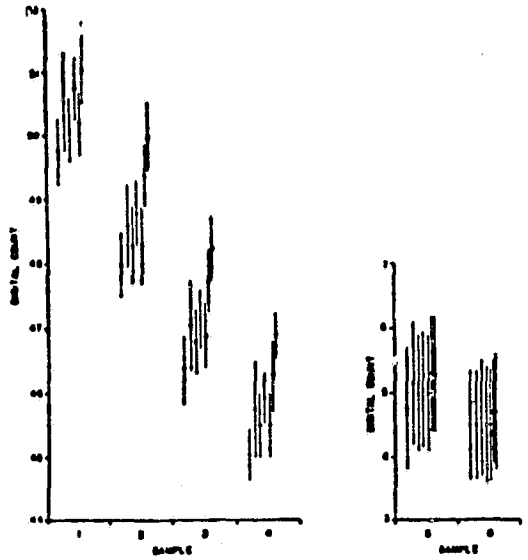

FIGURE 3.9

DETECTOR 10

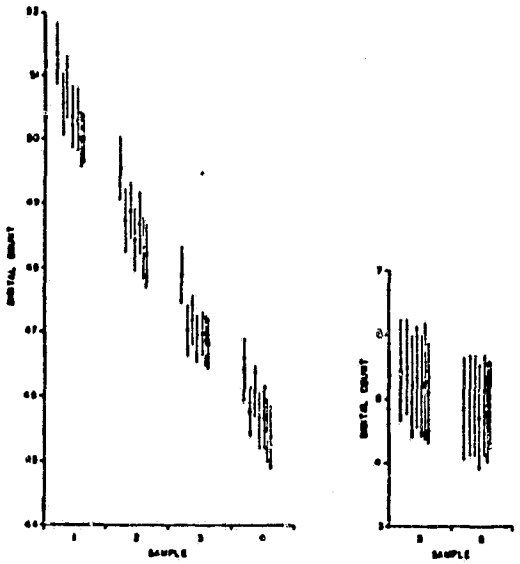

FIGURE 3.10

DETECTOR 11

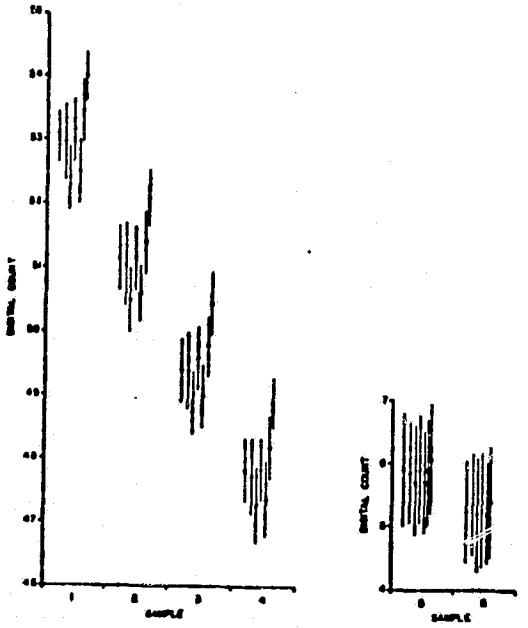

FIGURE 3.11

DETECTOR 12

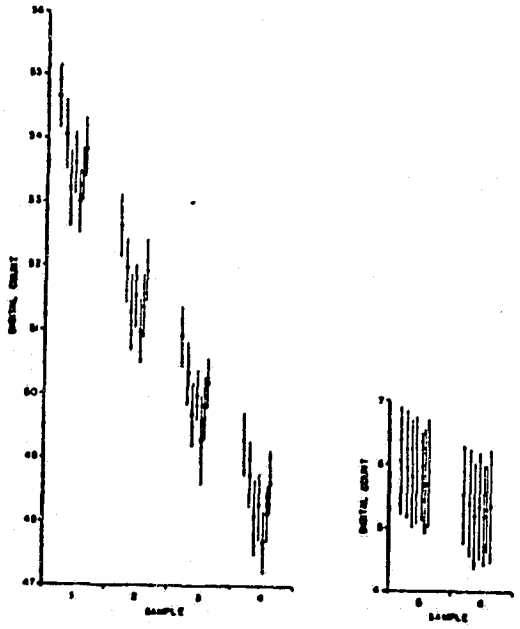

FIGURE 3.12

DETECTOR 13

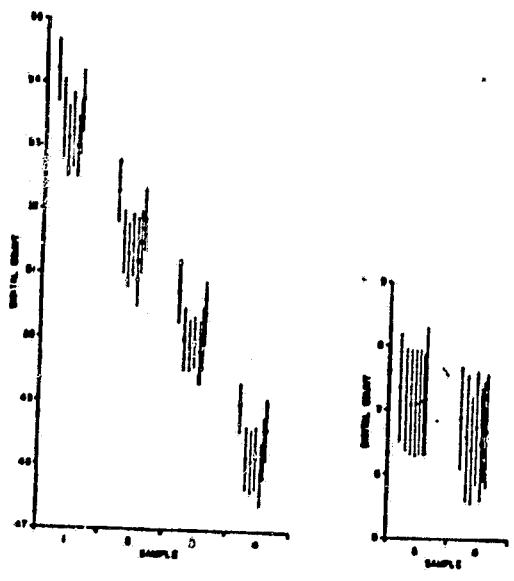

FIGURE 3.13

DETECTOR 14

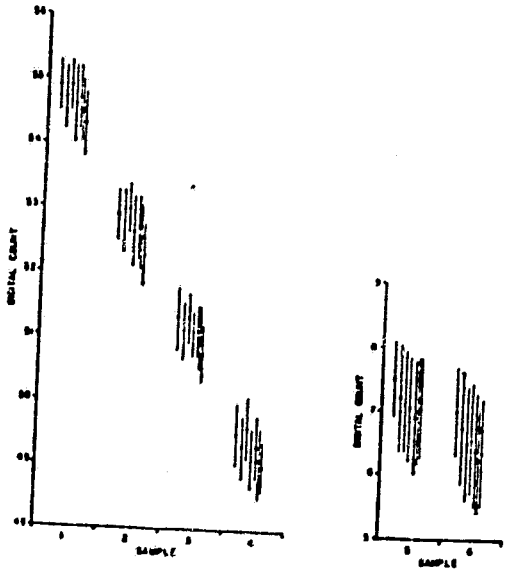

FIGURE 3.14

DETECTOR 15

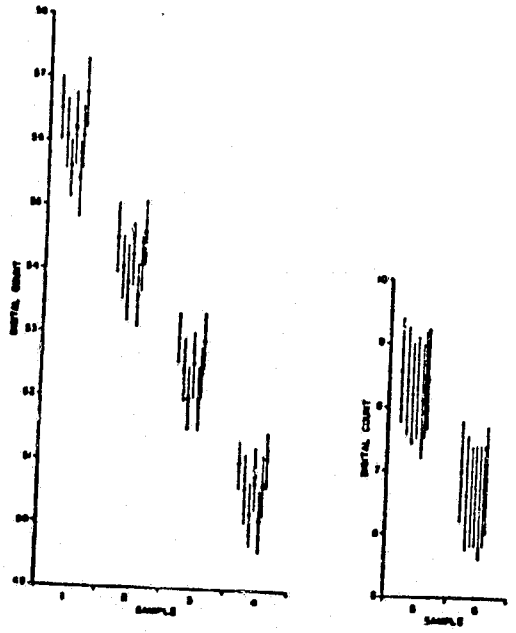

FIGURE 3.15

DETECTOR 16

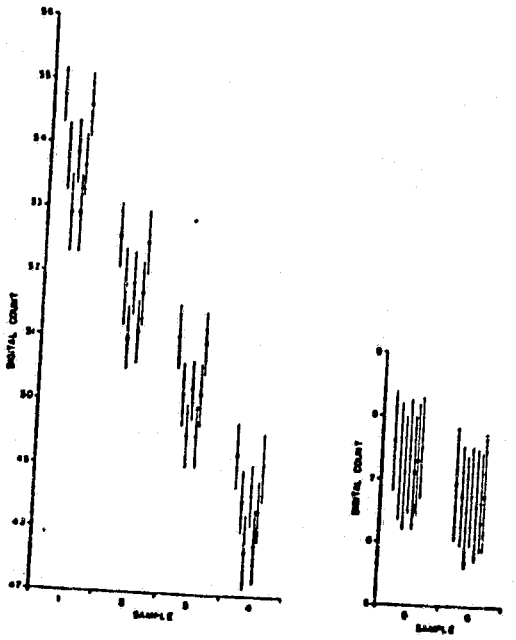

FIGURE 3.16

DETECTOR 17

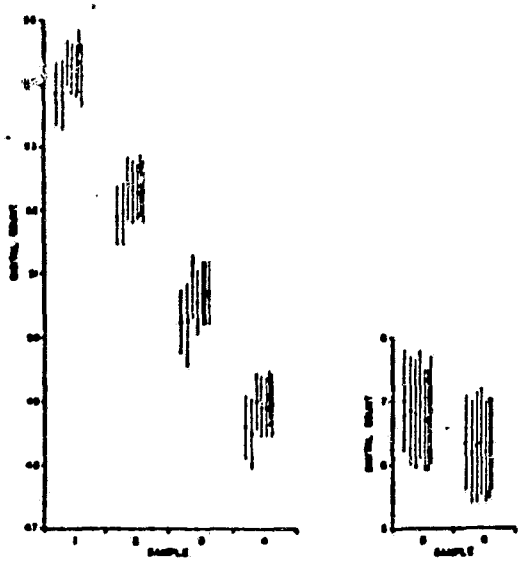

FIGURE 3.17

DETECTOR 18

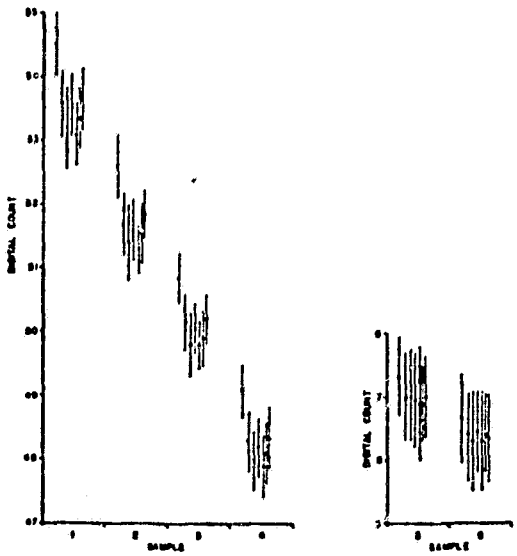

FIGURE 3.18

DETECTOR 19

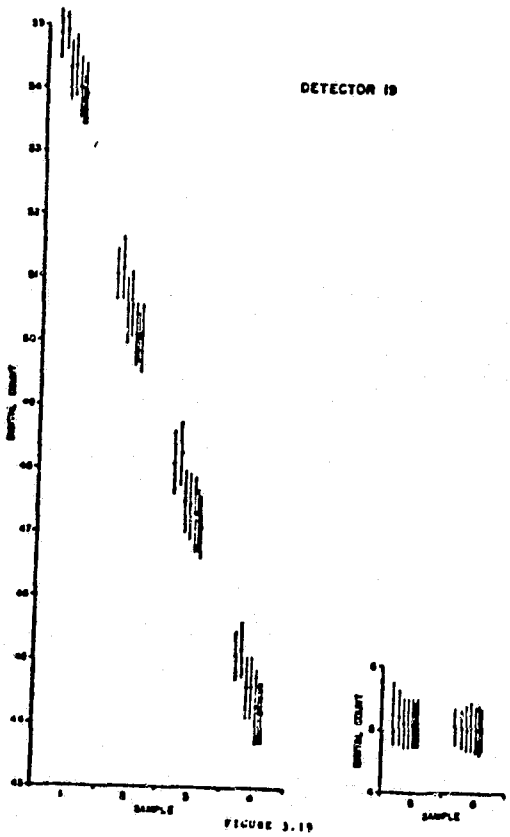

FIGURE 3.19

DETECTOR 20

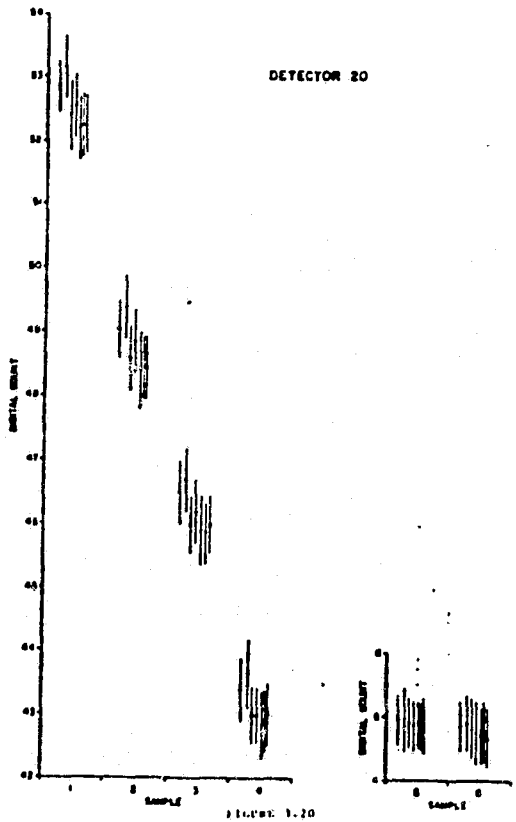

FIGURE 3.20

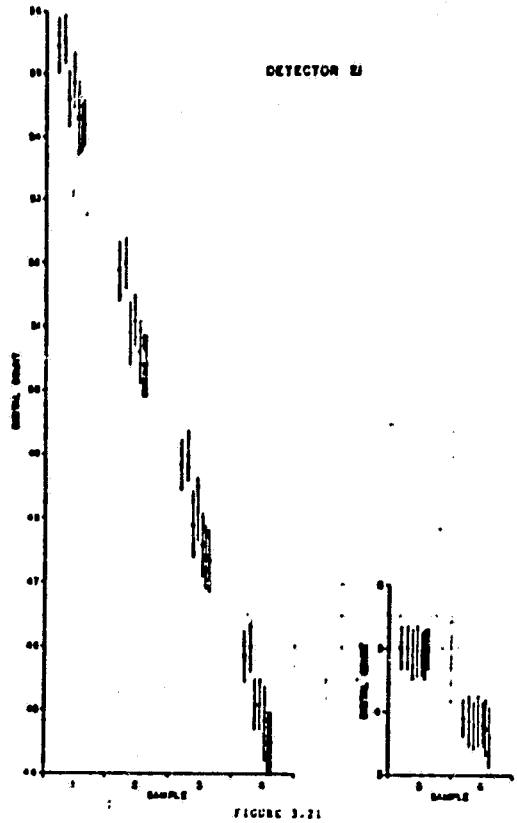

FIGURE 3.21

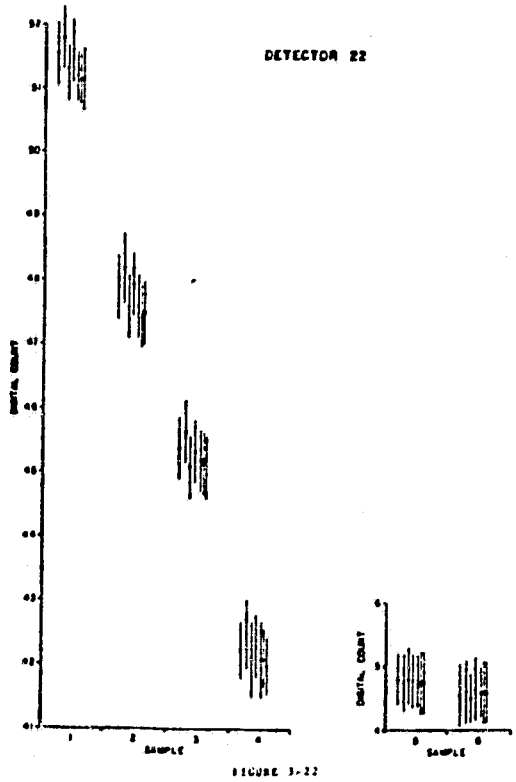

FIGURE 3.22

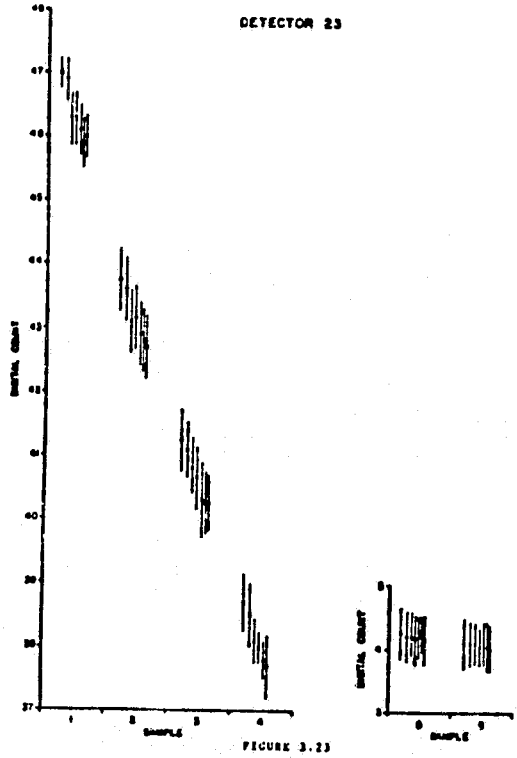

FIGURE 3.23

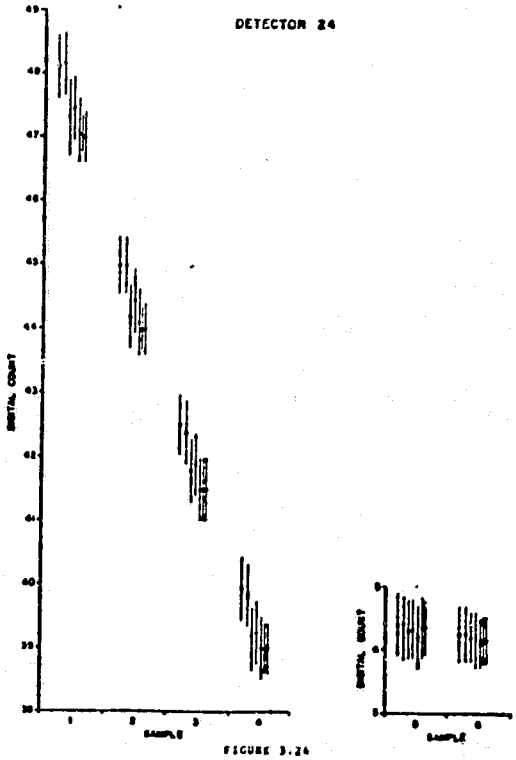

FIGURE 3.24

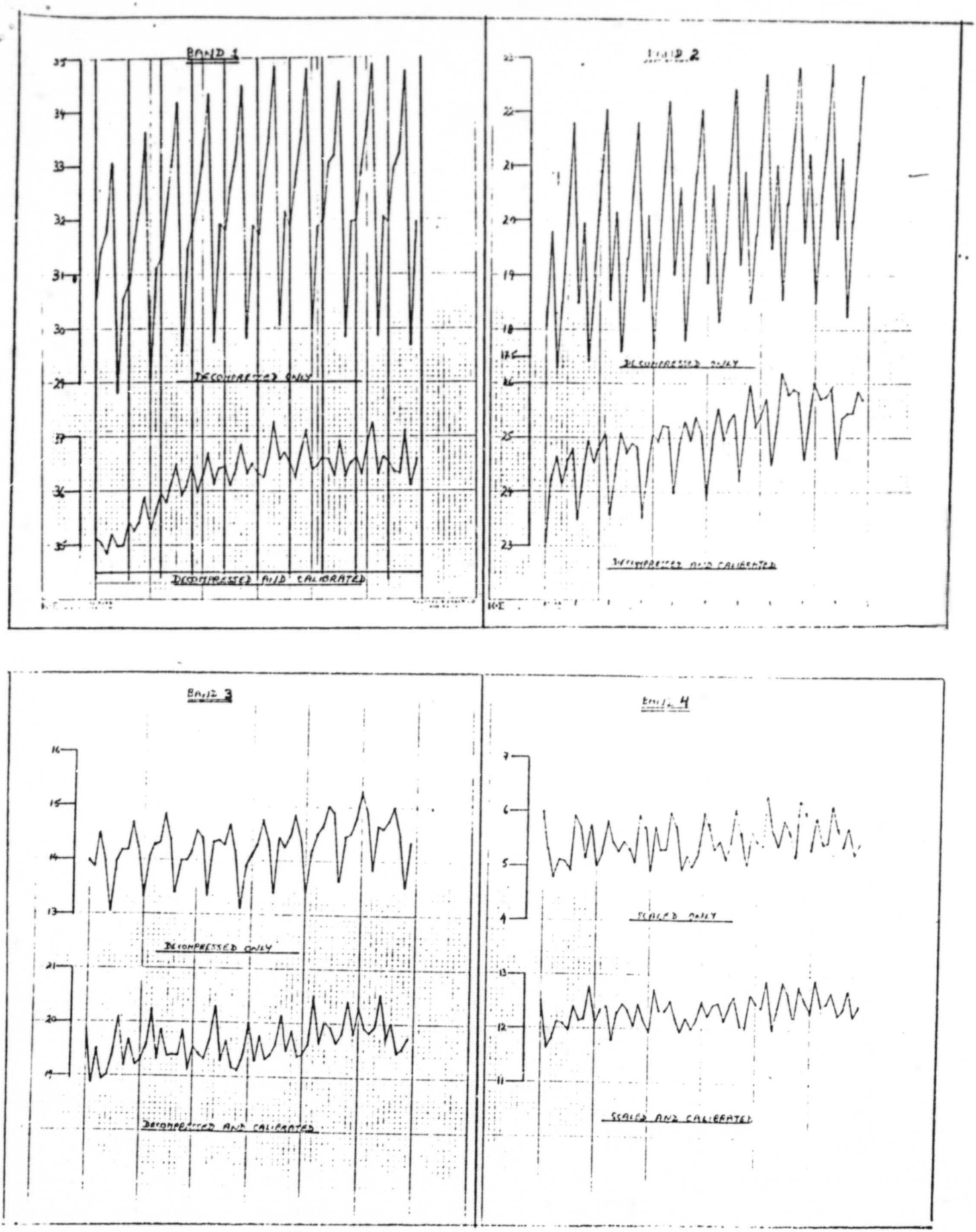

Figure 4.1 Residual Striping in Water

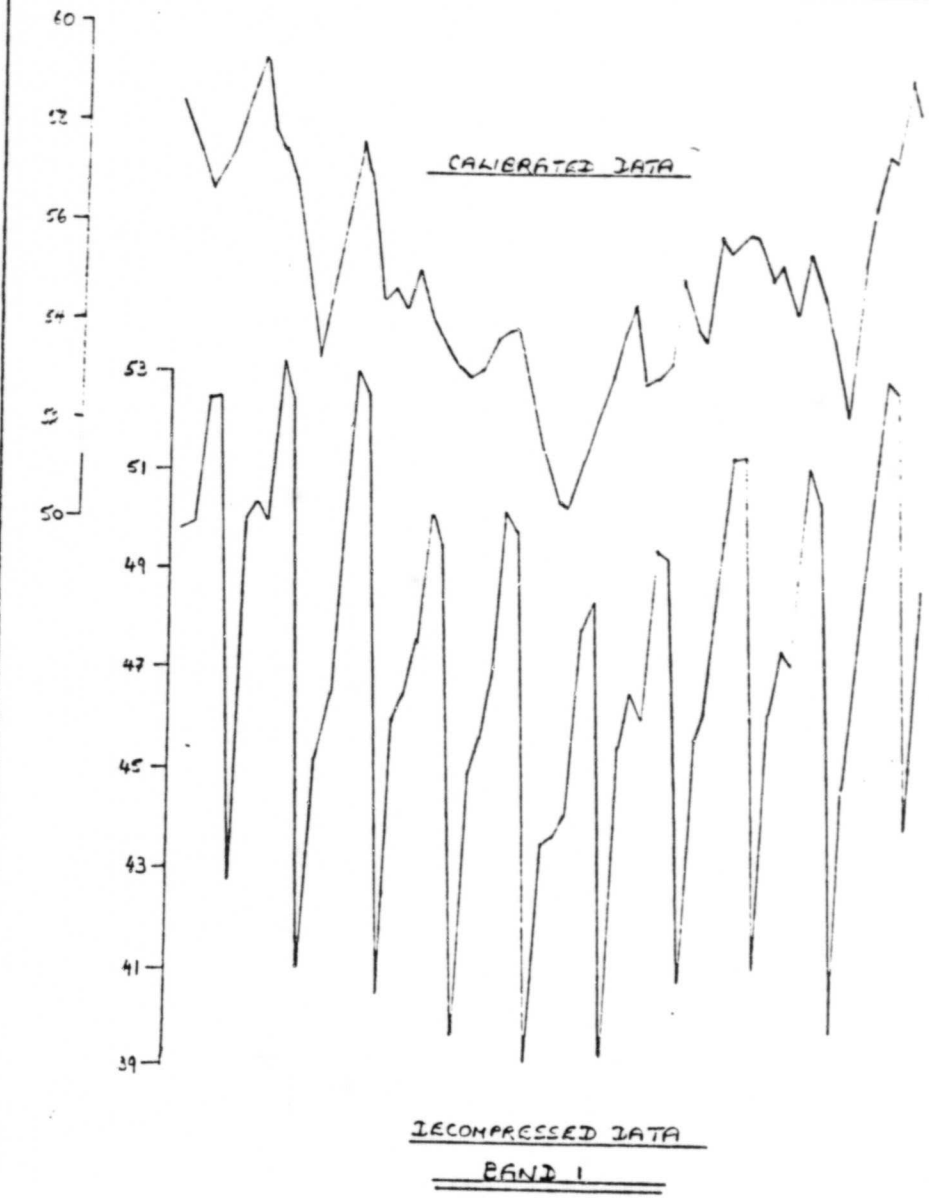

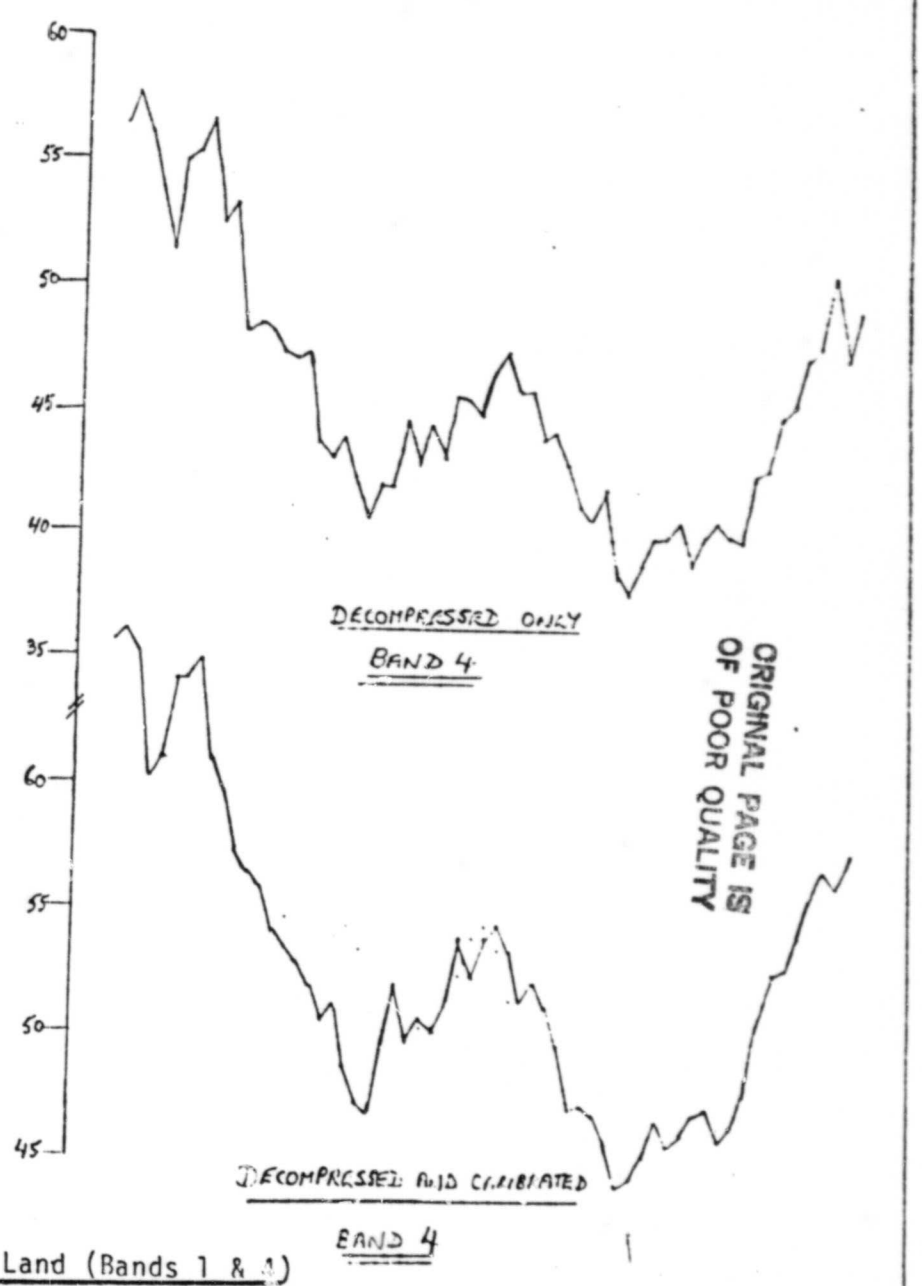

Figure 4.2a Residual Striping over Land (Bands 1 & 4)

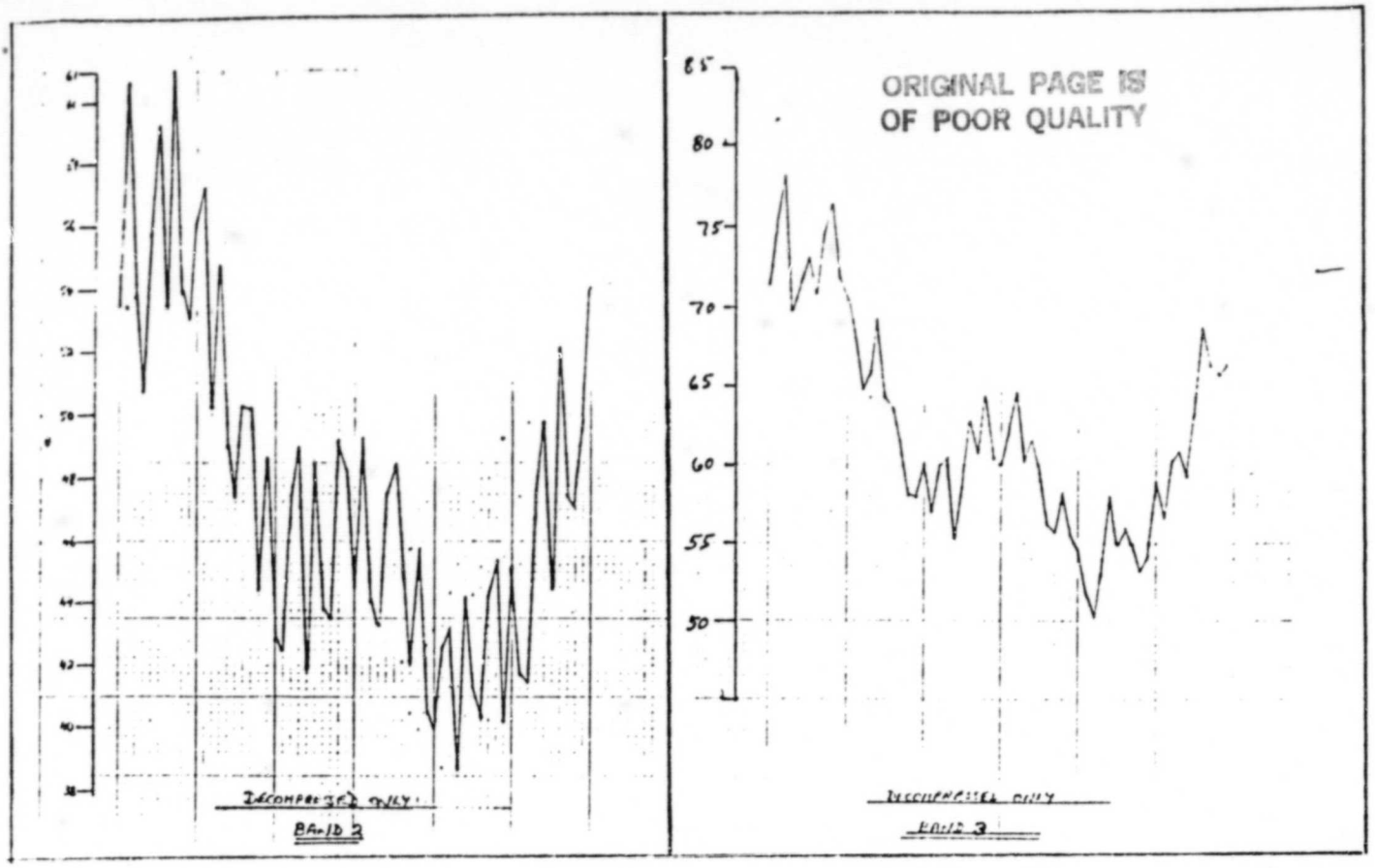

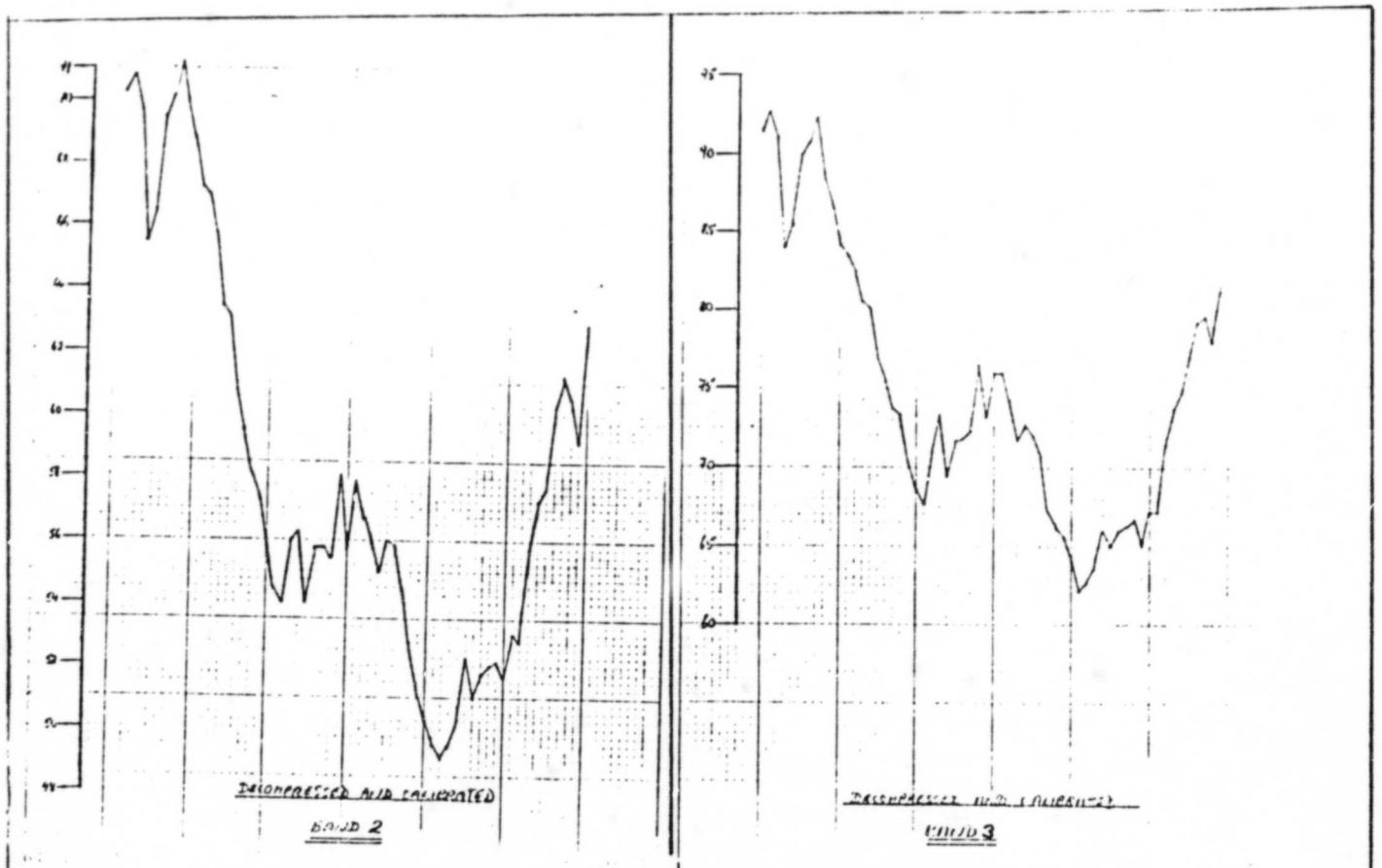

Figure 4.2b Residual Striping over Land (Bands 2 & 3)

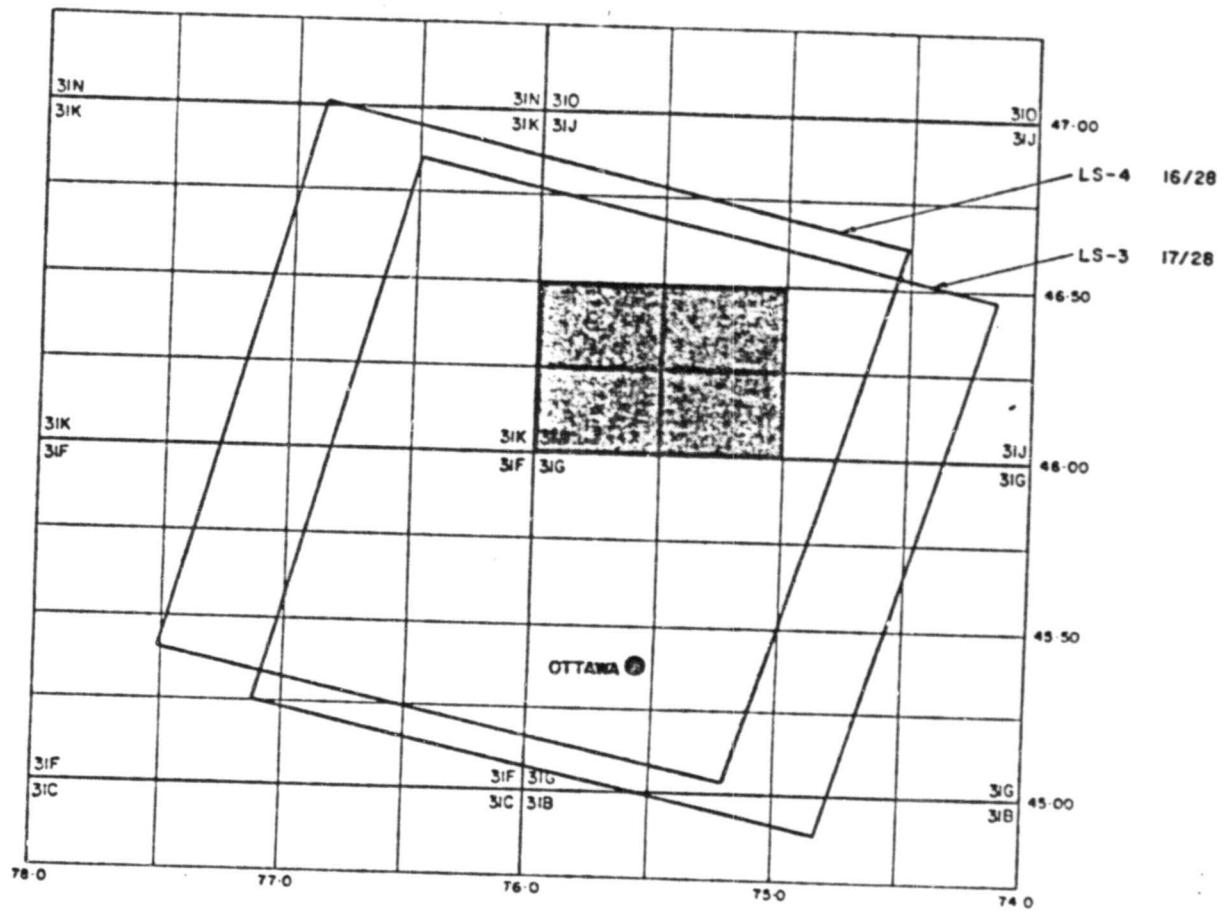

GEOCODED SUBSCENE DEFINITION

Figure 6.1

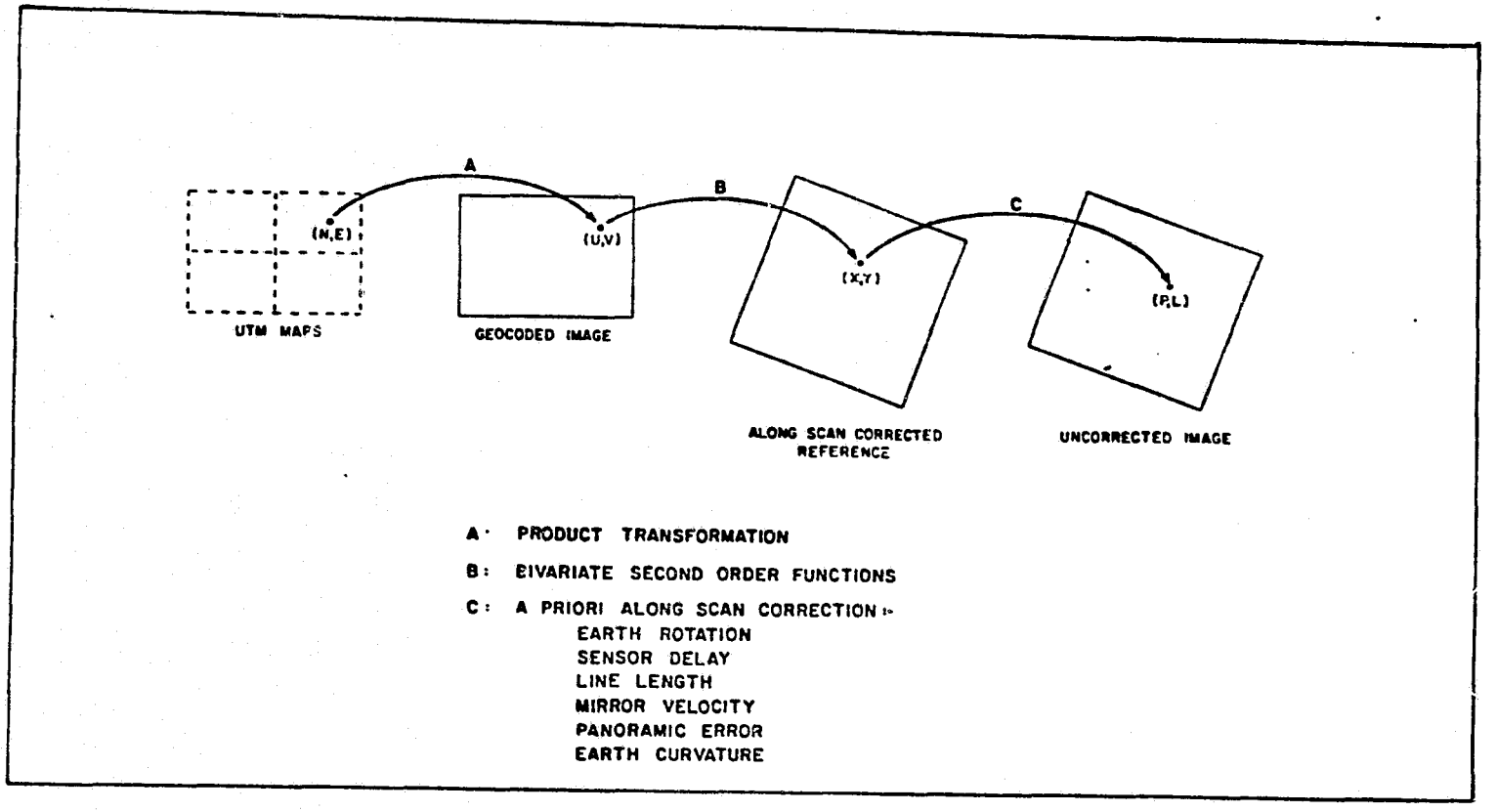

GEOMETRIC CORRECTION MODEL

Figure 6.2

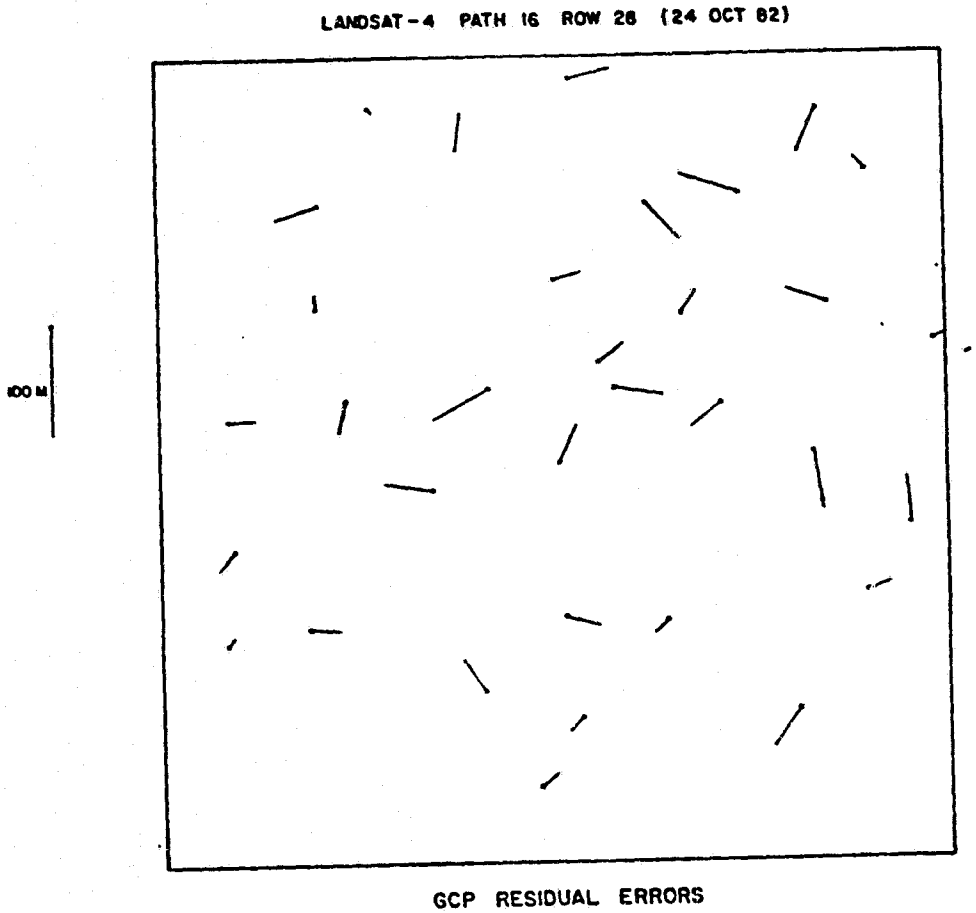

Figure 7.1

GCP RESIDUAL ERRORS COMPARISON

LANDSAT-1, 2, 3		LANDSAT-4		
SAT/PATH/ROW/CYCLE	RMS (METRES)	PATH/ROW/CYCLE	RMS (METRES)	LL
2 / 17 /24 / 093	33.5	16 / 24 / 003	42.6	(0-8)
1 / 17 / 28 / 079	30.0	16 / 28 / 005	39.7	(0-7)
2 / 17 / 28 / 071	38.7			
2 / 17 / 28 / 089	34.1			
2 / 17 / 28 / 084	43.0			
2 / 17 / 28 / 133	46.1			
3 / 17 / 28 / 085	34.6			
2 / 37 / 21 / 046	31.8	35 / 21 / 009	34.9	(0-8)
2 / 39 / 23 / 091	40.5	36 / 23 / 004	37.3	(0-2)
2 / 39 / 23 / 092	35.8			
2 / 39 / 23 / 132	33.0			
3 / 39 / 23 / 009	24.8			
2 / 42 / 22 / 050	29.4	39 / 22 / 005	36.9	(0-2)
2 / 42 / 22 / 092	40.7			
2 / 42 / 22 / 131	30.6			
	MEAN = 35.1 S.D. = 5.7		MEAN = 38.3	S.D. = 3.0

Table 7.2

LANDSAT-4 ABSOLUTE GEODETIC ERROR

PATH 16 ROW 28 CYCLE 005

GCP NO.	NORTHING ERROR (METRES)	EASTING ERROR (METRES)
1	-17	31
2	-47	4
3	23	-18
4	-15	12
5	40	38
6	18	-22
7	17	-1
8	32	-8
9	-30	33
10	-85	-10
11	-36	31
12	11	50
13	-10	-44
14	32	-54
MEAN	4.8	3.0
S.D.	36.0	31.4

Table 7.3

PRELIMINARY EVALUATION OF THE RADIOMETRIC CALIBRATION OF LANDSAT-4 THEMATIC MAPPER DATA BY THE CANADA CENTRE FOR REMOTE SENSING

Authors: J. Murphy, W. Park, A. Fitzgerald

Presented by: Jennifer Murphy

Canada Centre for Remote Sensing

2464 Sheffield Road

OTTAWA, Ontario

Canada K1A 0Y7

ABSTRACT

The technique being evaluated by the Canada Centre for Remote Sensing (CCRS) for the radiometric correction of LANDSAT-4 Thematic Mapper (TM) data is discussed. Preliminary results on the removal of radiometric striping, caused by inequalities in the calibration of individual detectors within each band, are presented. The destriping method was originally developed by CCRS for processing LANDSAT Multispectral Scanner (MSS) data and uses the scene histograms to equalize the responses of the individual detectors within each band. For the TM case, it may be applied to the forward and reverse scans either separately or in combination. CCRS is also evaluating the radiometric calibration of test scenes using the absolute pre-launch calibration tables supplied by NASA. Estimates of residual striping in the radiometrically corrected TM data are provided.

2.0 RAW DATA OBSERVATIONS

In this study three scenes have been used for the early testing of radiometric processing procedures. The first two are winter scenes acquired over Vancouver, British Columbia (path 48, row 26, November 11, 1982) and Ottawa, Ontario (path 16, row 28, December 12, 1982), respectively. The third, recorded over the coast of California (path 42, row 36, November 15, 1982) in the same time period was included in the test set in order to provide a greater dynamic range of raw TM data.

2.1 DETECTOR REPLACEMENT

The raw data has been examined in some detail to determine the signal-to-noise ratio of individual detectors within the seven bands. This forms part of an on-going study to determine the most appropriate replacement or smoothing techniques for dead or excessively noisy detectors. In the study reported here, the data from detector 3 of band 5 has simply been replaced with the data from detector 4 of band 5. Band 6 pixels and lines are replicated four times. For all other detectors, there is no data modification.

3.0 RADIOMETRIC CORRECTION METHOD

The radiometric correction process being evaluated for LANDSAT-4 TM data may be divided into three stages.

a) A reference detector is chosen for each spectral band, and the corrections required to place the data from this detector on an absolute scale are calculated, using in-flight calibration data, pre-launch calibration data and the maximum and minimum radiance values associated with the response of the band.

b) The relative differences between all other detectors in each band and the reference detector are calculated, using the means and standard deviations of the raw data values as calculated from the sums and the sums of the squares of the scene data values.

c) Finally, the absolute calibration of the reference detector for each band is combined with the relative calibration of the other detectors within the same band to provide an absolute calibration of all one hundred detectors.

3.3 RELATIVE GAIN AND OFFSET CALIBRATION

The histograms of the raw data for the Californian test scene were accumulated for all detectors of all bands, treating the forward scans and reverse scans separately. The histograms for all detectors of all bands for the first 1600 scan lines of the forward scans only are shown in Figures 3.1 to 3.7 for bands 1 to 7 respectively. The histograms for the forward and reverse sweeps were also combined, yielding one histogram for each detector of each band. These two sets of histograms were used to generate three different sets of relative gains and offsets, using the method outlined in Section 3.2. Firstly, the forward scans and reverse scans were treated independently, choosing a reference detector in each band for EACH scan direction, and setting its gain and offset to 1 and 0 respectively. These relative gains and offsets are shown in Table 3.1 for the forward scans and in Table 3.2 for the reverse scans. Secondly, the histograms for the forward scans and the reverse scans were added together, and the resulting relative gains and offsets, to be applied equally to the forward scans and reverse scans, are shown in Table 3.3. Thirdly, the forward scans and reverse scans were treated independently, but a reference detector in each band was chosen ONLY for the forward scan. The resulting relative gains and offsets are shown in Table 3.4 for the forward scans and in Table 3.5 for the reverse scans. Finally, the relative gains and offsets, assuming a reference detector number 1 for each band, were derived from the NASA pre-launch gains and offsets, and are shown in Table 3.6.

3.4 RELATIVE GAIN AND OFFSET OBSERVATIONS

Within each band, the largest variation in relative gain is seen to be 5%, with a maximum relative offset variation of approximately 1%. Comparison of Tables 3.1 and 3.2 shows that the relative intra-band calibration for the forward and reverse scans for all bands is almost identical. This factor is also reflected in the similarity between the relative intra-band calibration for either scan direction independently and for both scan directions combined. However, for the Californian test scene, the gain of the reverse scans relative to the gain of the forward scans is seen, from Table 3.5, to be 5% higher for bands 1, 2 and 3 and 1% higher for bands 4, 5, 6 and 7. Offsets are measured on a scale of 0-255.

The relative gains and offsets calculated from the NASA pre-launch calibration data indicate a similar relationship in the relative calibration of the detectors within each band, although the spread in relative gains is closer to 3% rather than to 5% as calculated from the histograms.

4.0 RESIDUAL RADIOMETRIC STRIPING

A simple method of assessing the radiometric striping in TM images consists of selecting arbitrary subscenes, and for each band plotting as a function of the line (or detector) number the radiometric intensity values averaged over a fixed number of pixels. In such profiles, the residual striping appears as a repetitive pattern with a period of sixteen lines which is added to the scene content. Because the scene data is averaged over a number of pixels, (for example 100 pixels), variations from line to line due to scene content tend to be small and gradual, particularly over uniform areas such as large water bodies. A detailed discussion and evaluation of this striping assessment method is given by Murphy (1981).

Figures 4.1 to 4.7 show the striping profiles for bands 1 to 7 respectively, on a 256 digital count scale, for a subscene extracted from a large ocean area in the Californian test scene. The striping both before and after calibration is shown for all bands using a 64-line by 50-pixel subscene.

For each band, a total of 5 graphs are shown, and they are identified as shown in Table 4.1.

TITLE	EXPLANATION
RAW	Raw data, before calibration.
METHOD 1	Forward and reverse scans corrected independently.
METHOD 2	Forward and reverse scans corrected using the same prelaunch gains and offsets.
METHOD 3	Forward and reverse scans corrected using one lookup table derived from combined forward and reverse histograms.
METHOD 4	Forward and reverse scans corrected independently, reference detector only in forward scan.

TABLE 4.1 SUMMARY OF DESTRIPING METHODS

For bands 2, 3, 4, 5 and 7, the striping before any corrections is seen to be less than 2 levels, and is reduced by all relative calibration procedures. For band 6, the striping is reduced from 3 levels to less than 1 level. In the uncorrected image for band 1, the striping is difficult to distinguish from the scene content. However, after corrections, the residual striping appears by this method to be between 1 and 2 levels.

5.0 RESULTS

Observations based on the residual striping estimates for a large ocean area in the Californian test scene using four different methods of relative calibration have shown no clear superiority of one method over the others. This indicates the need to quantify in more detail the differences between the radiometry of the forward and reverse scans as a function of line number within a full scene, using histograms of the raw data. An effective means of dealing with those detectors having significantly different singal-to-noise characteristics from the other detectors in the same band is required.

Observations of the histograms of the radiometrically corrected data show the necessity of choosing as reference detectors those which have the highest gain within a band. This will prevent the mapping of more than one raw digital level into the same output digital level. Discussion at the LANDSAT-4 Scientific Characterization Early Results Symposium focussed attention on the existence of "empty bins" and of "overpopulated bins" in the histograms of the corrected data from various sensors. This is to be expected with any system which quantizes analogue data and then performs digital intensity corrections. If the shape of the histograms is important in an analysis procedure, then the histogram should be used to estimate a probability density function. Strome (1980) discussed alternative methods for dealing with this problem for radiometrically corrected MSS data.

6.0 CONCLUSION

CCRS has initiated a study into the radiometric characteristics of the LANDSAT-4 TM sensor, with a view to developing absolute and relative radiometric calibration procedures. This early report has discussed the preliminary results from several different approaches to the relative correction of all detectors within each band. Further areas for study related to intra-band relative corrections have been outlined, and absolute calibration procedures will be developed using the internal calibration system.

REFERENCES

Butlin, T., Murphy, J. (1983) Early Processing of Thematic Mapper Data by the Canada Centre for Remote Sensing, Seventeenth International Symposium on Remote Sensing of Environment, Ann Arbor.

Murphy, J. (1981) A Refined Destriping Procedure for LANDSAT MSS Data Products, 7th Canadian Symposium on Remote Sensing, Winnipeg, pp. 454-470.

NASA (1982) Third LANDSAT Technical Working Group Meeting (LTWG), October.

Strome, W.M. et al. (1975) Format Specifications for Canadian LANDSAT MSS System Corrected Computer Compatible Tape, CCRS Research Report 75-3.

Strome, W.M., (1980) Histogram Estimation for Multiple Detector Sensors, 6th Canadian Symposium on Remote Sensing, Halifax.

DETECTOR	BAND 1		BAND 2		BAND 3		BAND 4	
	GAIN	OFFSET	GAIN	OFFSET	GAIN	OFFSET	GAIN	OFFSET
1	1.0000	0.0000	1.0000	0.0000	1.0000	0.0000	1.0000	0.0000
2	1.0051	-0.7881	0.9696	-0.0001	0.9808	-0.4033	0.9946	-1.0195
3	1.0147	-0.7633	0.9819	-0.6206	0.9837	-0.3435	1.0043	-0.5271
4	1.0132	-0.3259	0.9345	1.3503	0.9845	-0.8598	0.9990	-1.2205
5	1.0084	-0.9733	1.0064	-0.6684	0.9963	-0.7476	0.9926	-1.0335
6	1.0030	-0.8576	0.9939	-0.3946	0.9937	-0.6218	1.0024	-0.7828
7	0.9924	-0.9355	0.9787	-0.4762	0.9780	-0.4821	0.9933	-0.6278
8	1.0078	-0.9192	0.9782	-0.3961	0.9726	-0.4312	0.9969	-0.8669
9	1.0081	-1.5715	0.9892	-0.6510	0.9952	-0.8642	0.9925	-0.6424
10	1.0207	-1.2342	0.9888	-0.8439	0.9877	-0.6047	1.0345	-0.7959
11	1.0204	-2.1188	0.9889	-0.8172	0.9897	-1.0820	0.9859	-0.5398
12	1.0268	-1.2495	0.9847	-0.8172	1.0018	-0.8314	1.0045	-0.8770
13	1.0276	-2.0676	1.0101	-0.9393	1.0056	-1.0515	1.0126	-0.8800
14	1.0330	-2.2611	1.0048	-0.9155	1.0007	-0.6141	0.9966	-0.6112
15	1.0483	-2.7819	1.0251	-1.0311	1.0146	-1.0272	0.9896	-0.8195
16	1.0562	-2.8072	0.9917	-0.9283	0.9907	-0.6496	0.9980	-0.6104

DETECTOR	BAND 5		BAND 6		BAND 7	
	GAIN	OFFSET	GAIN**	OFFSET**	GAIN	OFFSET
1	1.0000	0.0000	1.0000	0.0000	1.0000	0.0000
2	0.9903	0.3304	1.0000	0.0000	0.9805	-0.1691
3	0.9946*	-0.0969*	1.0000	0.0000	0.9884	-0.2418
4	0.9946	-0.0969	1.0000	0.0000	0.9894	-0.3812
5	0.9949	-0.8718	1.0072	1.4032	0.9787	-0.5731
6	1.0112	-0.5493	1.0072	1.4032	0.9797	-0.2085
7	1.0204	-0.4570	1.0072	1.4032	0.9940	-0.6022
8	1.0171	-0.1845	1.0072	1.4032	0.9607	-0.1861
9	1.0155	-0.6614	0.9717	2.4665	0.9949	-0.5222
10	0.9971	-0.2960	0.9717	2.4665	0.9757	-0.3183
11	1.0356	-0.5915	0.9717	2.4665	0.9917	-0.4579
12	1.0363	-0.3753	0.9717	2.4665	0.9979	-0.2246
13	1.0241	-0.6168	1.0222	-0.2998	0.9844	-0.5178
14	1.0161	-0.3217	1.0222	-0.2998	0.9842	-0.2943
15	1.0091	-0.7547	1.0222	-0.2998	0.9707	-0.5193
16	1.0267	-0.4893	1.0222	-0.2998	1.0033	-0.2799

*Failed detector replaced by adjacent detector

**Replicated 4 times

RELATIVE GAINS AND OFFSETS,

USING HISTOGRAMS, REVERSE SCAN ONLY, CALIFORNIA SCENE

TABLE 3.2

DETECTOR	BAND 1		BAND 2		BAND 3		BAND 4	
	GAIN	OFFSET	GAIN	OFFSET	GAIN	OFFSET	GAIN	OFFSET
1	1.0000	0.0000	1.0000	0.0000	1.0000	0.0000	1.0000	0.0000
2	1.0039	-0.6416	0.9686	0.0320	0.9804	-0.3950	0.9934	-0.9306
3	1.0171	-0.9148	0.9861	-0.7299	0.9873	-0.4417	1.0060	-0.5541
4*	1.0139	-0.4417	0.9382	1.2030	0.9901	-1.0224	0.9989	-1.1325
5	1.0086	-1.0367	1.0140	-0.8926	1.0020	-0.9082	0.9940	-0.9847
6	1.0062	-1.0608	1.0065	-0.7763	1.0035	-0.9386	1.0048	-0.7736
7	1.0002	-1.4956	0.9962	-0.9986	0.9927	-0.9398	0.9999	-0.7847
8	1.0145	-1.4110	0.9974	-0.9919	0.9888	-0.9576	1.0036	-1.0330
9	1.0130	-1.9947	1.0058	-1.1820	1.0099	-1.3618	0.9996	-0.8654
10	1.0224	-1.4132	1.0003	-1.2268	0.9969	-0.9437	1.0377	-0.8744
11	1.0228	-2.3670	0.9999	-1.2037	0.9985	-1.4286	0.9913	-0.7320
12	1.0257	-1.3593	0.9936	-1.1430	1.0096	-1.1606	1.0093	-1.0941
13	1.0289	-2.2193	1.0209	-1.3010	1.0145	-1.3821	1.0193	-1.1426
14	1.0354	-2.4720	1.0170	-1.3211	1.0101	-0.9705	1.0031	-0.8770
15	1.0509	-3.0255	1.0379	-1.4728	1.0247	-1.4142	0.9985	-1.2094
16	1.0548	-2.8177	0.9989	-1.2146	0.9959	-0.9282	1.0013	-0.8034

DETECTOR	BAND 5		BAND 6		BAND 7		NOTES
	GAIN	OFFSET	GAIN**	OFFSET**	GAIN	OFFSET	
1	1.0000	0.0000	1.0000	0.0000	1.0000	0.0000	*Failed detector replaced by adjacent detector
2	0.9914	0.3457	1.0000	0.0000	0.9827	-0.1742	
3	0.9912*	0.3048*	1.0000	0.0000	0.9884	-0.1938	
4	0.9912	0.3048	1.0000	0.0000	0.9864	-0.1994	
5	0.9886	-0.2571	1.0078	1.3885	0.9713	-0.2827	**Replicated 4 times
6	1.0039	0.0575	1.0078	1.3885	0.9710	0.1022	
7	1.0136	0.0706	1.0078	1.3885	0.9870	-0.4106	
8	1.0101	0.3444	1.0078	1.3885	0.9520	0.0874	
9	1.0094	-0.2120	0.9694	2.7018	0.9864	-0.2858	
10	0.9923	0.0063	0.9694	2.7018	0.9662	-0.0536	
11	1.0288	-0.2332	0.9694	2.7018	0.9820	-0.2553	
12	1.0303	-0.0892	0.9694	2.7018	0.9887	-0.0302	
13	1.0195	-0.3601	1.0232	-0.4413	0.9766	-0.3438	
14	1.0133	-0.1651	1.0232	-0.4413	0.9780	-0.1559	
15	1.0047	-0.5183	1.0232	-0.4413	0.9634	-0.3696	
16	1.0201	-0.1233	1.0232	-0.4413	0.9939	-0.0507	

RELATIVE GAINS AND OFFSETS, USING HISTOGRAMS
CALIFORNIA SCENE
FORWARD SCAN

TABLE 3.4

DETECTOR	BAND 1		BAND 2		BAND 3		BAND 4	
	GAIN	OFFSET	GAIN	OFFSET	GAIN	OFFSET	GAIN	OFFSET
1	1.0360	-2.6076	1.0295	-0.9411	1.0273	-0.9541	1.0156	-0.6614
2	1.0413	-3.4089	0.9982	-0.9126	1.0075	-1.3390	1.0101	-1.6773
3	1.0513	-3.4093	1.0108	-1.5446	1.0105	-1.2820	1.0199	-1.1914
4	1.0497	-2.9679	0.9620	0.4709	1.0114	-1.7991	1.0145	-1.8813
5	1.0447	-3.6028	1.0361	-1.6155	1.0234	-1.6981	1.0081	-1.6900
6	1.0391	-3.4730	1.0232	-1.3299	1.0208	-1.5699	1.0180	-1.4458
7	1.0281	-3.5232	1.0076	-1.3973	1.0046	-1.4151	1.0088	-1.2848
8	1.0441	-3.5471	1.0070	-1.3166	0.9991	-1.3592	1.0124	-1.5254
9	1.0444	-4.2001	1.0184	-1.5819	1.0223	-1.8137	1.0079	-1.2988
10	1.0575	-3.8958	1.0180	-1.7744	1.0147	-1.5471	1.0506	-1.4801
11	1.0572	-4.7797	1.0181	-1.7478	1.0166	-2.0262	1.0013	-1.1919
12	1.0638	-3.9269	1.0137	-1.7439	1.0291	-1.7872	1.0201	-1.5414
13	1.0646	-4.7472	1.0399	-1.8898	1.0330	-2.0109	1.0284	-1.5497
14	1.0702	-4.9548	1.0344	-1.8610	1.0279	-1.5688	1.0121	-1.2704
15	1.0861	-5.5155	1.0553	-1.9958	1.0422	-1.9952	1.0051	-1.4741
16	1.0942	-5.5613	1.0210	-1.8616	1.0177	-1.5948	1.0136	-1.2705

DETECTOR	BAND 5		BAND 6		BAND 7		NOTES
	GAIN	OFFSET	GAIN**	OFFSET**	GAIN	OFFSET	
1	1.0067	-0.3869	1.0130	-1.2717	1.0095	-0.2692	* Failed detector replaced by adjacent detector
2	0.9970	-0.0528	1.0130	-1.2717	0.9898	-0.4331	
3	1.0013	-0.4817*	1.0130	-1.2717	0.9978	-0.5079	
4	1.0013	-0.4817	1.0130	-1.2717	0.9988	-0.6476	
5	1.0016	-1.2567	1.0203	0.1223	0.9879	-0.8366	** Replicated 4 times
6	1.0180	-0.9405	1.0203	0.1223	0.9890	-0.4723	
7	1.0272	-0.8518	1.0203	0.1223	1.0034	-0.8699	
8	1.0239	-0.5781	1.0203	0.1223	0.9698	-0.4448	
9	1.0224	-1.0544	0.9843	1.2309	1.0043	-0.7901	
10	1.0038	-0.6819	0.9843	1.2309	0.9849	-0.5810	
11	1.0425	-0.9922	0.9843	1.2309	1.0011	-0.7249	
12	1.0433	-0.7763	0.9843	1.2309	1.0074	-0.4933	
13	1.0310	-1.0131	1.0355	-1.5997	0.9938	-0.7828	
14	1.0229	-0.7148	1.0355	-1.5997	0.9936	-0.5593	
15	1.0159	-1.1452	1.0355	-1.5997	0.9799	-0.7807	
16	1.0336	-0.8866	1.0355	-1.5997	1.0129	-0.5500	

RELATIVE GAINS AND OFFSETS,
USING HISTOGRAMS, REVERSE SCAN ONLY, USING DETECTOR 1
OF FORWARD SCAN AS REFERENCE DETECTOR,
CALIFORNIA SCENE

TABLE 3.5

DETECTOR	BAND 1		BAND 2		BAND 3		BAND 4	
	GAIN	OFFSET	GAIN	OFFSET	GAIN	OFFSET	GAIN	OFFSET
1	1.0000	0.0000	1.0000	0.0000	1.0000	0.0000	1.0000	0.0000
2	1.0074	-0.8103	0.9930	-0.6475	0.9837	-0.5143	0.9858	-0.5562
3	1.0180	-0.5904	0.9804	-0.5280	0.9826	-0.1937	1.0042	-0.5830
4	1.0180	-0.6555	0.9963	-0.5436	0.9771	-0.6168	0.9871	-0.6763
5	1.0104	-0.5451	1.0026	-0.5762	0.9858	-0.5055	0.9854	-0.7374
6	1.0055	-0.6889	1.0010	-0.4559	0.9894	-0.4837	0.9964	-0.5694
7	1.0025	-0.6104	0.9856	-0.6341	0.9818	-0.5371	0.9856	-0.2803
8	1.0069	-0.6458	0.9883	-0.4457	0.9766	-0.5423	0.9914	-0.6800
9	1.0113	-0.5840	0.9879	-0.5755	0.9877	-0.5629	0.9898	-0.6195
10	1.0136	-0.7535	0.9900	-0.6215	0.9804	-0.5935	1.0290	-0.8721
11	1.0025	-0.6632	0.9784	-0.5685	0.9780	-0.6064	0.9800	-0.5527
12	1.0108	-0.7104	0.9803	-0.6049	0.9875	-0.6048	0.9935	-0.7284
13	1.0030	-0.6319	0.9926	-0.5970	0.9914	-0.6661	1.0076	-0.8815
14	1.0071	-0.7707	0.9959	-0.5134	0.9872	-0.4352	0.9944	-0.6032
15	1.0086	-0.6271	1.0025	-0.6274	0.9992	-0.5922	0.9816	-0.7929
16	1.0144	-0.8593	0.9761	-0.4990	0.9728	-0.4316	0.9869	-0.5022

DETECTOR	BAND 5		BAND 6		BAND 7		
	GAIN	OFFSET	GAIN	OFFSET	GAIN	OFFSET	NOTES
1	1.0000	0.0000			1.0000	0.0000	
2	1.0034	-0.3471	NO DATA		0.9901	-0.5524	*Failed detector
3	1.0148*	-0.4737*			0.9963	-0.5657	replaced by
4	1.0148	-0.4737	AVAILABLE		0.9965	-0.5138	adjacent detector
5	1.0031	-0.2859			0.9966	-0.6725	
6	1.0042	-0.2630			0.9896	-0.4596	
7	1.0110	-0.3060			0.9972	-0.6603	
8	1.0078	-0.1602			0.9805	-0.5138	
9	1.0052	-0.2702			0.9978	-0.6028	
10	1.0051	-0.3712			0.9765	-0.4286	
11	1.0143	-0.2866			0.9915	-0.6133	
12	1.0155	-0.4462			0.9980	-0.4515	
13	1.0129	-0.2138			0.9859	-0.7494	
14	1.0090	-0.3577			0.9968	-0.3641	
15	1.0097	-0.1654			0.9863	-0.7546	
16	1.0153	-0.3540			1.0017	-0.3848	

RELATIVE GAINS AND OFFSETS, USING NASA PRELAUNCH CALIBRATION DATA

TABLE 3.6

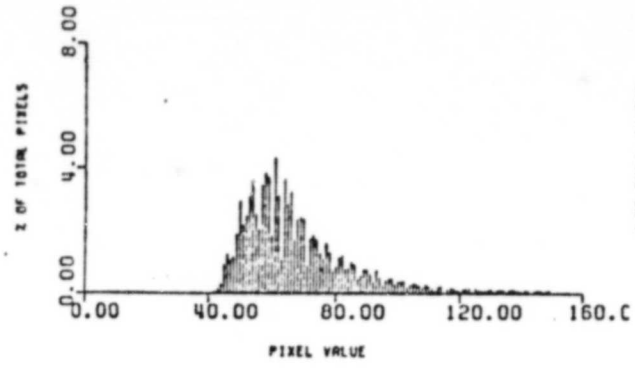

END OF PLOT FOR BAND 1 DETECTOR 1

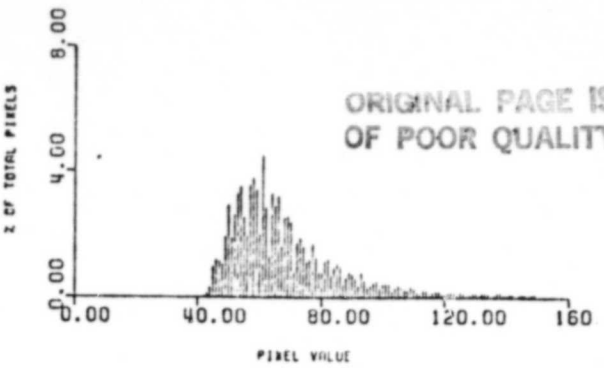

END OF PLOT FOR BAND 1 DETECTOR 3

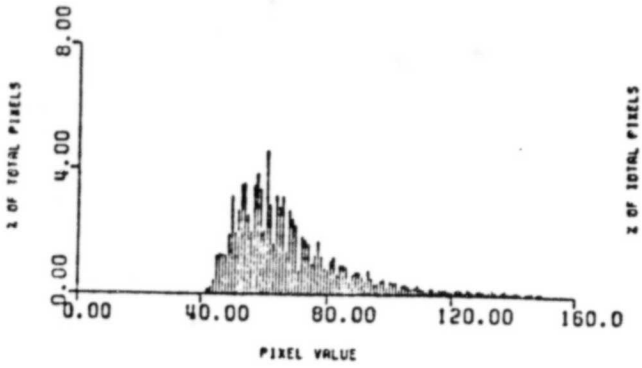

END OF PLOT FOR BAND 1 DETECTOR 2

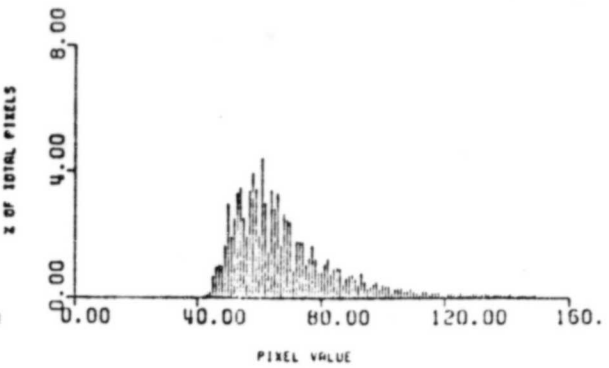

END OF PLOT FOR BAND 1 DETECTOR 4

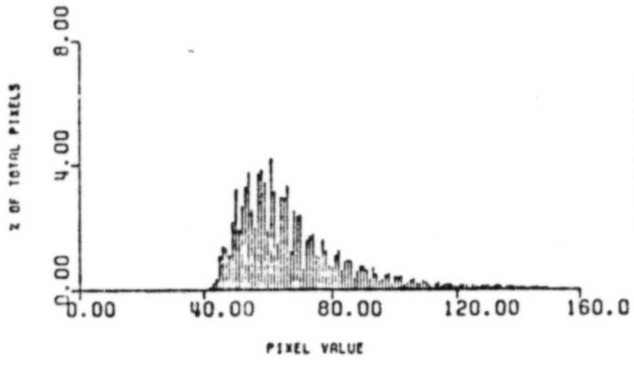

END OF PLOT FOR BAND 1 DETECTOR 5

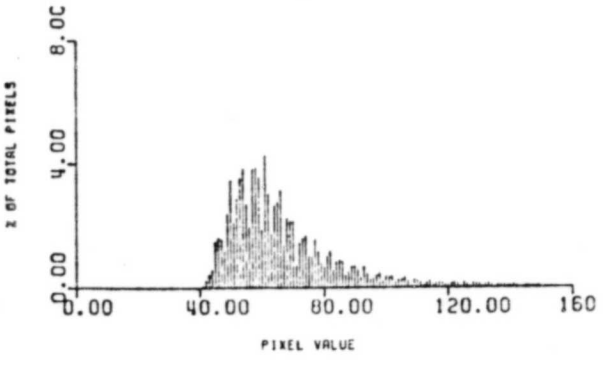

END OF PLOT FOR BAND 1 DETECTOR 7

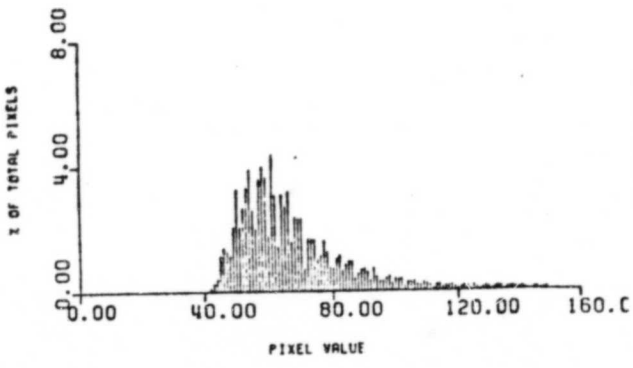

END OF PLOT FOR BAND 1 DETECTOR 6

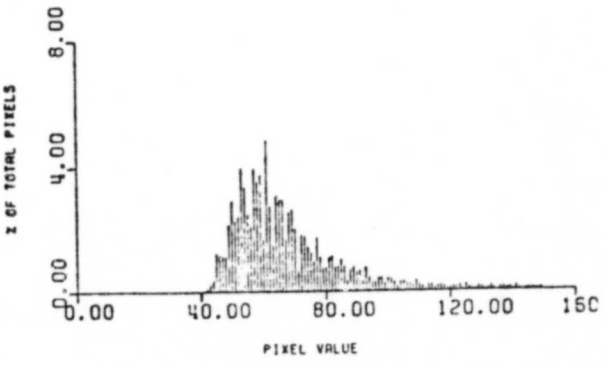

END OF PLOT FOR BAND 1 DETECTOR 8

FIGURE 3.1 BAND 1 HISTOGRAMS

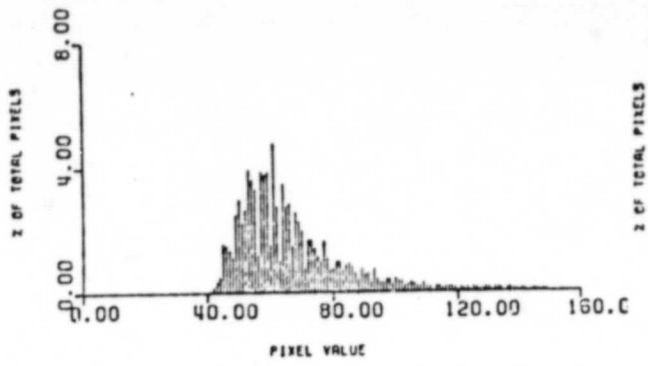

END OF PLOT FOR BAND 1 DETECTOR 9

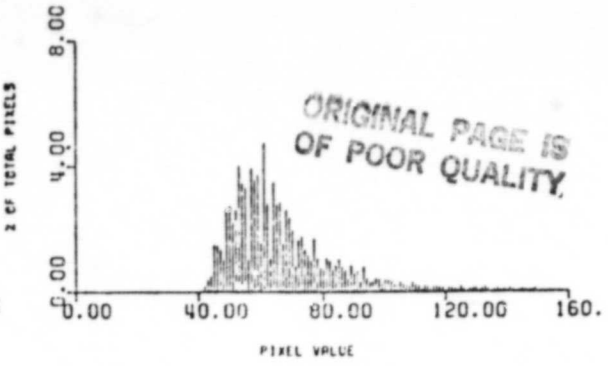

END OF PLOT FOR BAND 1 DETECTOR 11

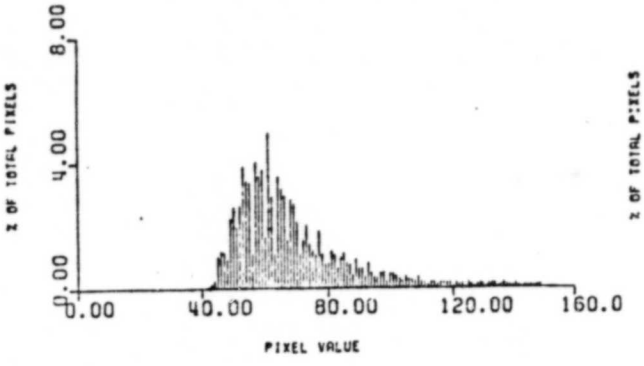

END OF PLOT FOR BAND 1 DETECTOR 10

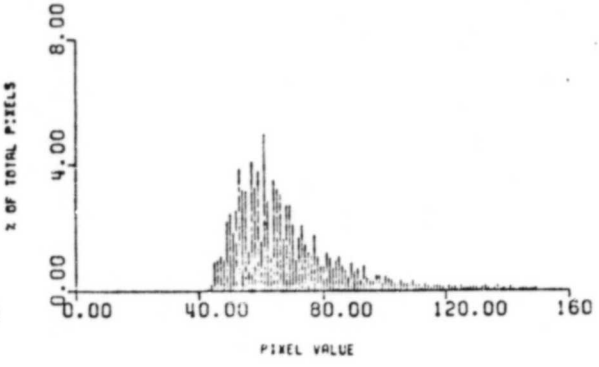

END OF PLOT FOR BAND 1 DETECTOR 12

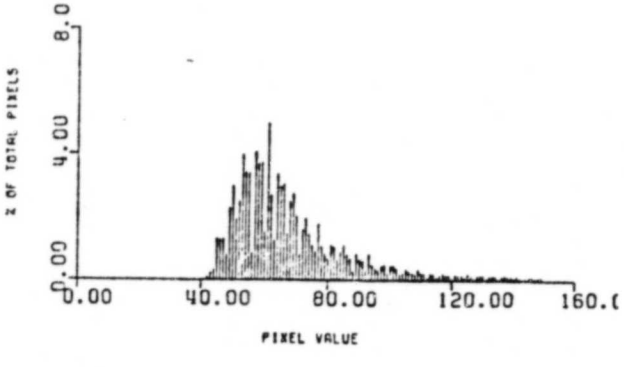

END OF PLOT FOR BAND 1 DETECTOR 13

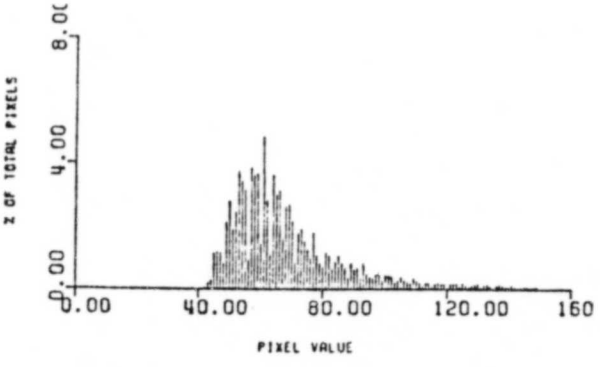

END OF PLOT FOR BAND 1 DETECTOR 15

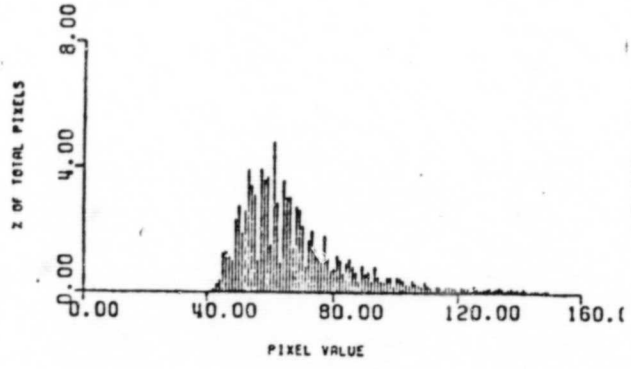

END OF PLOT FOR BAND 1 DETECTOR 14

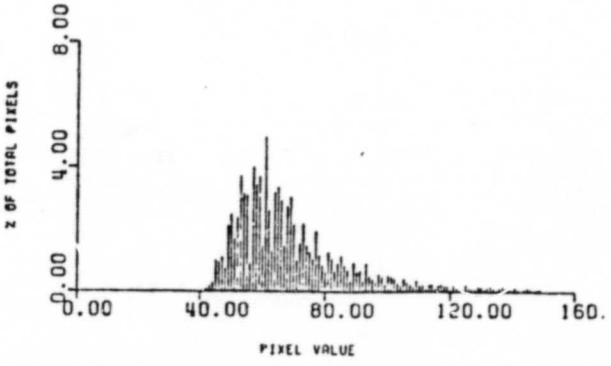

END OF PLOT FOR BAND 1 DETECTOR 16

FIGURE 3.1 (CONT) BAND 1 HISTOGRAMS

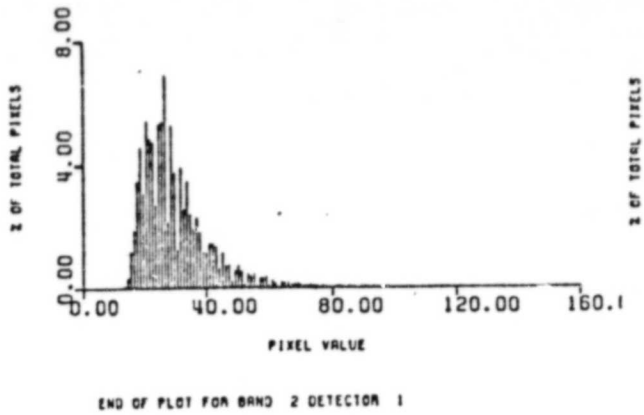

END OF PLOT FOR BAND 2 DETECTOR 1

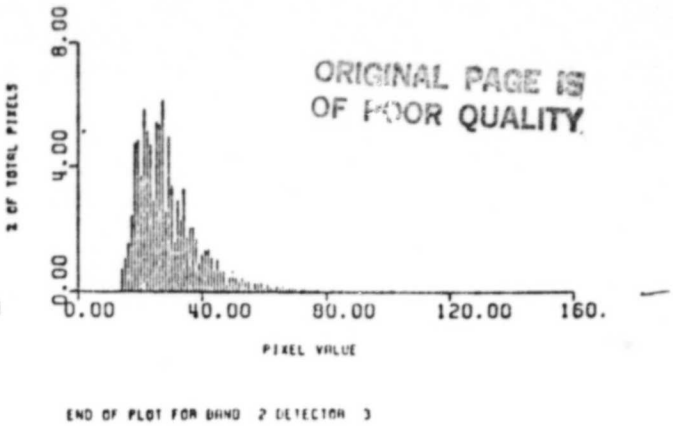

END OF PLOT FOR BAND 2 DETECTOR 3

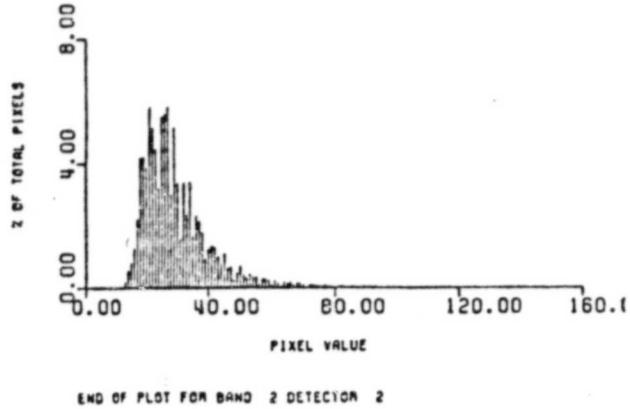

END OF PLOT FOR BAND 2 DETECTOR 2

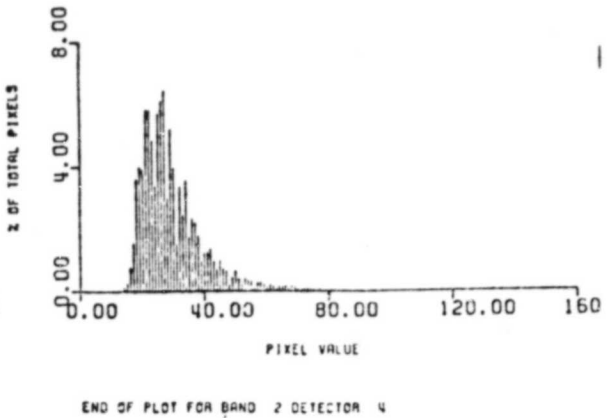

END OF PLOT FOR BAND 2 DETECTOR 4

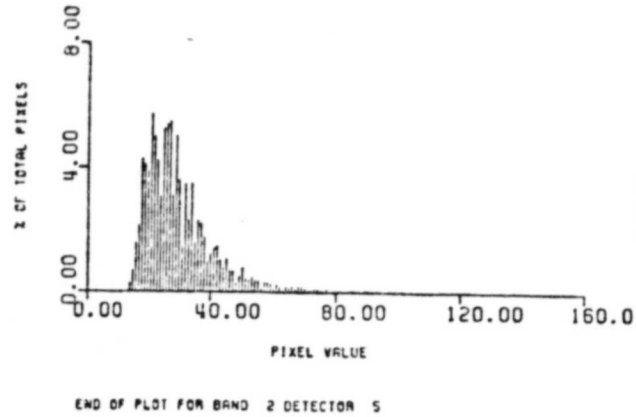

END OF PLOT FOR BAND 2 DETECTOR 5

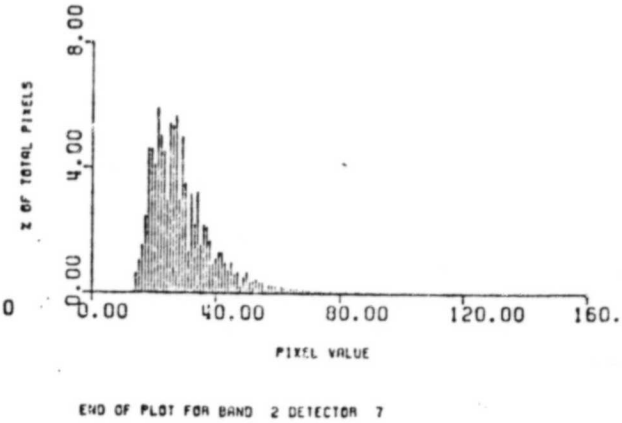

END OF PLOT FOR BAND 2 DETECTOR 7

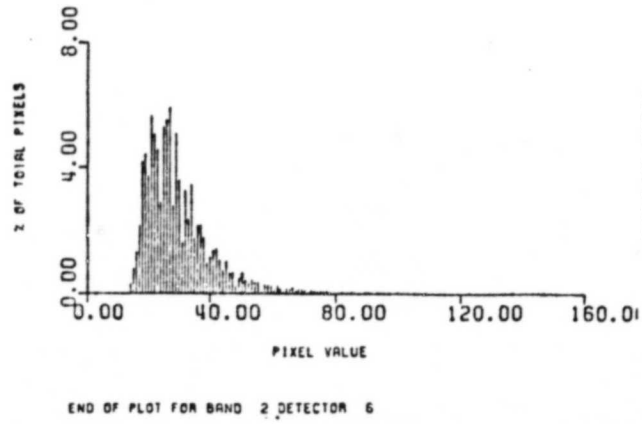

END OF PLOT FOR BAND 2 DETECTOR 6

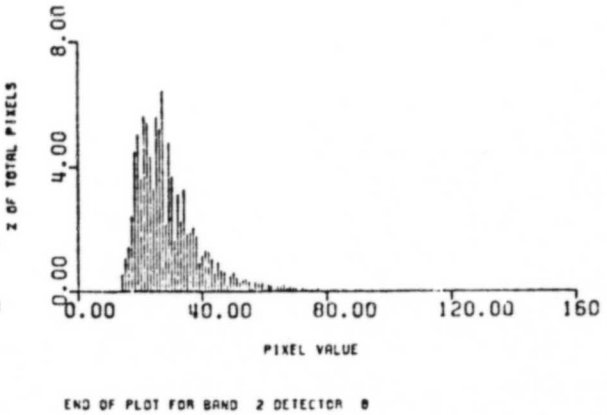

END OF PLOT FOR BAND 2 DETECTOR 8

FIGURE 3.2 BAND 2 HISTOGRAMS

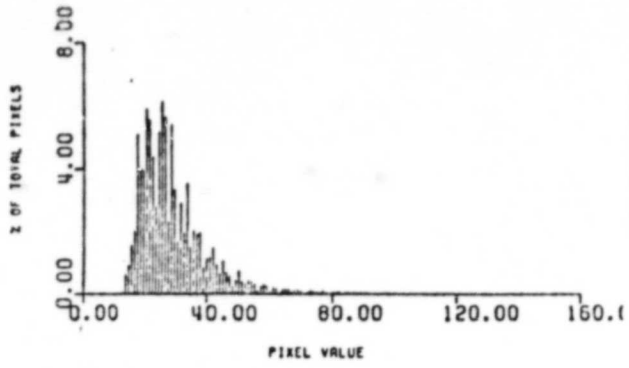

END OF PLOT FOR BAND 2 DETECTOR 9

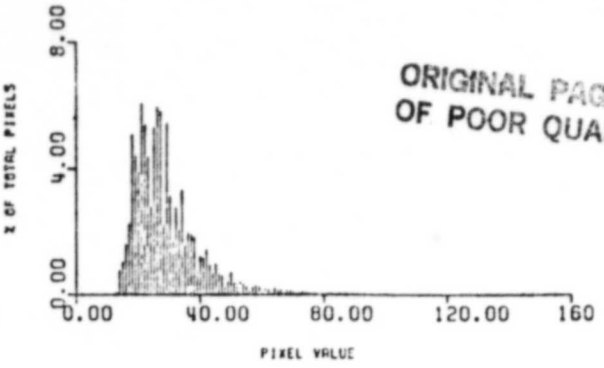

END OF PLOT FOR BAND 2 DETECTOR 11

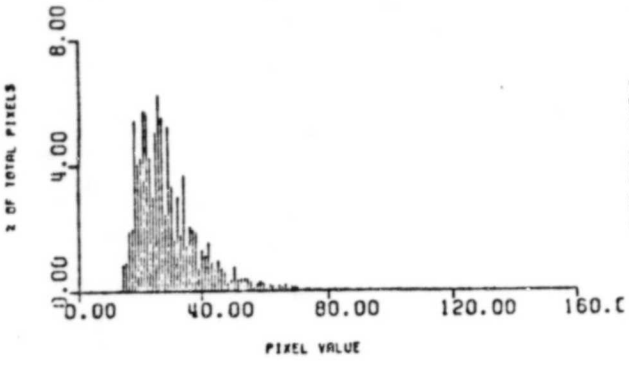

END OF PLOT FOR BAND 2 DETECTOR 10

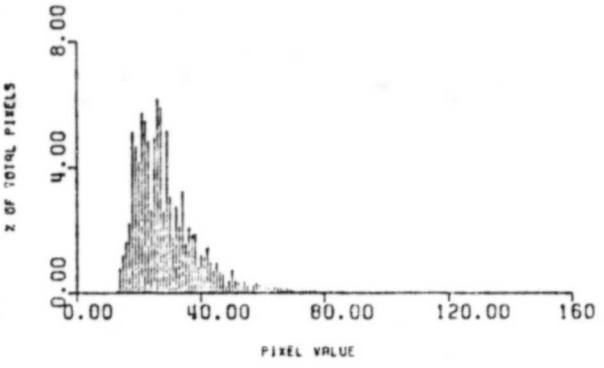

END OF PLOT FOR BAND 2 DETECTOR 12

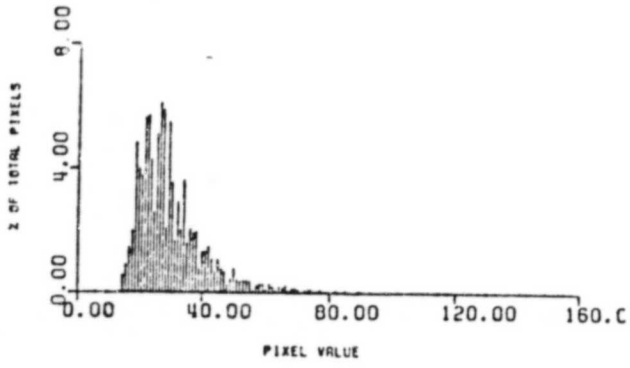

END OF PLOT FOR BAND 2 DETECTOR 13

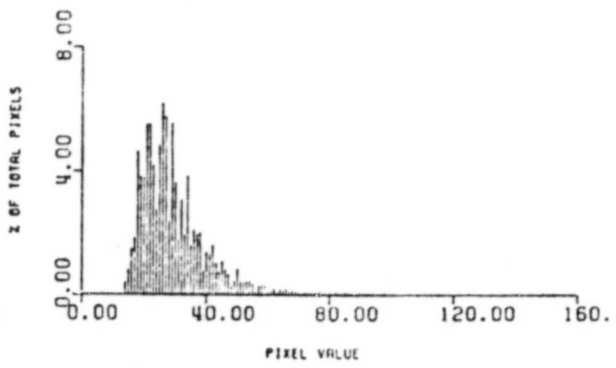

END OF PLOT FOR BAND 2 DETECTOR 15

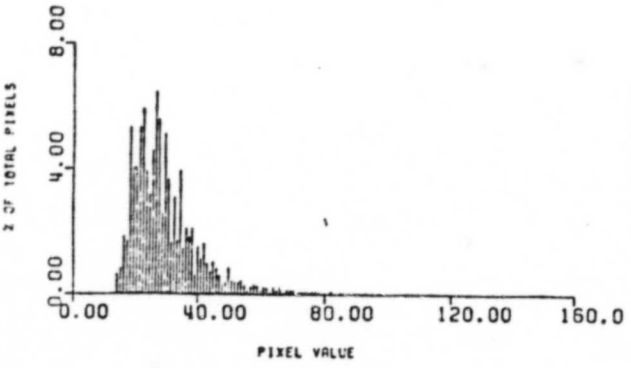

END OF PLOT FOR BAND 2 DETECTOR 14

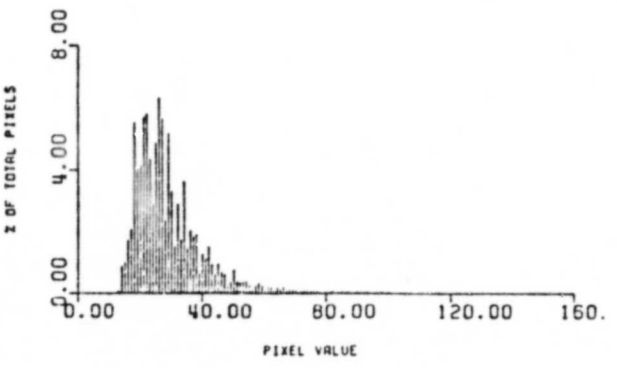

END OF PLOT FOR BAND 2 DETECTOR 16

FIGURE 3.2 (CONT) BAND 2 HISTOGRAMS

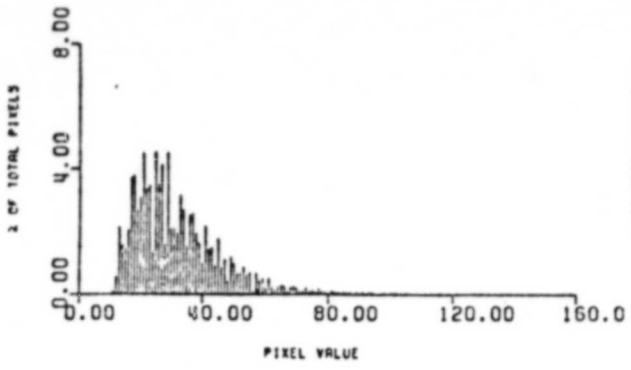

END OF PLOT FOR BAND 3 DETECTOR 9

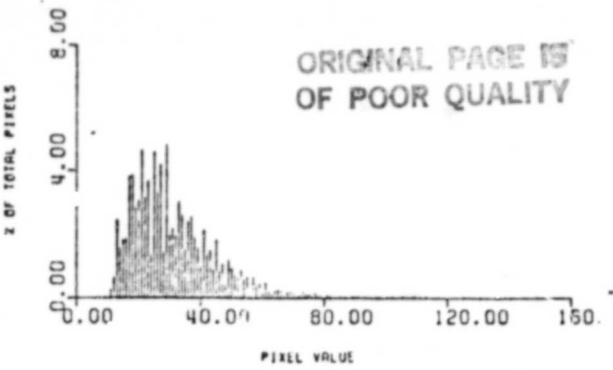

END OF PLOT FOR BAND 3 DETECTOR 11

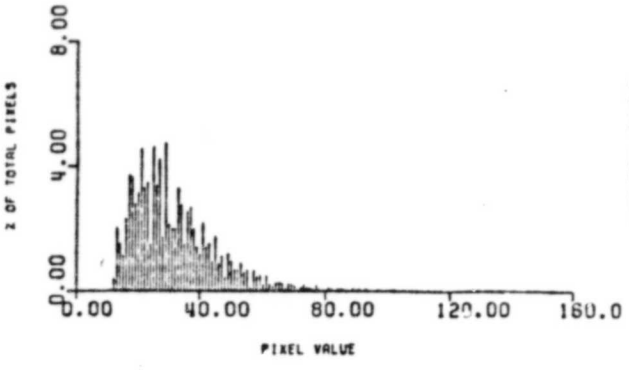

END OF PLOT FOR BAND 3 DETECTOR 10

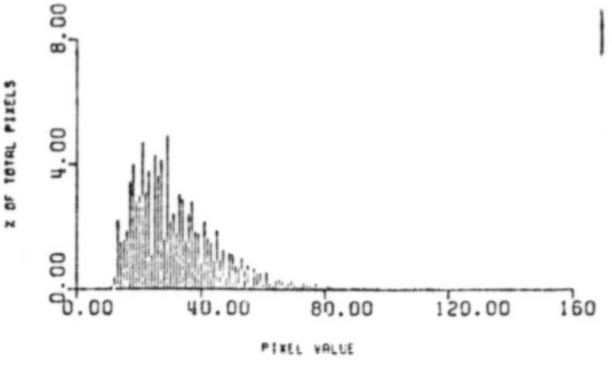

END OF PLOT FOR BAND 3 DETECTOR 12

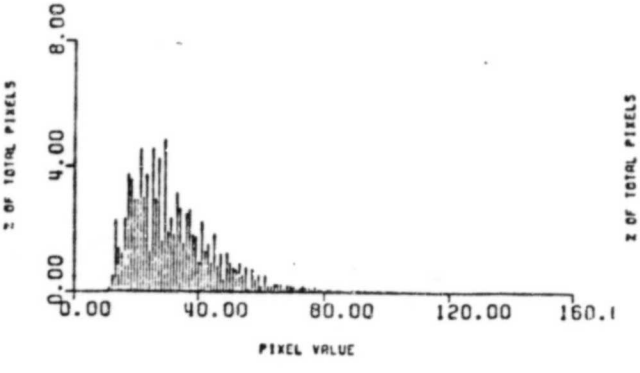

END OF PLOT FOR BAND 3 DETECTOR 13

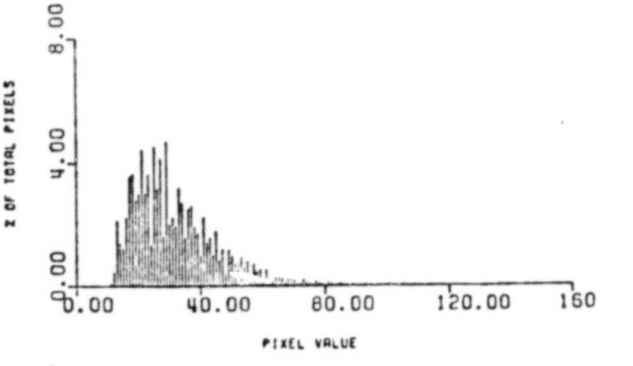

END OF PLOT FOR BAND 3 DETECTOR 15

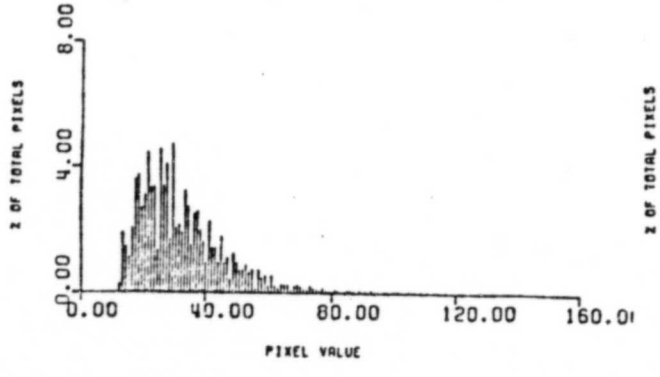

END OF PLOT FOR BAND 3 DETECTOR 14

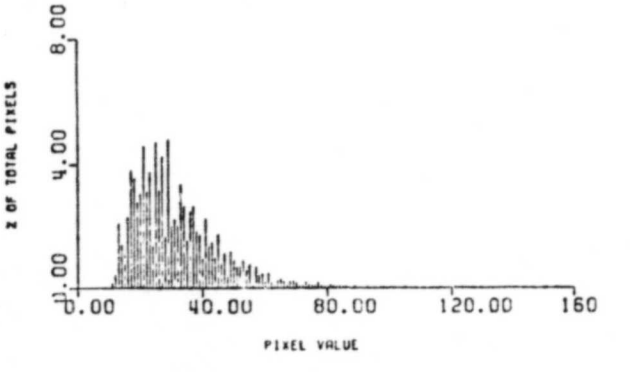

END OF PLOT FOR BAND 3 DETECTOR 16

FIGURE 3.3 (CONT) BAND 3 HISTOGRAMS

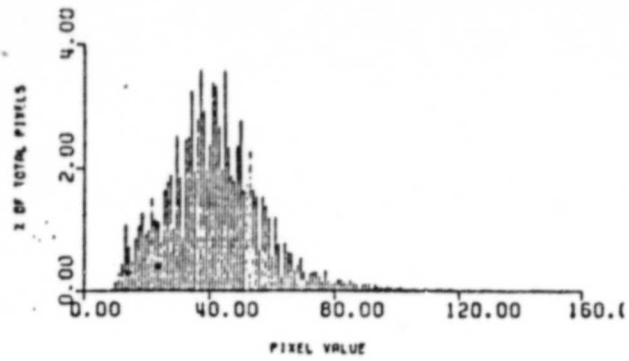

END OF PLOT FOR BAND 4 DETECTOR 1

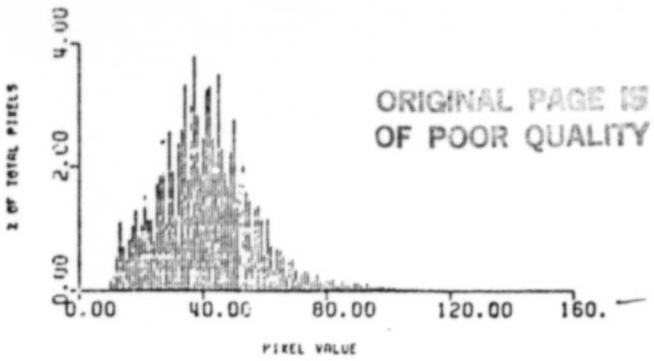

END OF PLOT FOR BAND 4 DETECTOR 3

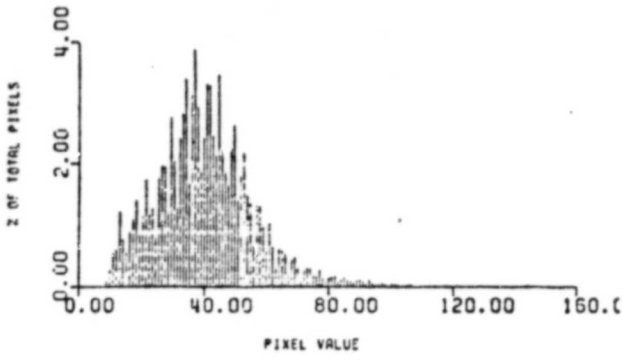

END OF PLOT FOR BAND 4 DETECTOR 2

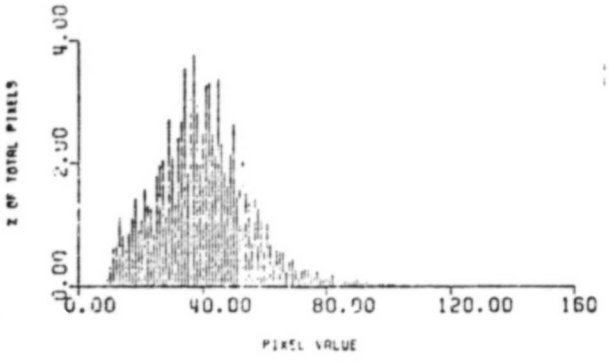

END OF PLOT FOR BAND 4 DETECTOR 4

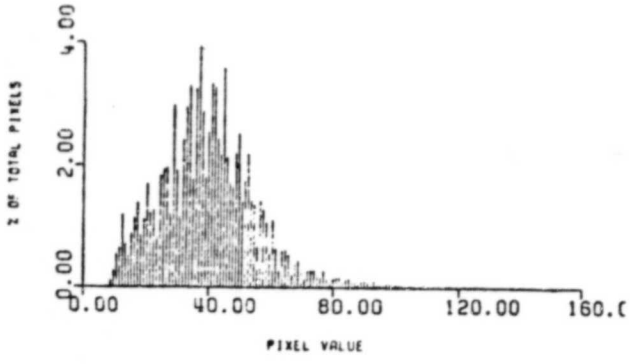

END OF PLOT FOR BAND 4 DETECTOR 5

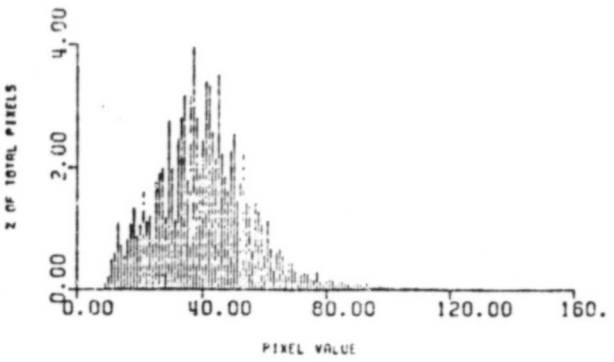

END OF PLOT FOR BAND 4 DETECTOR 7

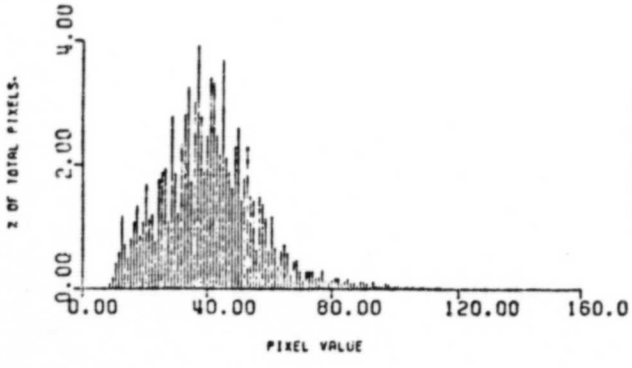

END OF PLOT FOR BAND 4 DETECTOR 6

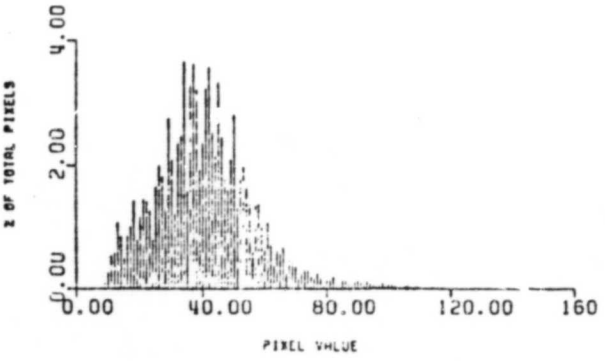

END OF PLOT FOR BAND 4 DETECTOR 8

FIGURE 3.4 BAND 4 HISTOGRAMS

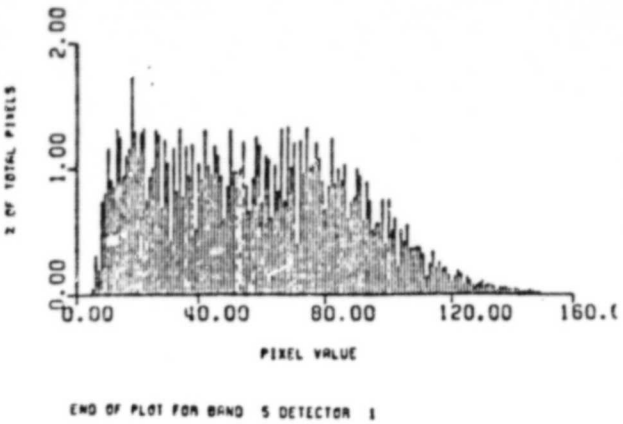

END OF PLOT FOR BAND 5 DETECTOR 1

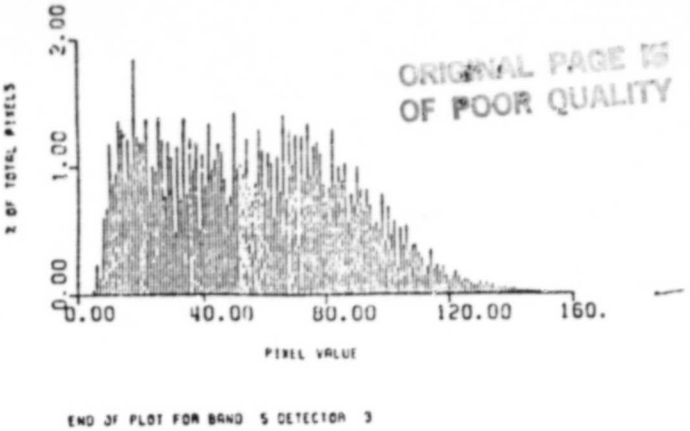

END OF PLOT FOR BAND 5 DETECTOR 3

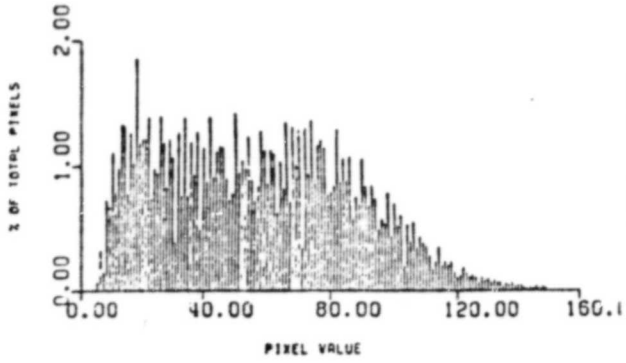

END OF PLOT FOR BAND 5 DETECTOR 2

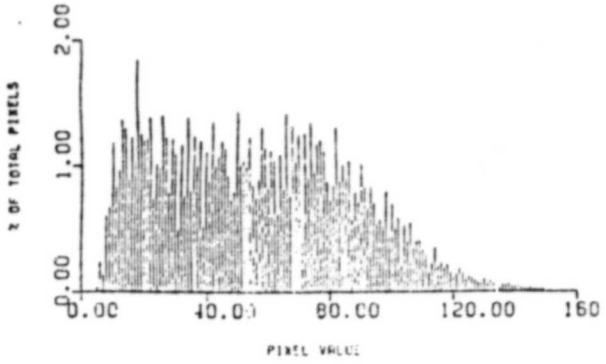

END OF PLOT FOR BAND 5 DETECTOR 4

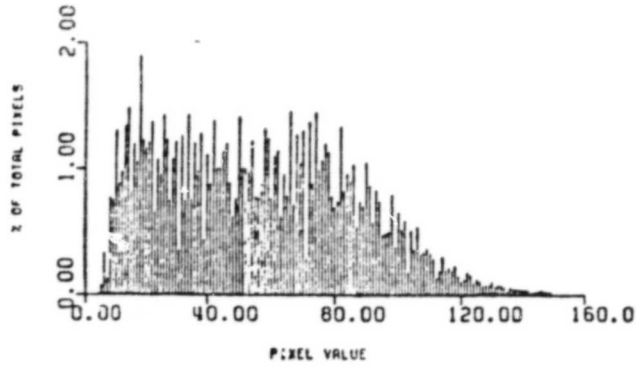

END OF PLOT FOR BAND 5 DETECTOR 5

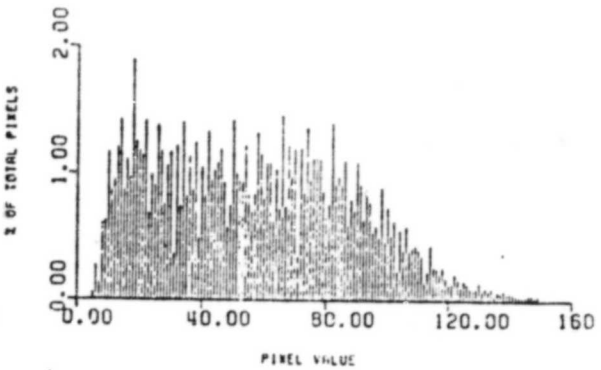

END OF PLOT FOR BAND 5 DETECTOR 7

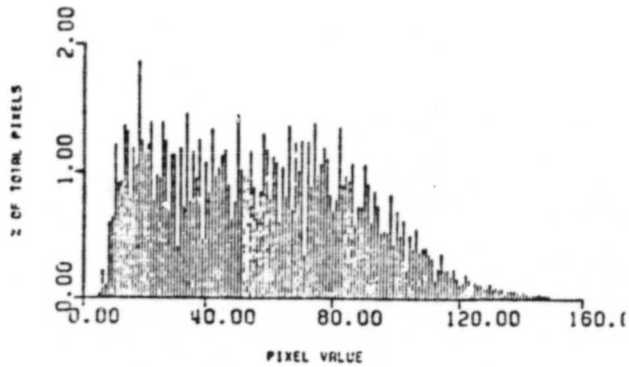

END OF PLOT FOR BAND 5 DETECTOR 6

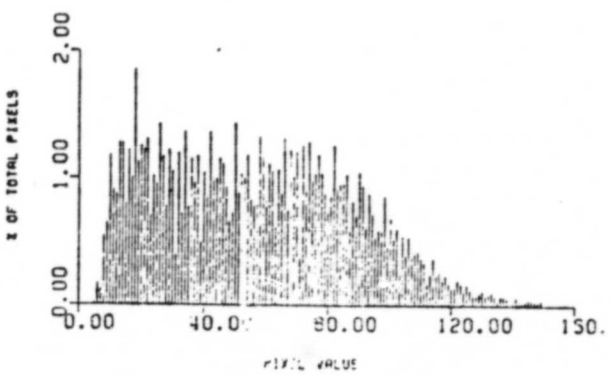

END OF PLOT FOR BAND 5 DETECTOR 8

FIGURE 3.5 BAND 5 HISTOGRAMS

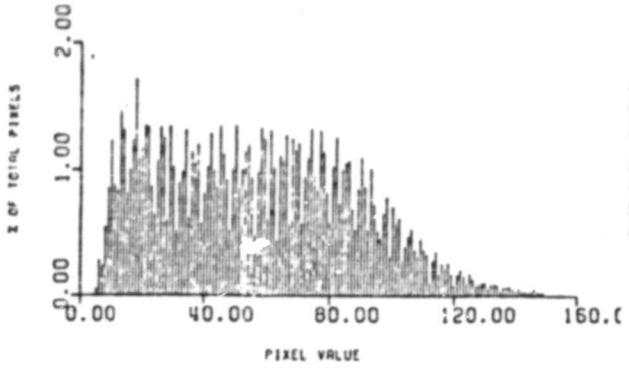

END OF PLOT FOR BAND 5 DETECTOR 9

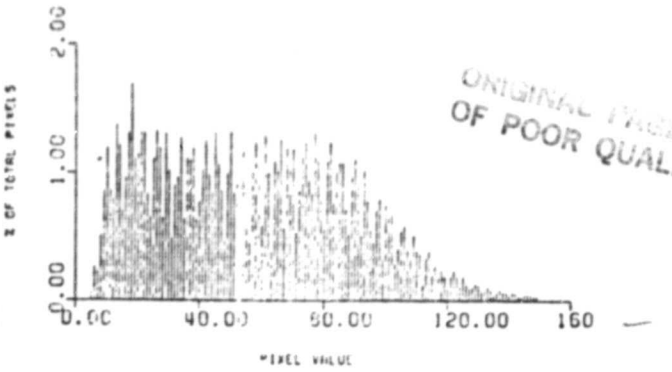

END OF PLOT FOR BAND 5 DETECTOR 11

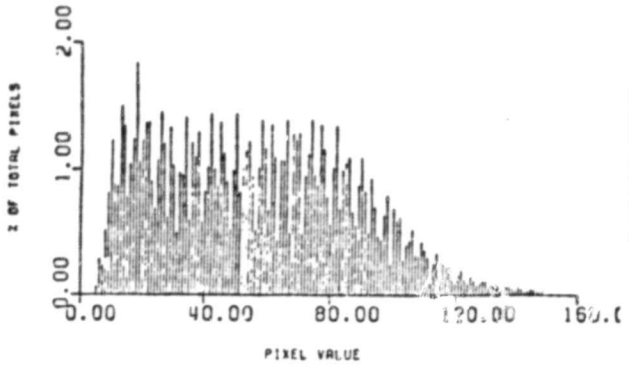

END OF PLOT FOR BAND 5 DETECTOR 10

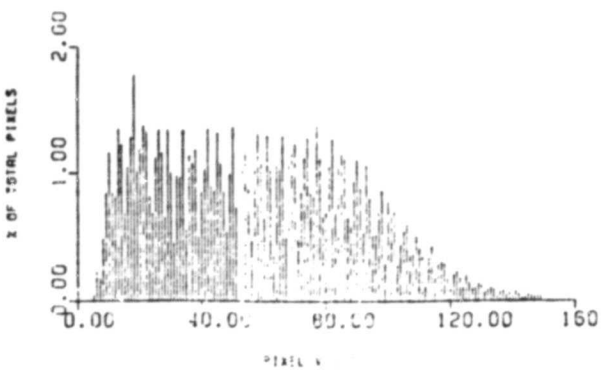

END OF PLOT FOR BAND 5 DETECTOR 12

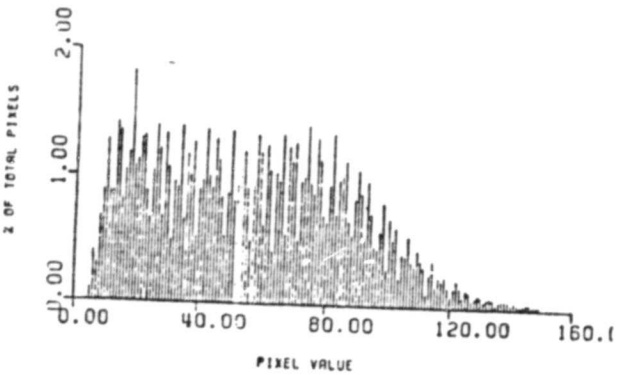

END OF PLOT FOR BAND 5 DETECTOR 15

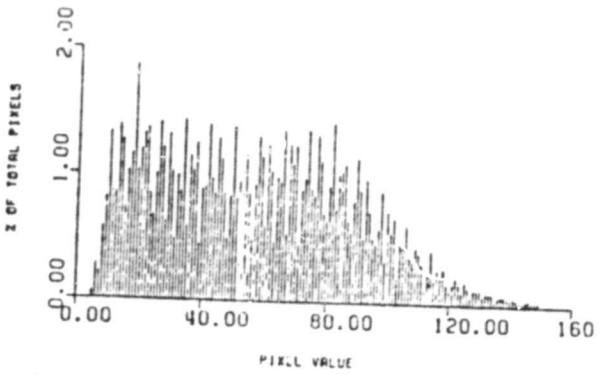

END OF PLOT FOR BAND 5 DETECTOR 13

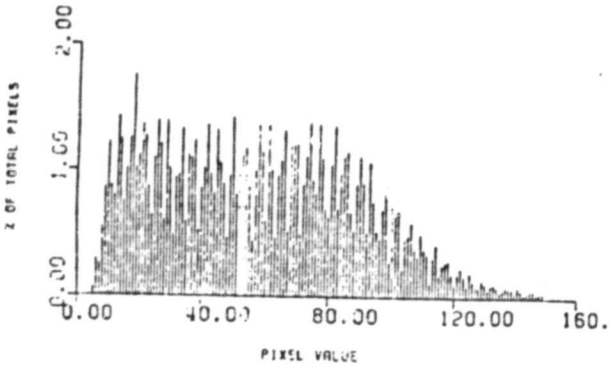

END OF PLOT FOR BAND 5 DETECTOR 16

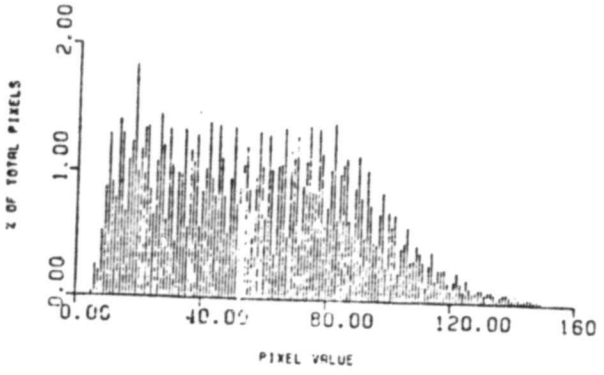

END OF PLOT FOR BAND 5 DETECTOR 14

FIGURE 3.5 (CONT) BAND 5 HISTOGRAMS

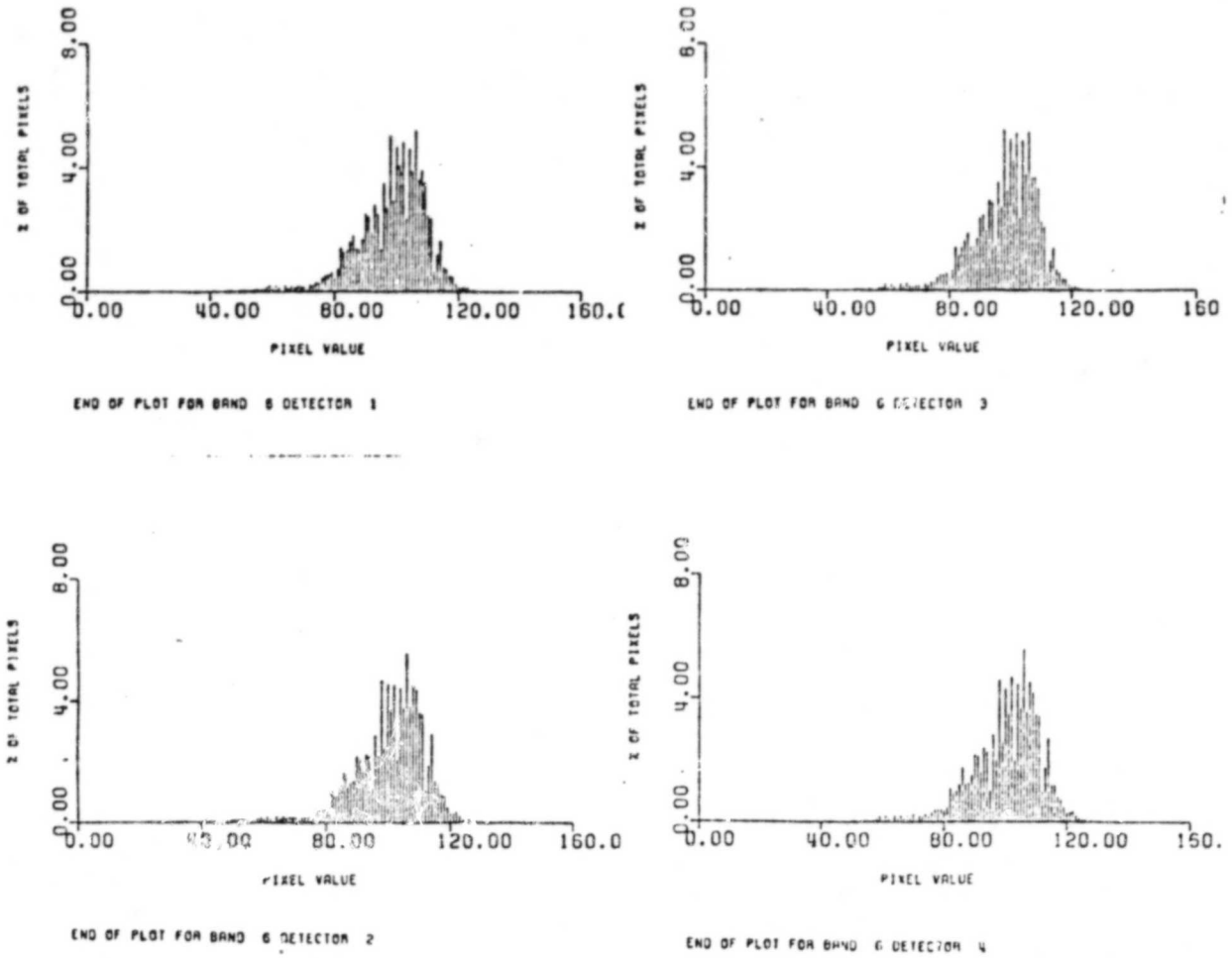

FIGURE 3.6 BAND 6 HISTOGRAMS

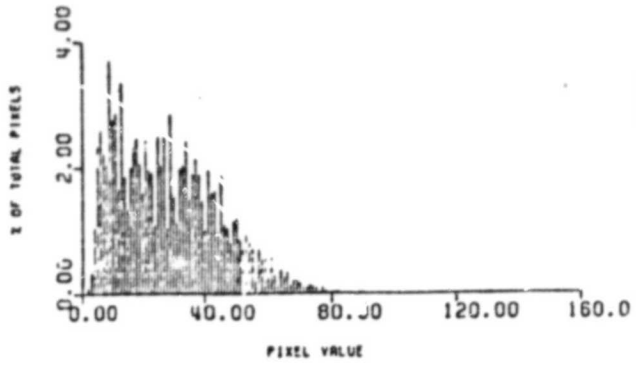

END OF PLOT FOR BAND 7 DETECTOR 1

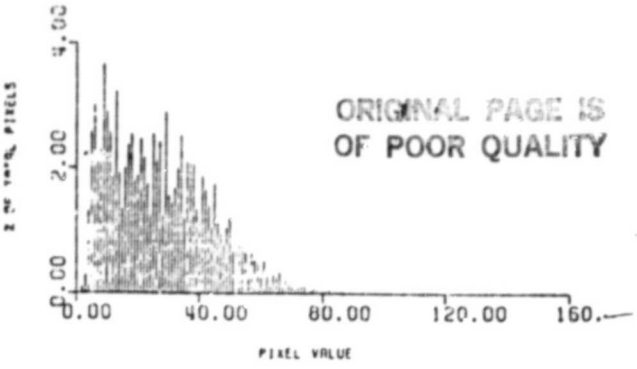

END OF PLOT FOR BAND 7 DETECTOR 3

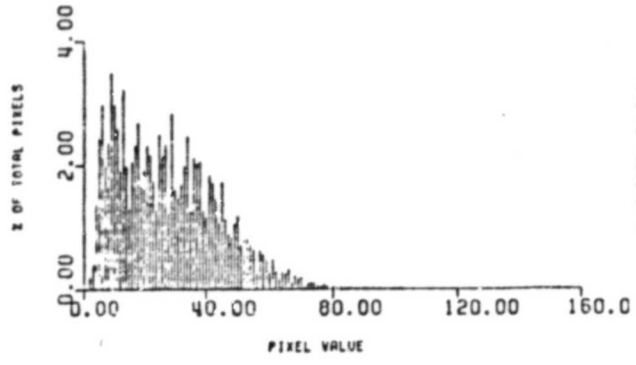

END OF PLOT FOR BAND 7 DETECTOR 2

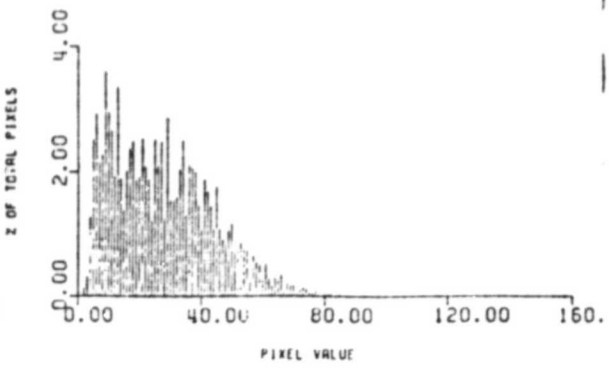

END OF PLOT FOR BAND 7 DETECTOR 4

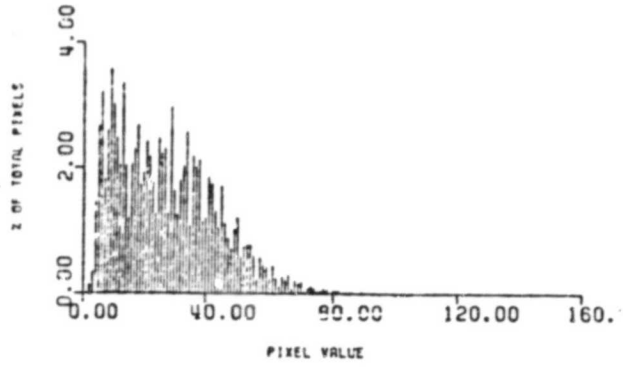

END OF PLOT FOR BAND 7 DETECTOR 5

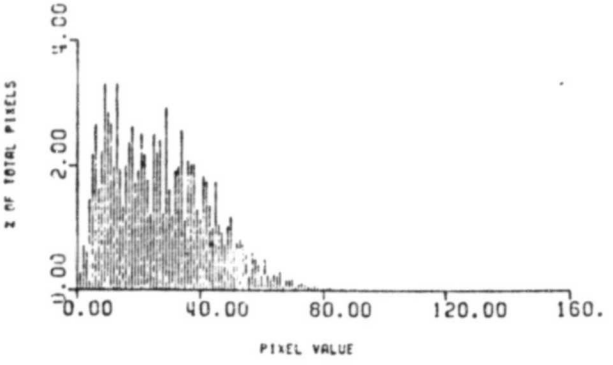

END OF PLOT FOR BAND 7 DETECTOR 7

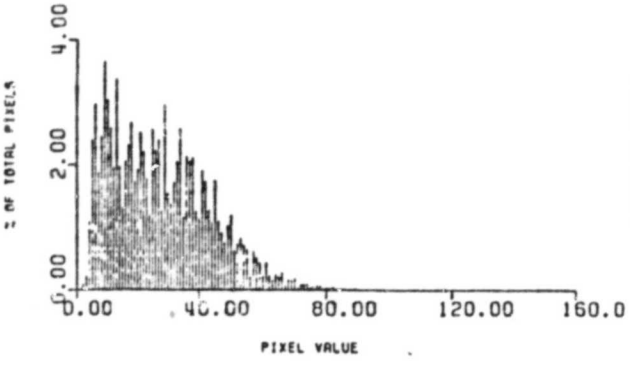

END OF PLOT FOR BAND 7 DETECTOR 6

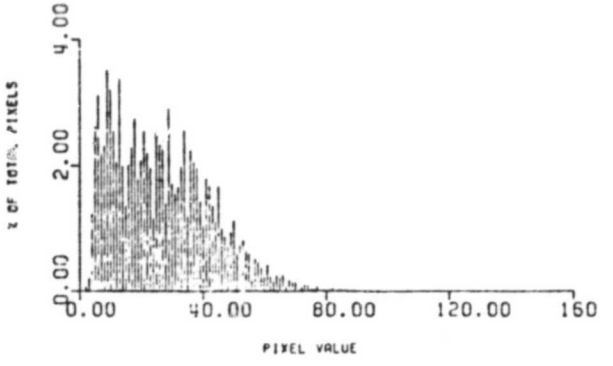

END OF PLOT FOR BAND 7 DETECTOR 8

FIGURE 3.7 BAND 7 HISTOGRAMS

FIGURE 4.1 Residual Striping Over Water - Band 1

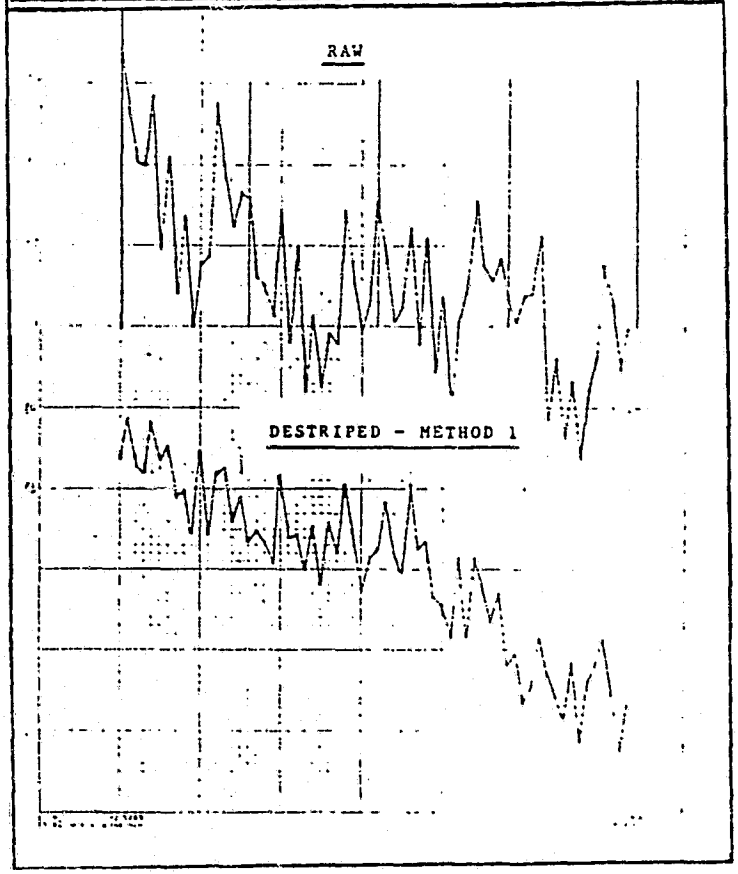

FIGURE 4.1 (Cont) Residual Striping Over Water - Band 1

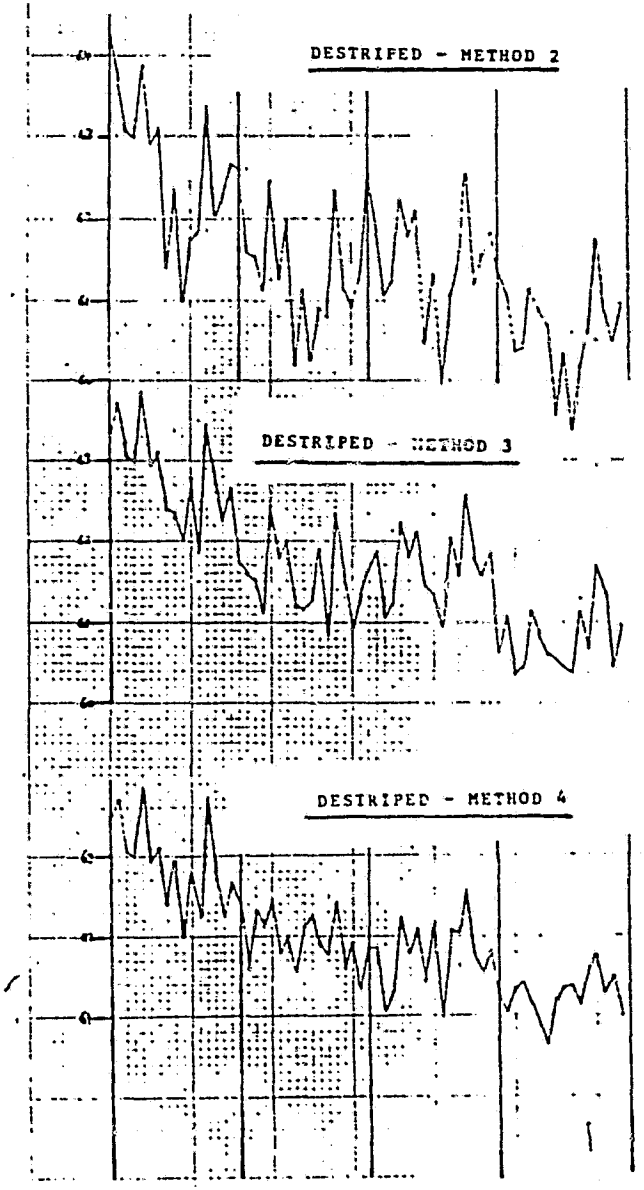

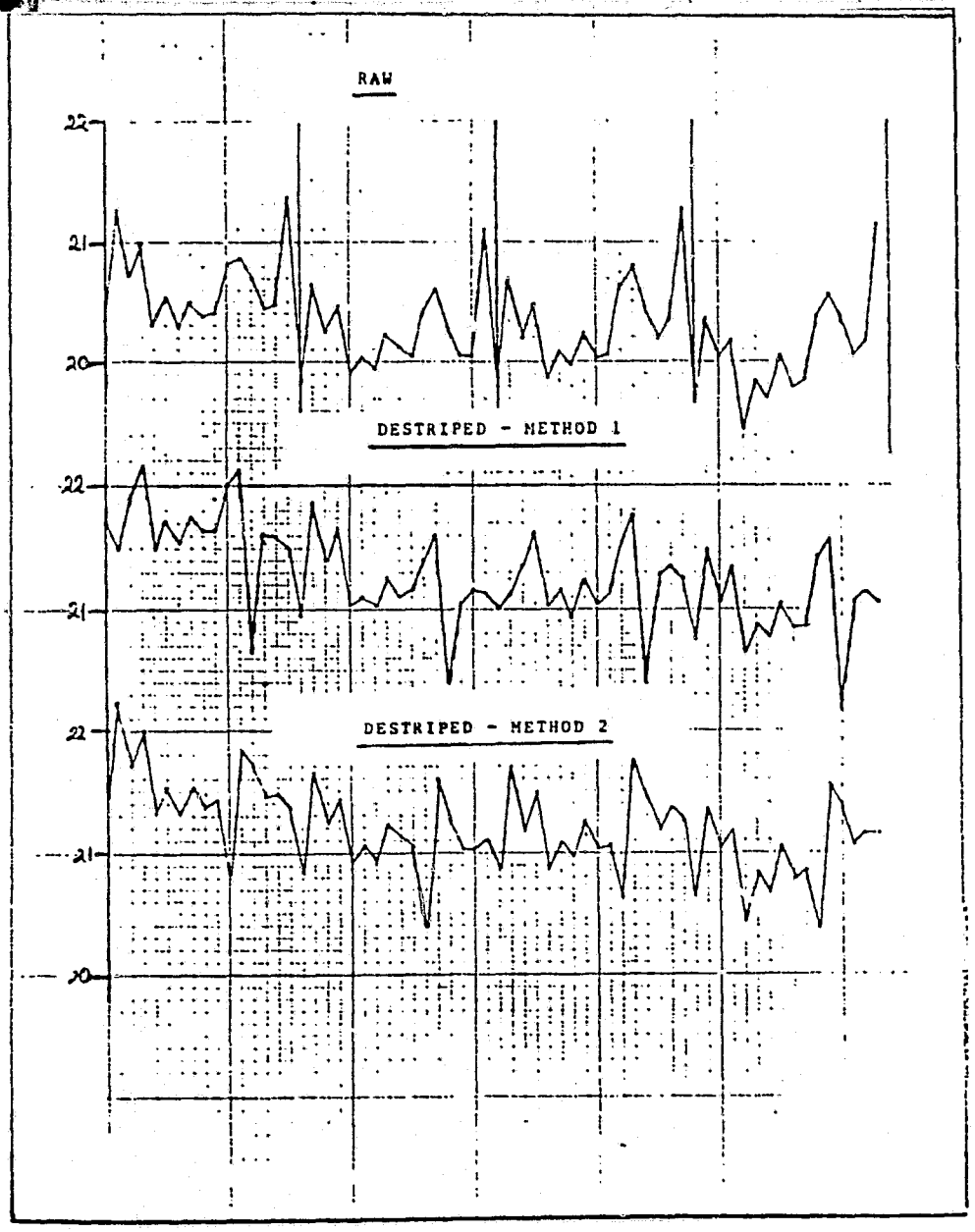

FIGURE 4.2 (Cont) Residual Striping Over Water - Band 2

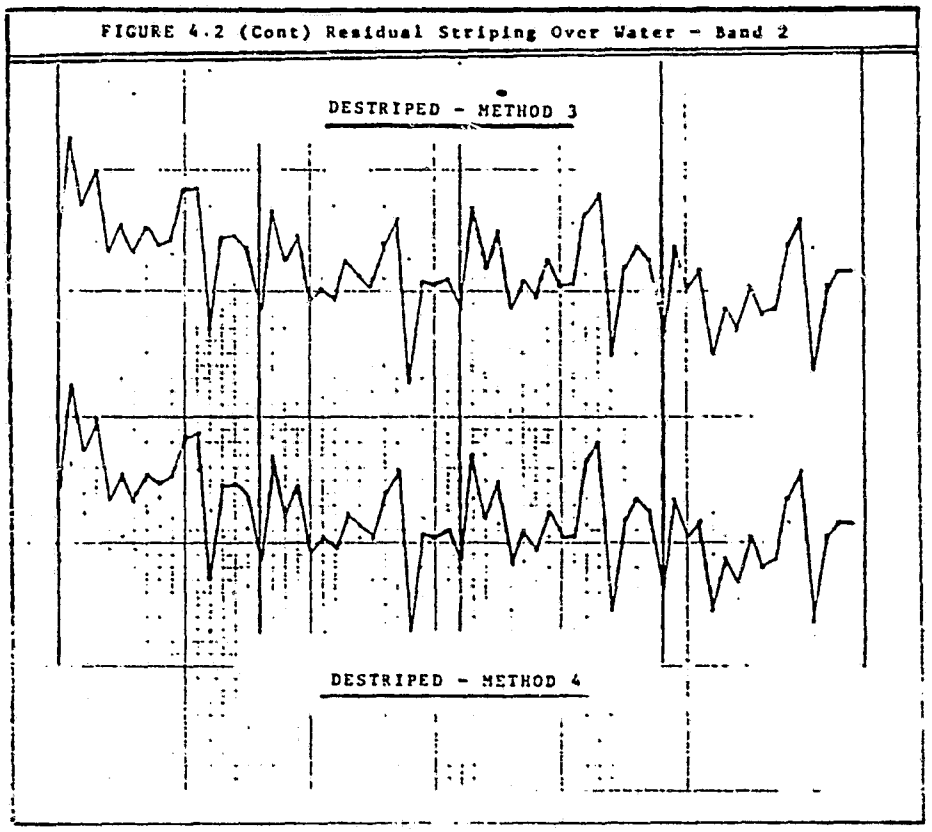

FIGURE 4.3 Residual Striping Over Water - Band 3

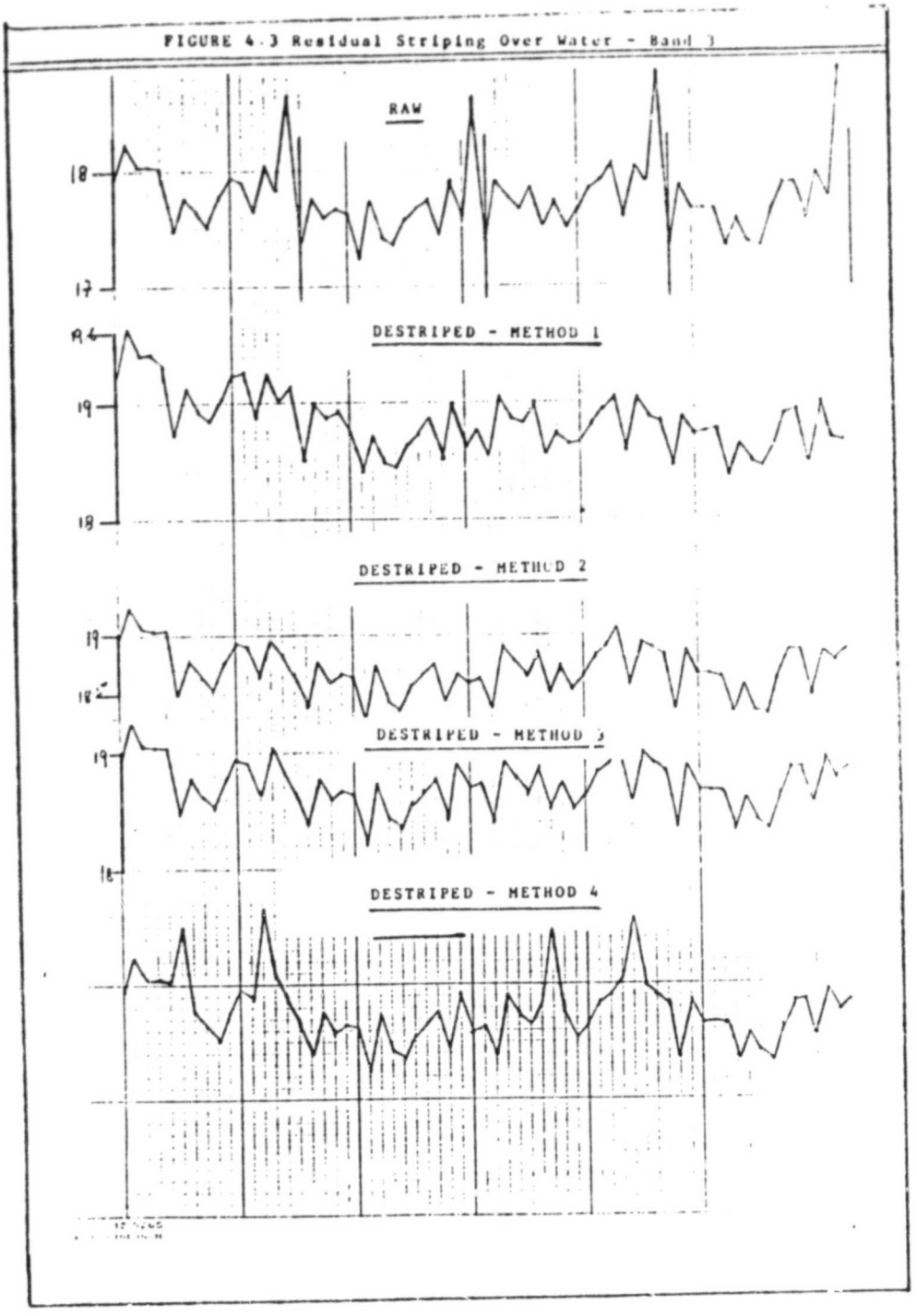

FIGURE 4.4 Residual Striping Over Water - Band 4

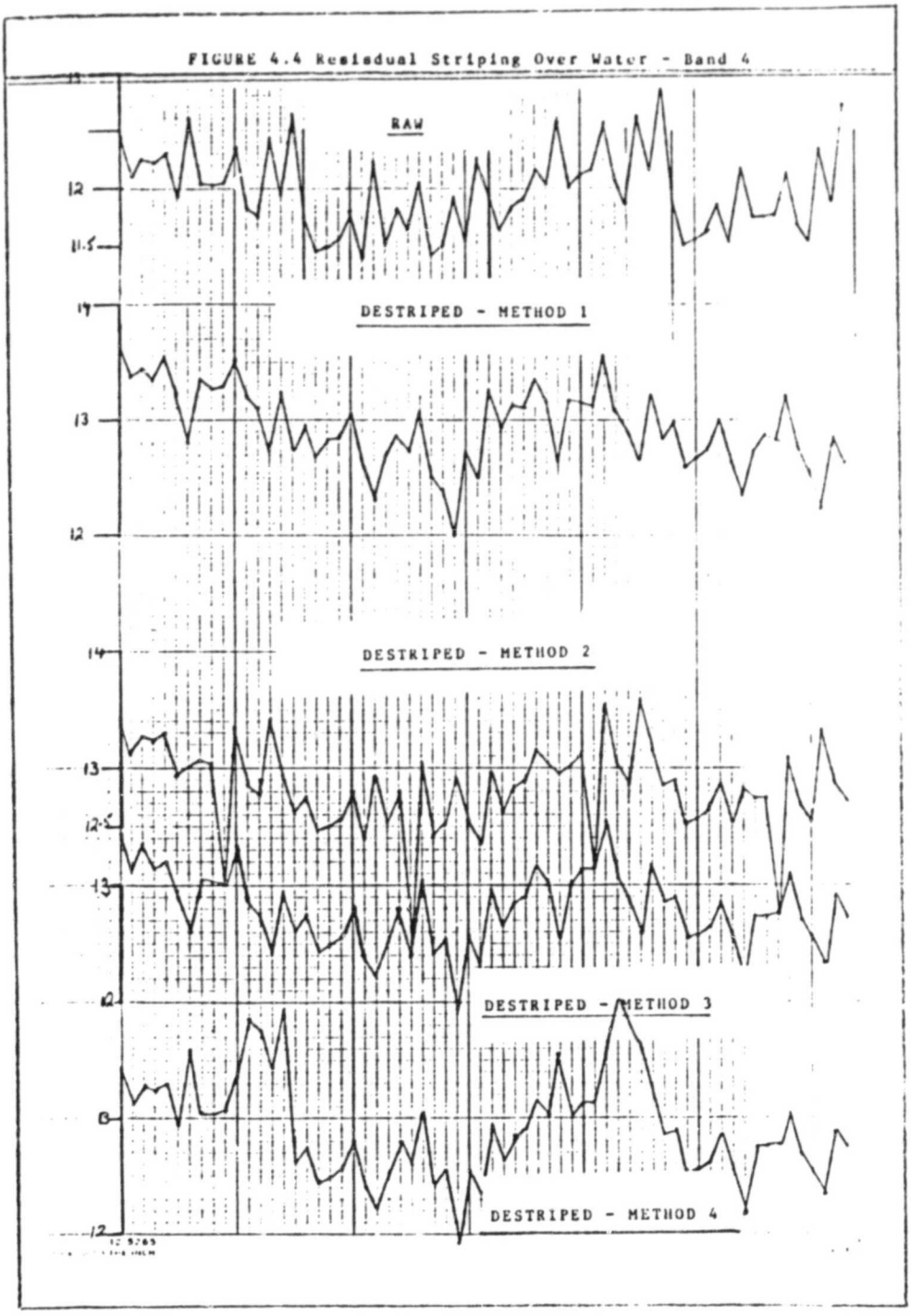

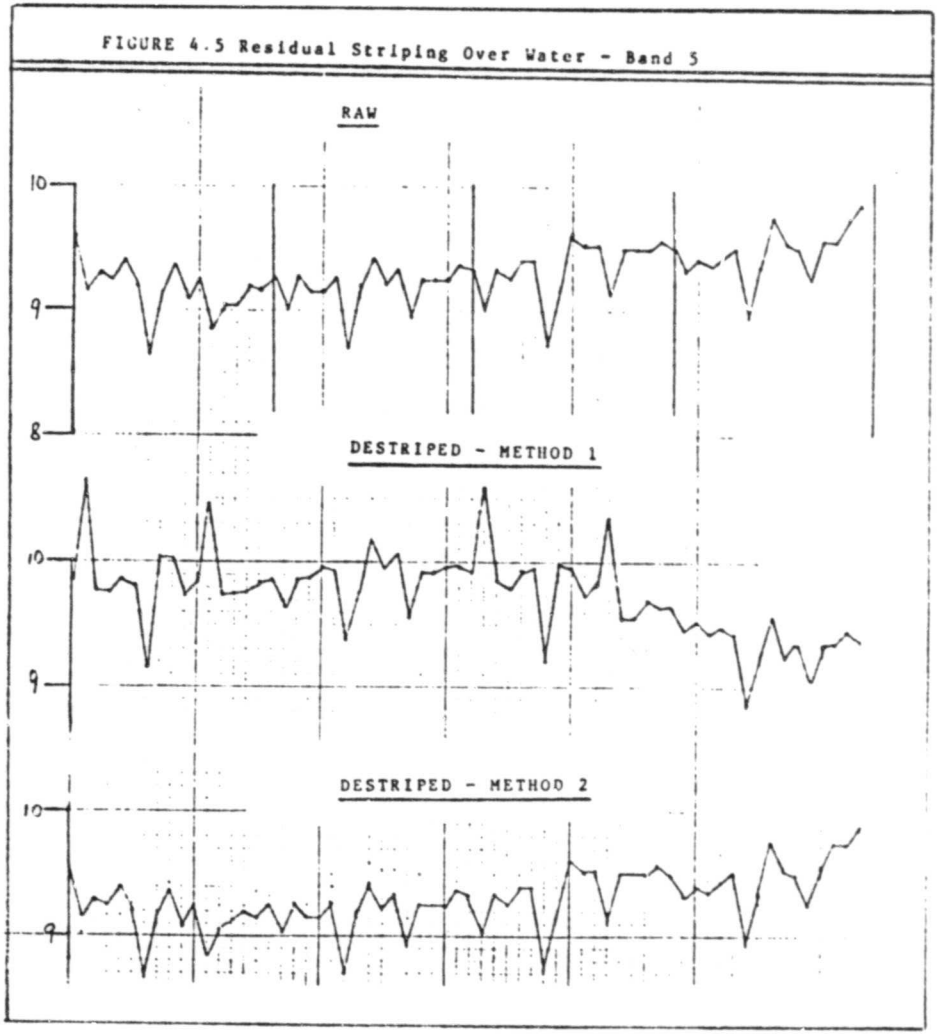

FIGURE 4.5 Residual Striping Over Water - Band 5

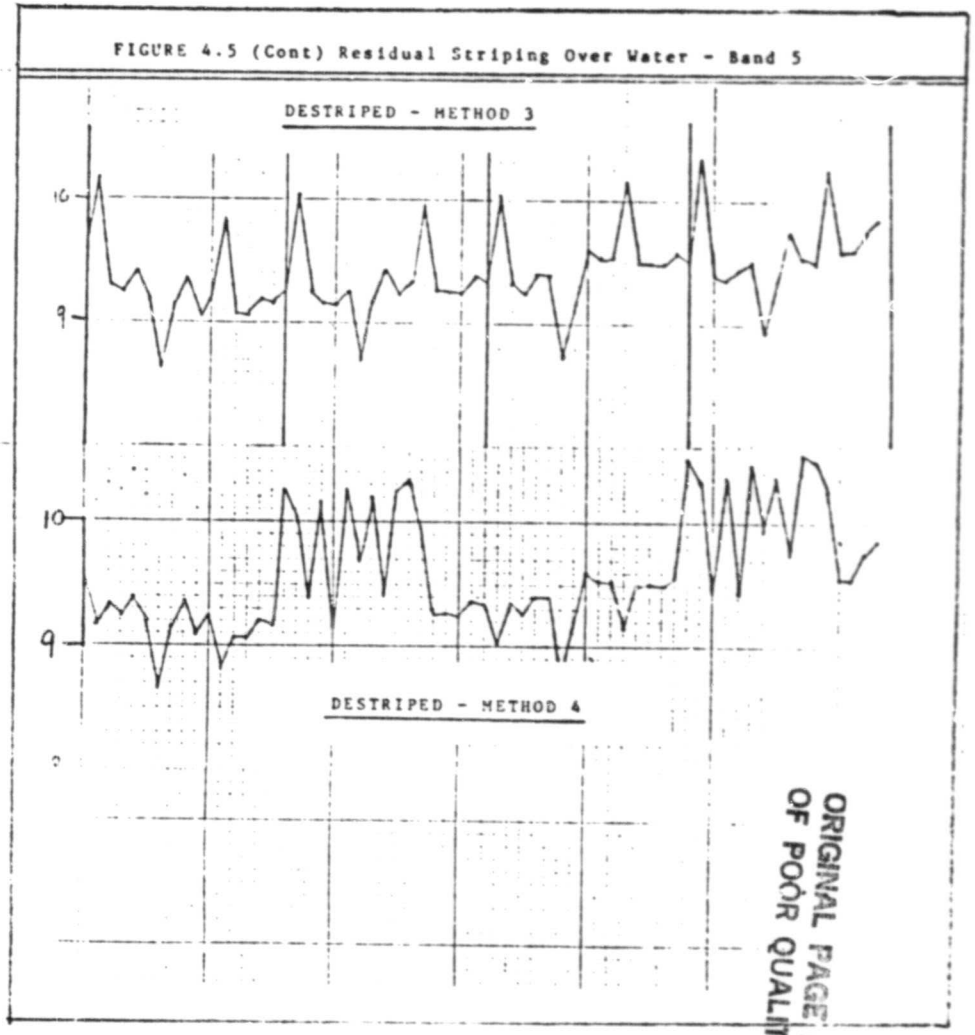

FIGURE 4.5 (Cont) Residual Striping Over Water - Band 5

FIGURE 4.6 Residual Striping Over Water - Band 6

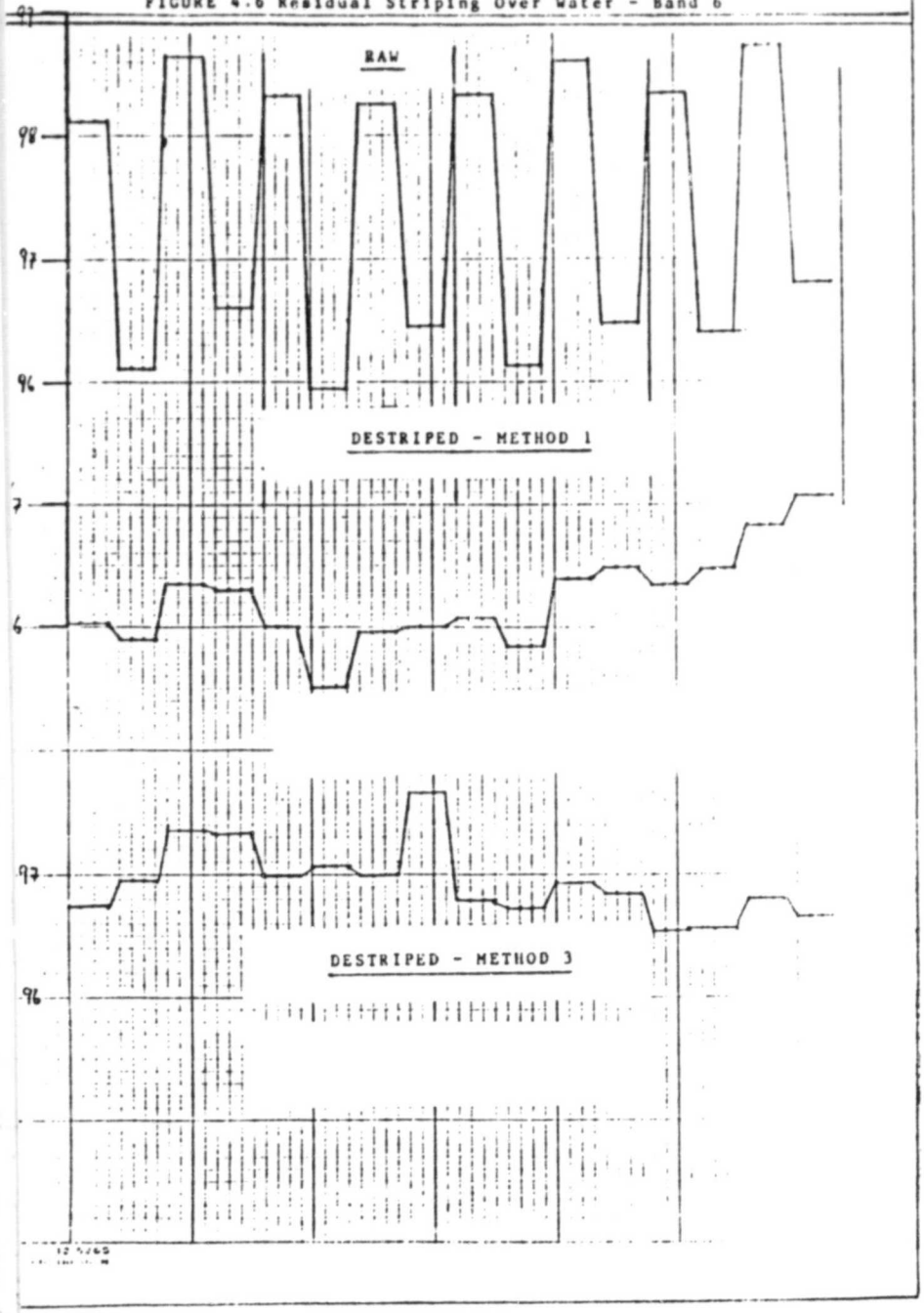

FIGURE 4.7 Residual Striping Over Water - Band 7